2018년 8월

박사학위논문

C_1 화학분야에 대한 DBD 플라즈마와 금속 촉매의 상호작용 및 활용 연구

조선대학교 대학원

항공우주공학과

이 충 준

C_1 화학분야에 대한 DBD 플라즈마와 금속 촉매의 상호작용 및 활용 연구

The research on interaction and utilization of DBD plasma and metal catalyst for C_1 chemistry

2018년 8월 24일

조선대학교 대학원

항공우주공학과

이 충 준

C_1 화학에 대한 DBD 플라즈마와 금속 촉매의 상호작용 및 활용 연구

지도교수 김 태 규

이 논문을 공학 박사학위신청 논문으로 제출함

2018 년 04 월

조선대학교 대학원

항공우주공학과

이 충 준

이충준의 박사학위 논문을 인준함

위원장 한국기계연구원 책임연구원 이 대 훈 (인)

위 원 조선대학교 교수 이 현 재 (인)

위 원 조선대학교 교수 김 태 규 (인)

위 원 조선대학교 교수 이 창 열 (인)

위 원 한국기계연구원 선임연구원 조 성 권 (인)

2018 년 06 월

조 선 대 학 교 대 학 원

CONTENTS

LIST OF FIGURES

LIST OF TABLES

NOMENCLATURE

Abbreviations

AC	Alternating Current
CCD	Charge-Coupled Device
DBD	Dielectric Barrier Discharge
DMFC	Direct-Methanol Fuel Cell
EDS/EDX	Energy Dispersive X-ray Spectroscopy
FT-IR	Fourier-Transform Infra-Red spectroscopy
GC	Gas Chromatography
GHSV	Gas Hourly Space Velocity
GTL	Gas-to-Liquid
LTS	Low-Temperature Shift
MFC	Mass Flow Controller
NASA	National Aeronautics and Space Administration
OES	Optical Emission Spectroscopy
P2G	Power-to-Gas
PC	Personal Computer
PEMFC	Proton Exchange Membrane Fuel Cell
	Polymer Electrolyte Membrane Fuel Cell
RMFC	Reformed-Methanol Fuel Cell
SED	Specific Energy Density
SEM	Scanning Electron Microscopy
SNG	Substitute Natural Gas
	Synthetic Natural Gas
SUS	Steel Use Stainless

Chemistry

γ-Al_2O_3	Gamma-phase alumina
Al	Aluminum
Al_2O_3	Alumina
C	Carbon
C_2H_2	Acetylene
C_2H_4	Ethylene
C_2H_6	Ethane
C_3H_8	Propane
CH_3OH	Methanol
CH_4	Methane
CO	Carbon Monoxide
CO_2	Carbon Dioxide
Cu	Copper
Fe	Iron
H	Hydrogen
Mg	Magnesium
Mn	Manganese
N	Nitrogen
Ni	Nickel
NO_x	Nitrogen Oxides
O	Oxygen
Os	Osmium
Pd	Palladium
Pt	Platinum
Rh	Rhodium

Ru	Ruthenium
Ti	Titanium
Zn	Zinc

Electric

C_a	Air gap capacitance
C_d	Dielectric capacitance
f	Frequency
Hz	Unit of frequency, Hertz
F	Unit of capacitance, Farad
Q	Electric charge
V	Unit of voltage, Volt
V_0	Breakdown voltage
V_m	Maximum voltage
W	Unit of electric power, Watt

Units

℃	Unit of temperature, degree Celsius
atm	Unit of pressure
g	Unit of mass, Gram
mL	Unit of volume, Milliliter
mL/min	Unit of flow rate
mm	Unit of length, Millimeter
$ml \cdot h^{-1} \cdot g_{cat.}^{-1}$	Unit of space velocity

ABSTRACT

The research on interaction and utilization of DBD plasma and metal catalyst for C_1 chemistry

by Lee, Chung Jun

Advisor : Prof. Kim, Taegyu, Ph. D.

Department of Aerospace Engineering,

Graduate School of Chosun University

C_1 화학분야는 단일 탄소 원자와 기타 원소들이 결합된 화학 결합물을 이용하는 모든 분야를 통틀어 지칭하는 용어로써, 현대 사회의 생활/경제/에너지 분야에 큰 영향을 미치고 있다. 하지만 이러한 C_1 화학분야에 속한 일부는 최근 큰 이슈가 되고 있는 환경문제 중 하나인 지구 온실 기체인 이산화탄소 및 메탄의 배출과 같은 문제에도 매우 밀접한 관계를 가지는 두 얼굴을 가지고 있다. 이러한 배경으로 인하여 C_1 화학분야와 관련된 다양한 연구가 진행되고 있는데, 대표적인 사례로는 에너지원 혹은 원천재료에 대한 메탄올 및 메탄의 개질/전환에 관한 연구와 지구 온실기체 제거 및 감소와 관련된 이산화탄소 및 메탄의 분해에 대한 연구를 예로 들 수 있다.

일반적으로 메탄올 및 메탄의 개질/전환, 이산화탄소 및 메탄의 분해는 일정 이상의 온도 조건에서 촉매를 이용한 화학반응을 이용하여 이루어지게 된다. 가령 메탄올은 섭씨 약 300도 이내의 조건에서 구리 기반의 촉매를 이용하여 개질/전환 반응이 대표적이며, 메탄은 섭씨 약 800도 이상에서 니켈 기반으로 구성된 촉매를 이용하여 개질/전환 반응을 수행하게 된다. 이러한 촉매 기반의 개질/전환 혹은 분해 반응을 보다 촉진시키기 위하여 이산화탄소, 수증기, 산소 등과 같은 추가 첨가물을 이용하여 공정 효율을 향상시키는 방법이 일반적으로 사용되고 있다. 하지만, 최근에는 첨가물 및 고온

에 의존하지 않고 보다 낮은 온도에서 첨가물 없이 공정의 효율을 올리기 위해 저온 혹은 비열 플라즈마를 이용하는 방법이 그 대표적인 사례라고 할 수 있다.

대표적인 저온 혹은 비열 플라즈마를 이용하는 방법을 살펴보면, 전극 사이에 절연 물질을 위치시키고 고전압을 인가하는 유전체 장벽 방전을 이용하여 저온 플라즈마를 형성시키는 방법이 매우 활발하게 연구되고 있는데, 이는 바로 유전체 장벽 방전의 구성 난이도가 낮고 넓은 범위에 걸쳐 플라즈마를 생성할 수 있는 것을 그 이유로 들 수 있다. 현재 많은 기존 연구에서 유전체 장벽 방전을 이용하여 촉매 상에 플라즈마를 형성하여 다양한 반응에서 성능이 향상되었다는 결과들이 보고된 바 있지만, 이러한 성능의 향상의 원인에 대해서는 아직도 명확하게 밝혀지지 않고 있기에 화학 공정에 대한 적극적으로 활용할 수 있는지 여부에 대한 해답도 여전히 논쟁거리가 되고 있다. 이러한 이유로 본 C_1 화학공정에 대해서 유전체 장벽 방전 플라즈마와 금속 촉매의 혼종 구성을 이용하는 화학 공정에 대해서 다음과 같이 연구를 수행하였다.

첫 번째로는 유전체 장벽 방전 플라즈마와 촉매에 대한 기본 특성 이해를 위해 메탄올 전환 반응을 수행하였다. 상대적으로 저온 영역에서 활발한 촉매 반응을 보이는 메탄올에 대해서 촉매 혹은 촉매 주변에 플라즈마를 발생시켜 이로 인한 영향력과 특성에 대한 이해를 수행하였다. 플라즈마의 인가로 인하여 촉매-화학반응과 다른 양상이 발생하는 현상을 확인하였으며, 플라즈마와 촉매의 상대적인 위치, 그리고 유전체 장벽 방전을 위한 전극 사이에 위치하는 촉매와 같은 물질에 따라서도 전혀 다른 반응 양상이 발생하는 것을 확인하였다.

두 번째로는 유전체 장벽 방전 플라즈마가 촉매의 종류 혹은 유전체 장벽 방전 그리고 그 결과로 플라즈마가 발생되는 영역에 위치하는 물질에 따라 성능이 크게 변화할 수 있음을 검증하기 위한 연구를 메탄 전환 반응에 대해 수행하였다. 이를 확인하기 위해 구리-아연 촉매 상에 10%의 조촉매가 포함되도록 조절하였다. 일반적으로 촉매에 의한 메탄의 전환 반응이 잘 발생하지 않는 조건을 실험 환경으로 설정하였음에도 조촉매 원소에 따라 결과가 크게 달라지는 것을 확인하였다. 이를 바탕으로 유전체 장벽 방전 플라즈마와 촉매는 일방적인 보조-성능 향상의 관계가 아닌 상호간 영향을 미치는 상호작용이 존재한다는 가설을 설립하고 이를 증명하기 위한 방법을 고안하였

다.

세 번째로 수행된 연구는 유전체 장벽 방전 플라즈마와 촉매 사이의 상호작용을 증명하는 일환으로 촉매를 구성하는 원소에 의한 유전체 장벽 방전 플라즈마의 성능 변화를 직접 관측하는 가시화에 대한 연구를 수행하였다. 통상적으로 유체의 흐름을 제어하기 위해 연구되고 있는 비대칭형 유전체 장벽 방전 플라즈마 액츄에이터가 연구에 사용되었으며, 전극 사이에 촉매를 위치시키고 서로 다른 촉매 원소에 따라 플라즈마 스트리머의 발달이 변화됨을 가시화 촬영을 통해 확인하였고, 촉매의 원소 이외에도 촉매의 산화/환원 상태도 영향을 미치는 것을 확인할 수 있었다. 앞서 수행한 메탄올, 메탄을 이용한 연구의 결과와 가시화 연구의 결과를 바탕으로 유전체 장벽 방전이 일어나는 공간 내에 위치하는 촉매와 같은 물질은 플라즈마 형성에 큰 영향을 미치며, 이는 다시 형성된 플라즈마가 유전 가열이나 전자의 충돌로 원자 및 분자의 여기 및 라디칼 생성과 같은 특성으로 촉매 반응에 다시금 영향을 줄 수 있는 상호작용이 발생한다는 결론을 도출하였다.

네 번째로 수행된 연구는 이러한 유전체 장벽 방전 플라즈마와 촉매의 상호작용을 활용할 수 있는 응용 방법에 대해 수행되었으며, 플라즈마의 전자 충돌 특성을 이용하여 통상적으로 고온 영역에서 분해가 시작되는 물질을 강제로 분해시키고 동시에 유전 가열로 부분적인 촉매 활성화를 유도할 수 있는 대상을 탐색한 결과, 이산화탄소와 수소를 이용한 메탄 합성 공정을 그 응용 연구의 주제로 결정하였다. 특히, 선행되었던 메탄 전환 실험의 결과와 탐색 실험 과정에서 확인한 소수의 탄소에 대한 다수의 활성/여기 상태의 수소가 존재할 경우 안정된 구조인 메탄을 형성하려는 경향성이 매우 강하다는 것을 확인하였기 때문에 이러한 메탄화 과정을 가속화시킬 촉매에 대한 탐색을 먼저 수행하였다. 메탄화 반응에 일반적으로 사용되는 원소들에 대해 유전체 장벽 방전 플라즈마 환경에서의 상호작용 특성을 살펴본 결과, 루테늄 촉매가 가장 바람직한 상호작용을 구현할 수 있음을 확인하였고 이를 바탕으로 유전체 장벽 방전 플라즈마와 촉매의 상호작용을 이용하여 파워-투-가스 공정의 사례 중 하나로 주목받고 있는 이산화탄소와 수소를 이용하여 메탄을 합성하는 공정을 상온/상압 조건에서 실현 가능함을 확인하였다.

다섯 번째로는 이러한 긍정적인 상호작용이 아닌 실제 응용분야에 활용에 있어 가장 문제가 될 수 있는 부정적인 작용에 대한 탐구를 수행하였다. 유전체 장벽 방전은 전자의 충돌, 활성종 생성 그리고 유전가열 등으로 인하여 긍정적인 상호작용도 발생시켰으나, 반대로 함침 촉매의 표면에 큰 손상을 가할 수 있는 요소들이 확인되었다. 따라서, 이에 대한 손상이 가해지는 조건 및 메커니즘에 대한 가설을 제시함으로써 유전체 장벽 방전 플라즈마와 촉매의 상호작용을 이해하고 이에 대한 C_1 화학 분야에 대한 응용 가능성에 대해 제시하였다.

I. Introduction

1. Background

1.1 Dielectric barrier discharge and plasma generation

Dielectric barrier discharge is one of the electrical discharge technique[1, 2]. It is also known as DBD (abbreviation) or silent discharge. Figure 1 is schematic of typical configurations about dielectric barrier discharge. Most distinguishing feature of dielectric barrier discharge is insulation material barrier between electrodes. Normally, insulation material is disturb electrical discharge but electron can be passed through the insulation material or dielectric barrier when discharge voltage is higher enough. When discharge voltage is also higher enough against gas and dielectric barrier between electrodes, electrical discharges will be occurred. It called electrical breakdown and causes plasma generation because electrons are collided with gas molecules. Especially, massive micro-discharges are generated by dielectric barrier discharge.

Dielectric barrier discharge was first reported by Ernst Werner von Siemens in mid-19th century. He invented dielectric barrier discharge to convert oxygen into ozone. After dielectric barrier discharge was invented, it was used and studied to generate ozone for a long time. In early 1930s, electrical engineer K. Buss found out breakdown of dielectric barrier discharge in atmospheric pressure. He was reported that large number of tiny short-lived current filaments are generated between planar parallel electrodes which was covered by dielectric barrier. After 10 years later, T. C. Manley was proposed about determination method of dissipated power by dielectric barrier discharge[3].

The studies about dielectric barrier discharge was originally focused on ozone generation. However, lot of possibilities and potentials of dielectric barrier discharge are discovered during the study for ozone generation. As a result, dielectric barrier discharge is studied for many fields such as chemistry for environment or energy conversion, agriculture for sterilization, aerospace engineering for flow control and industry for surface treatment or

pollutant control or chemical applications. Especially, utilization for chemical industry is very interesting field in today. People expect that some characteristics of DBD plasma can improved performance of many chemical processes[4-10].

The DBD plasma have a fast responsibility and low power consumption characteristic. It can be also used at atmospheric pressure and temperature. Moreover, DBD plasma is non-thermal plasma which is not in thermodynamic equilibrium. It indicates that DBD plasma is not increase temperature of discharge media extremely because its ion and electron temperature is different. Therefore, people expect that DBD plasma can be improving the industrial applications like a hydrocarbon reforming process due to the fast start time, low pre-heating requirements, low electrical power consumption, and inability to be poisoned or deactivated[11-15].

1.2 DBD plasma assisted catalyst process

Many DBD plasma for chemical process is used with catalyst. This combined operation of DBD plasma and catalyst is called in many different ways such as hybrid catalytic-DBD plasma, DBD plasma assisted catalyst process or etc. The advantage of this combined operation is performance improvement on chemical process. Many studies has reported conversion improvement or specific selectivity improvement[11, 16-34]. However, it is not always contribute positively with some catalysts or some processes. Moreover, performance of some catalysts are decreased under DBD plasma assisted condition. Therefore, using DBD plasma with proper catalyst and proper chemical process is very important parameter to make positive effect.

The DBD plasma assisted catalyst process is actively discussed and studied for chemical energy conversion processes such as hydrocarbon reforming or hydrogen production. Especially, hydrocarbon reforming like a methane to higher hydrocarbon and hydrogen production from hydrogen carrier such as methane, methanol is received attention because it can be used on fuel-cell application or feedstocks.

However, DBD plasma assisted catalyst process have a many arguments[35]. One of the actively discussed argument is presence of synergy effect between DBD plasma and catalyst. This argument is also carried over into its mechanism and source of performance enhancement from DBD plasma assisted catalyst process. However, aforementioned performance enhancement and synergy effect is not clearly identified yet. Especially, dielectric heating can be generated from DBD plasma in higher discharge frequency and many studies are used higher discharge frequency because they want to maximize performance enhancement in plasma discharge condition. In higher discharge frequency and higher dielectric heating condition, contribution of dielectric heating on catalytic enhancement is may be higher than expected. Actually, dielectric heating is not a negative or undesirable characteristic on chemical conversion or reforming process because catalytic performance can be increased by temperature. However, only using dielectric heating is completely ineffective than thermal plasma because thermal plasma can provide much higher thermal energy in short time. Except the efficiency, reaction product of DBD plasma assisted catalyst process is not same as pure catalytic process. Therefore, DBD plasma assisted catalyst process is still makes lot of arguments and discussions.

1.3 DBD plasma and C_1 chemistry

The C_1 chemistry is refers to the specific chemical compounds what contains single carbon atom in molecule and its related conversion processes. This C_1 chemistry is one of the important interest in today because it is very closely connected with modern life of human. Fossil fuels such as gasoline, diesel and natural gas contains carbon and dependence of fossil fuels are still higher than another fuels. In 2014, global market share of fossil fuel is still over an 80 percent. Therefore, fossil fuel what include carbon is very important on human life and modern economy system[36].

However, it is not always good for human life because carbon dioxide is emitted by fossil fuel combustion. This carbon dioxide is well-known as greenhouse gas and it has

high global warming potential. Therefore, this carbon dioxide emission is very sensitive issue on environment[37, 38].

DBD plasma assisted catalyst for C_1 chemistry is widely studied in today. For example, alternative fuel productions and synthesize fuels from hydrocarbons such as hydrogen production and hydrocarbon reforming or upgrading are studied with DBD plasma assisted catalyst process. Methanol decomposition is a good example of alternative fuel production. The methanol is well-known hydrogen carrier because one mole of methanol contain 4 hydrogen atoms and one of carbon and oxygen (Chemical Formula of methanol : CH_3OH). Copper-based catalysts are usually used for methanol decomposition or reforming reaction. This methanol decomposition is the one of the famous low temperature shift (LTS) reaction.

In the other study, about fuel synthesis is mainly studied with methane. The methane has a simple structure which is consisted of one carbon atom and four hydrogen atoms (Chemical Formula of methane : CH_4). It is main component of natural gas and far cheaper than oil and especially with the recent discovery and development of shale deposits in the United States and elsewhere. The methane can convert into hydrocarbon fuel by using upgrading or reforming process. Dry reforming, steam reforming and gas-to-liquid (GTL) is typical processes about methane to synthetic fuel. Therefore, upgrading or reforming of methane to higher hydrocarbon have a great potential in today. Those hydrocarbons related C_1 chemistry is closely connected with economical and economical side.

On the contrary, DBD plasma assisted catalyst process on oxidized carbon is mainly studied for environment applications. For example, carbon monoxide is studied on plasma-assisted catalytic partial oxidation and carbon monoxide is studied on plasma assisted catalytic decomposition. The partial oxidation of carbon monoxide can be decrease harmful oxide gases such as NO_x (nitrogen oxides), and decomposition such as carbon dioxide into carbon monoxide or carbon and oxygen can contribute removal or decrease of

carbon dioxide concentrations.

Other oxidized carbon, carbon dioxide is also widely studied in many fields, including DBD plasma assisted catalyst process. It related fossil fuels what composed mainly hydrocarbons and produce carbon dioxide via combustion process. Modern human life is based on fossil fuel infrastructure and is closely connected with our economic system. For example, generation of heat, electrical power or mechanical or other forms of energy is usually achieved by combustion of fossil fuel. Alternative energy source such as renewable energy or hydrogen energy is still difficult to replace most of the fossil fuel applications. For these reasons, carbon dioxide emission is very sensitive issue in today. Major reason to worry about carbon dioxide emission is related to climate change and global warming because carbon dioxide traps heat in atmosphere. The Kyoto Protocol (1997) and Paris Agreement (2016) is good examples what attentions and concerns about carbon dioxide emission. Therefore, carbon dioxide removal or decomposition is actively studied in today.

1.4 Recent research on DBD plasma assisted catalyst process

The DBD plasma assisted catalyst process have been studied for chemical conversion process. Many chemical processes are already studied with DBD plasma assisted catalyst process. Especially, pollutant removal such as NO_x decomposition or hydrocarbon conversion such as CH_4 reforming/conversion with DBD plasma assisted catalyst process is actively studied in today[16-34]. Also, researches on positive or synergy effect mechanism is also performed with many analysis methods. Some people was used Fourier-Transform Infrared Spectroscopy (FT-IR) and some people was used Optical Emission Spectroscopy (OES) to reveal its mechanism. However, it is still not clearly identified yet.

1.5 Recent research on C_1 chemistry

The C_1 chemistry is play an important role in energy supply and many products. At the

same time, it is also related with environmental issues such as global warming and climate change. In energy supply, methane is widely studied for conversion and reforming process. This methane is rich in natural gas and can coverted into higher hydrocarbons such as propane, butane or diesel. It also can be convert into petrochemical products such as asphalt, plastics and polyethylene. Except case of methane, methanol is also widely studied for fuel, hydrogen production and conversion into synthesis gas or chemical industry. As above examples, hydrocarbon related C_1 chemistry is closely connected with modern human life and modern industry and economy[39].

In environmental case, oxidized C_1 chemistry like a carbon dioxide is also important because it causes greenhouse effect and climate change. This carbon dioxide related studies are mainly conducted to decompose or deoxygenation of carbon dioxide. However, carbon dioxide is too stable and its bonding energy is quite strong. It means that decomposition or deoxygenation of carbon dioxide is required high energy supply. Even if using novel catalyst, this decomposition of carbon dioxide is required over a 1,000°C high temperature[40, 41]. Therefore, many researches are still investigated to reduce energy consumption for decomposition or increase decomposition efficiency.

The researches what can simultaneously achieve aforementioned both objectives are also existed. The carbon dioxide and hydrogen can be synthesized to methane and water. This methane synthesis reaction is well-known as Sabatier reaction. One of famous case of Sabatier reaction is carbon dioxide removal and water generation system of NASA which has tested from 2010[42, 43]. Of course, methane is also greenhouse gas but it can be used as gas fuel or converted into higher hydrocarbon. Generally, Sabatier reaction is conducted with the platinum-group metal catalyst such as ruthenium, rhodium, palladium, osmium, iridium, and platinum. In the background of this research, we can found out reason from the renewable energy. The growth of renewable energy is kept accelerated in today due to the growing concern regarding issues such as environment and rise of global oil price. The renewable energy generates electric power and its growth means available

electricity will be increased. However, it also causes oversupply of electricity and dissipation of energy when available electricity is too much. Power to Gas (P2G) is one of the idea what utilizing those surplus electricity and convert into storable form such as hydrogen or methane gas.

Since, Tohoku University and Hitachi Zosen demonstrates their prototype and pilot plant, challenges about test and commercial plant are actively conducted in many European countries and United States and Japan. Above all, Germany is leading country in Power-to-Gas researches and commercializations. The German automaker Audi had started project about industrial scale CO_2 methanation based Power-to-Gas facility in 2013, and 250kW class research plant is started in Stuttgart and many places around the same time. They also participate “STORE & GO Project” what 27 partner organizations and companies from all over Europe collaborated project to integrate Power-to-Gas technology into the future European energy system since 2015. The “STORE & GO Project” is focus on methanation technologies and will be implemented and tested by established private enterprises on three demonstration sites in Germany, Switzerland and Italy[44-46].

2. Research overview

2.1 Motivation of research

Many advantages of DBD plasma has been already reported from many researchers. They also expect that advantages are result of synergy effect between catalyst and DBD plasma. However, this synergy effect is not always occurred in some processes and enhancement mechanism of DBD plasma assisted catalytic technology is not clearly identified yet. Therefore, DBD plasma assisted process is still controversial what DBD plasma makes synergy effect on catalyst or not. Moreover, many studies used high discharge frequencies to generate DBD plasma. It means that dielectric heating effect is higher enough than their expected. Actually, dielectric heating effect of DBD plasma is not

a negative effect on catalyst because catalyst will be well activated and its performance will be increased by dielectric heating effect. However, if most of the contribution from DBD plasma is heating effect, role of DBD plasma is same as electric heater or other heating device, and it is not a synergy effect. Moreover, using the dielectric heating characteristic of DBD plasma for chemical process is quite inefficient because it is classified as non-equilibrium or non-thermal plasma not like a thermal plasma.

Except above dielectric heating issue, enhancement mechanism of DBD plasma assisted catalytic technology have been focused on catalytic performance. For example, people who have a skeptical response on DBD plasma assisted process contend dielectric heating related issue. On the contrary, people who have a favorable response contend DBD plasma can enhance catalytic performance of catalyst. Aforementioned dielectric heating issue is also focused on catalytic performance.

Therefore, we decide to study about synergy effect mechanism of the DBD plasma assisted catalytic technology and effects between DBD plasma and catalyst. The motivation for this research is to identify synergy effect of DBD plasma assisted process and its mechanism.

2.2 Objective of research

The aim of my research is investigation of DBD plasma assisted catalytic process in low-temperature and atmosphere pressure condition. The major reason of aimed temperature and pressure condition is related with energy consumption, endurance and environment. In higher temperature and pressure, catalytic performance can increased and it is a well-known scientific fact. However, higher temperature and pressure condition is required more energy to maintain the condition and is unfavorable to endurance on catalyst and reactor. For this reason, we have aimed operating condition of DBD plasma assisted catalytic process in near an atmosphere temperature and pressure condition, if possible.

The primary objective of my research is investigation about synergy effect mechanism of

the DBD plasma assisted catalytic process in low-temperature and atmosphere pressure. There have been studies what already investigated its synergy effect mechanism. However, most of the studies are focused on catalysis of catalyst and it is still not clearly identified yet. Therefore, we set the primary objective of my research as above.

The secondary objective is investigation about utilization of synergy effect mechanism in suitable process or application and verify its effectiveness. The reason for this is related with verification my theory to derived through conducting above primary objective. Moreover, investigation on drawback characteristic and its countermeasure is also included in this research.

2.3 Experimental method and application overview

The experiments for investigation on DBD plasma assisted catalytic process is performed with methanol and methane what is well-known compounds in C_1 chemistry. After methanol and methane experiments, target C_1 chemistry is change to carbon dioxide. The fundamental characteristic of DBD plasma assisted catalytic process is investigated with methanol. Based on this result, parameter study of DBD plasma assisted catalytic process is conducted with methane and modified asymmetric DBD plasma actuator and optical emission spectroscopy. Subsequently, investigation of application experiments are conducted with removal of deposit carbon in H_2 rich gas flow. Finally, DBD plasma assisted catalytic carbon dioxide to methane experiment is conducted to verify its applicability.

Basically, conversion experiments of methanol and methane and carbon dioxide into methane is conducted with quartz-glass tube reactor, and it can placed packed catalyst in middle of the area. Two electrodes are installed on this reactor to generate DBD plasma which has used alternating current input. This input is real-time monitored and analyzed by digital oscilloscope and V-Q Lissajous method. The input gas is always controlled by mass flow controller (MFC) and output gas is analyzed by gas chromatography.

The catalyst which is used for experiment has prepared by incipient wetness

impregnation method. This impregnation method is most famous catalyst preparation method because it is easy to control and maintain uniformity and loading of catalyst. If there is no particular reason, packed catalyst has always used fresh catalyst and only used single time at each experiments. More detailed information and changes of experiment and application is described in each subject chapter.

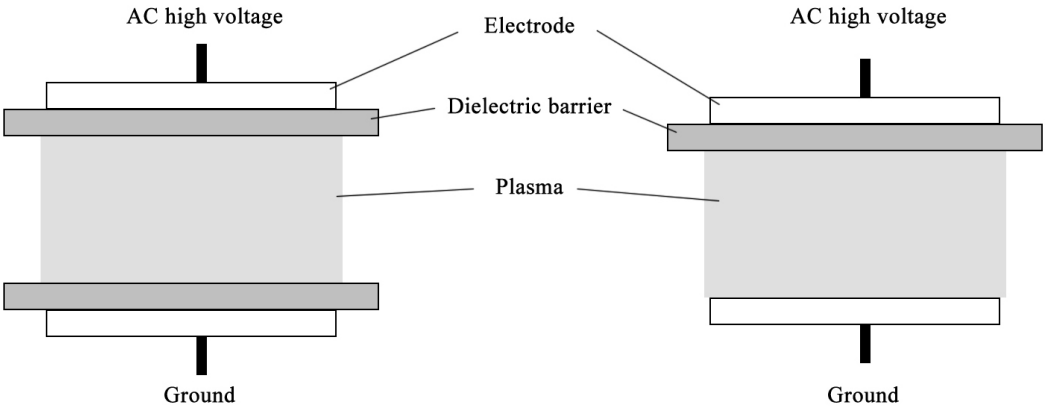

Figure 2. Typical configuration of dielectric barrier discharge

Figure 3. Ernst Werner von Siemens (1816-1892)

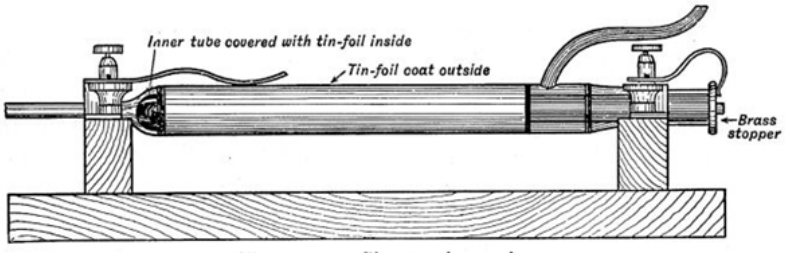

Figure 4. Ozone discharge tube of W. Siemens, 1857

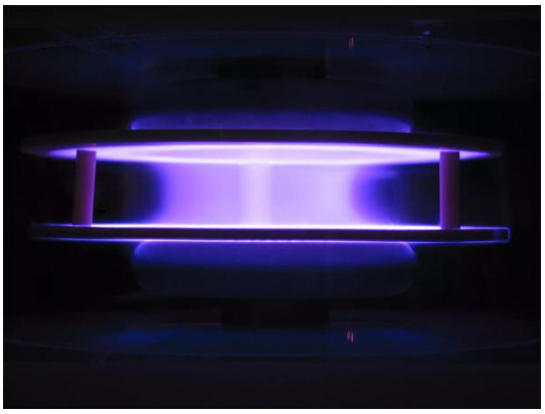

Figure 5. Plasma generation of dielectric barrier discharge

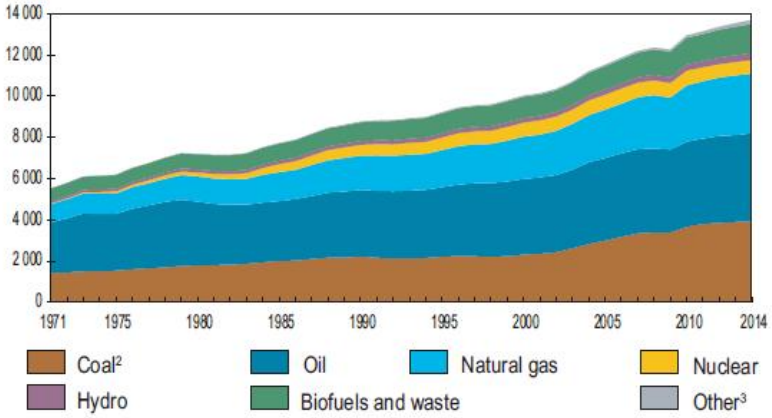

Figure 6. World total primary energy supply from 1971 to 2014 by fuel

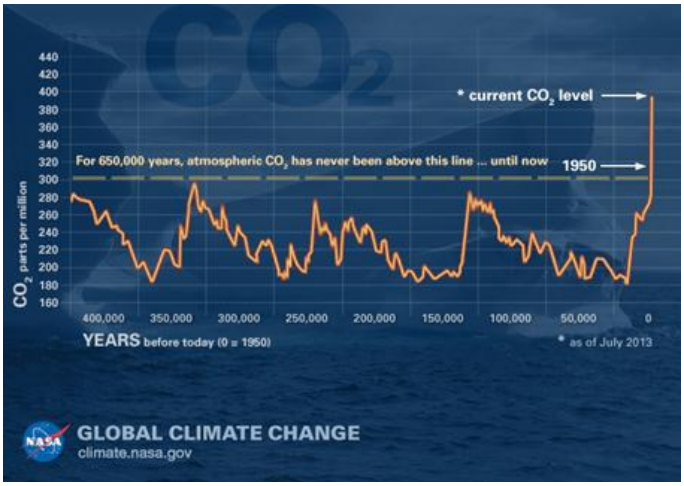

Figure 7. Levels of carbon dioxide in the atmosphere

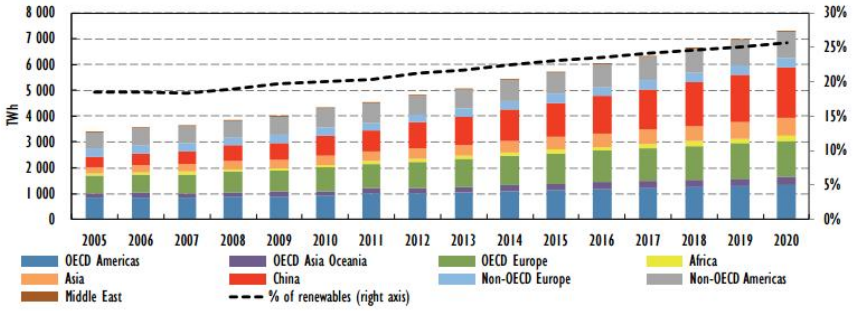

Figure 8. Global renewable electricity production by region, historical and projected

Figure 9. German automaker Audi's e-gas (Power-to-Gas) plant in Werlte, Germany

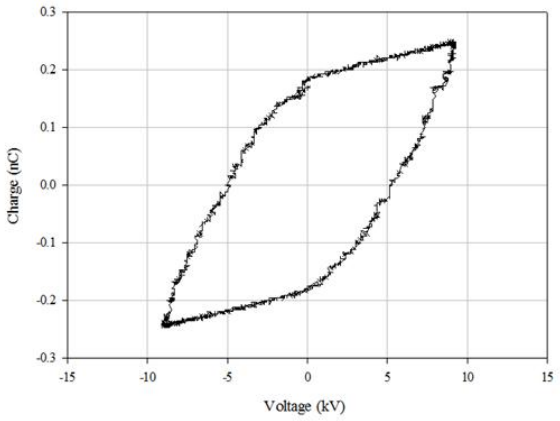

Figure 10. Typical example of V-Q Lissajous diagram for dielectric barrier discharge

II. Methanol Conversion

1. Overview of methanol

The methanol or methyl alcohol is the simplest alcohol and useful energy carrier in today. It consists of single carbon and oxygen atom and four hydrogen atoms (Chemical formula : CH_3OH). This methanol is important feedstock for many applications including fuels and petrochemical products. For example, foams, resins, plastics, paints, polyester and a variety of health and pharmaceutical products can produced by using methanol.

Moreover, methanol is also used to fuel on internal combustion engine or fuel-cells such as DMFC (Direct-methanol fuel cell) and RMFC (Reformed-methanol fuel cell). In case of internal combustion engine, pure methanol fuel (M100) is often used in car racing and small applications such as radio-controlled aircraft, and blended methanol fuel like a methanol/gasoline and methanol/diesel fuel is also studied to increase energy density.

In fuel cell applications, pure methanol is used to fuel of DMFC and RMFC. The hydrogen which is contained in methanol can released by decomposition or conversion process, and used to fuel of hydrogen fuel cells such as PEMFC (Proton exchange membrane fuel cell or polymer electrolyte membrane fuel cell). Methanol to fuel is also achieved by higher hydrocarbon upgrading process such as conversion and reforming process.

For above-mentioned reasons, methanol is very attractive alternative fuel source in today. Typically, it is easily converted with thermal conversion process or copper-based catalyst at low temperature condition. Therefore, we decided to study DBD plasma assisted process in methanol conversion reaction. In my research, methanol conversion was investigated to produce hydrogen and upgrade into higher hydrocarbon by using DBD plasma assisted process, and a matter of primary concern was focused on understanding principle characteristics of DBD plasma assisted process.

2. Experimental

2.1 Catalyst preparation

The catalyst on methanol experiment was used copper-based catalyst and was prepared by using incipient wetness impregnation method[47-49]. This copper-based catalyst was impregnated on gamma-phase alumina support. The alumina which has pellet-shaped and sphere-shaped was tested in initial stage of the methanol experiment but this paper was based and wrote experiments what had performed with sphere-shaped alumina only. The reasons of using sphere-shaped alumina instead of pellet-shaped alumina is related with repeatability and reliability because generation of DBD plasma was not uniformly and discharge power and streamer generation is very unstable in some cases which has use pellet-shaped alumina support. The unstable DBD plasma generation is also causes unstable conversion activity of methanol. It is also affected on conversion performance of methanol even without using catalyst. The pellet-shaped alumina was also caused spatial interference in internal space of the reactor. This interference is frequently causes surface or structural damage on catalyst in preparation phase and it also directly affected on conversion performance of methanol.

Besides, contents of the catalyst was also tested in initial stage of the methanol experiment. The pure copper or copper-zinc what is about various mix ratio is tested and finally 3:7 of copper-zinc mix ratio was chosen by reason of reliability. The none or low mix-ratio of zinc on copper-zinc catalyst was shown fast deactivation during the experiment. On the contrary, higher zinc mix ratio of copper-zinc catalyst was shown better reliability within experimental range. Therefore, only experiments which has conducted with sphere-shaped and 3:7 mix ratio of copper-zinc catalyst will be mentioned in this paper.

The preparation of precursor solution was used copper (II) nitrate trihydrate ($Cu(NO_3)_2 \cdot 3H_2O$, 77.0~80.0%, Samchun Pure Chemical) and zinc nitrate hexahydrate ($Zn(NO_3)_2 \cdot 3H_2O$, 98.0%, Samchun Pure Chemical), and molar ratio of copper-zinc mixture was

adjusted 3 and 7. The precursor mixture was dissolved in the water what is minimum quantity to dissolve, and then precursor solution was diluted 3 times by acetone (99.98%, Burdick & Jackson). γ-Al_2O_3 support was impregnated with a prepared precursor solution. After impregnation the support was dried at room condition overnight and calcined at 300°C for 1 hour. Finally, 27.11wt.% loading of Cu_3Zn_7/γ-Al_2O_3 catalyst was obtained.

2.2 Catalyst-DBD plasma hybrid reactor

The reactor for DBD plasma assisted catalytic process on methanol conversion reaction is considered to use catalyst and DBD plasma. Figure 14 shows the schematics of catalyst-DBD plasma hybrid reactor for methanol conversion. Quartz glass and SUS (Steel Use Stainless) material pipe fitting were used for catalyst-DBD plasma hybrid reactor. The quartz glass tube that has co-axial shaped and 12.9 × 10.8 × 400.0 mm (outer diameter x inner diameter x length) dimensions was used. The quartz glass tube is also played a role like a dielectric barrier for DBD plasma discharge. The quartz glass tube is also has a 2.1 mm wall thickness.

The SUS rod and aluminum film were installed on catalyst-DBD plasma hybrid reactor for DBD plasma discharge. SUS material rod which was used inner electrode has a 3.15 mm diameter and installed center of the reactor. Aluminum thin film has wrapped around outside wall of the reactor and it used to outer electrode. The overlapped length of both electrodes is 50.0 mm and DBD plasma has generated within this overlapped area.

The SUS material pipe fittings were connected on both end of quartz glass for methanol and carrier gas feeding and transfer product gas into the analysis device. Especially, supply tube of the methanol was connected into the inside of reactor and vaporized into gas phase at the end of the supply tube.

In initial stage, thermocouple was installed to measure catalyst temperature but electrical surge was occurred by thermocouple. This electrical surge was caused unstable generation of DBD plasma. It was also caused interruption and electrical damage into data acquisition

systems. Therefore, thermocouple was removed from the reactor and temperature was measured by using infrared thermometer.

2.3 Experimental apparatus

The experiments were conducted by using various experimental apparatus. The apparatus are consists of the reactor, gas/methanol supply, temperature control, plasma generation and gas analysis device. The gas and methanol supply device was used mass flow controller and programmable syringe pump (KDS-100). Mass flow controller (Bronkhorst EL-FLOW) was controlled and maintained nitrogen flow into the reactor, and programmable syringe pump was used to supply liquid-state methanol into the reactor. The supplied nitrogen and methanol was passed through the reactor which was vertically placed inside of digital programmable furnace.

The reactor is also connected with plasma generation device and function generator (Agilent 33220A) with high voltage amplifier (Trek Model 20/20C) was used to supply high voltage. This high voltage caused DBD plasma generation and was monitored by using digital storage oscilloscope (LeCroy WaveSurfer 424), high-voltage probe (Tektronix P6015A) and 1024 pF capacitors. It also used to measure dissipated power which has known as discharge power between the electrodes by V-Q Lissajous method.

The after passed catalyst-DBD plasma area, product gas is move to outlet of the reactor. Electric band heater was used to maintain temperature of the product above 120°C and prevent condensation of product at outlet which has exposed outside of the furnace. Therefore, the gas-phase product was move to the dehydration chamber and then it was move into the inlet of gas chromatography device (YL6100GC).

2.4 Experimental condition and parameters

Experimental condition was considered to clarify the DBD plasma effect on methanol

reforming. The reaction temperature and feed rate of methanol and carrier gas are greatly influenced to methanol reforming[50, 51]. Therefore, we performed fundamental experiments before fixing the experimental condition and parameters.

Synthesized $Cu_3Zn_7/\gamma\text{-}Al_2O_3$ catalyst (C_3Z_7A) showed 80% conversion of methanol when feed of methanol was 0.1 mL/min and N_2 carrier gas was 10.0 mL/min and reaction temperature is 220°C. Based on this result, experimental condition was fixed at 220°C and methanol feed is 0.1 mL/min and N_2 feed is 10.0 mL/min.

The experimental parameter like a catalyst and DBD plasma was considered. The parameters were defined to verify the interaction between catalyst and DBD plasma. Especially, effect of DBD plasma for methanol reforming can be verified by parameter for DBD plasma discharge. Also, performance improvement source can be clarified by parameter for catalysts. Experimental parameter was consists of catalyst, DBD plasma discharge and discharge location. The definition of conversion and selectivity is presented as below equation (1) to (6) and detailed parameter is presented in Table 1.

$$\text{Conversion of } CH_3OH\ (\%) = \frac{\text{Mass of converted product from } CH_3OH}{\text{Mass of introduced } CH_3OH} \times 100 \quad (1)$$

$$\text{Selectivity of } H_2\ (\%) = \frac{\text{Mole of produced } H_2}{2 \times \text{Moles of converted } CH_3OH} \times 100 \quad (2)$$

$$\text{Selectivity of CO}\ (\%) = \frac{\text{Mole of produced CO}}{\text{Moles of converted } CH_3OH} \times 100 \quad (3)$$

$$\text{Selectivity of } CO_2\ (\%) = \frac{\text{Mole of produced } CO_2}{\text{Moles of converted } CH_3OH} \times 100 \quad (4)$$

$$\text{Selectivity of } CH_4\ (\%) = \frac{\text{Mole of produced } CH_4}{\text{Moles of converted } CH_3OH} \times 100 \quad (5)$$

$$\text{Selectivity of } C_xH_y\ (\%) = \frac{\text{Mole of produced } C_xH_y}{x \times \text{Moles of converted } CH_3OH} \times 100 \quad (6)$$

3. Results and discussions

3.1 Methanol conversion and DBD plasma

Figure 17and Table 2 shows methanol conversion increment and discharge power for DBD plasma discharge. Basically, copper-zinc shows the best methanol conversion when DBD plasma discharge was not used. Also, methanol conversion of none of catalyst and γ-Al_2O_3 shows nearly zero conversion when DBD plasma was not used. However, methanol conversion of none of catalyst and γ-Al_2O_3 was increased by DBD plasma discharge. About 12.18% of conversion was increased by pure DBD plasma discharge. The γ-Al_2O_3 and Cu_3Zn_7/γ-Al_2O_3 catalyst shows 12.35% and 14.63% conversion increment, respectively. On the contrary, conversion increment was not detected when DBD plasma was not discharged on Cu_3Zn_7/γ-Al_2O_3 catalyst.

The DBD plasma discharged Cu_3Zn_7/γ-Al_2O_3 catalyst shows the best conversion and conversion increment for DBD plasma discharge. It shows extra higher conversion increment (2.45%) than summation of individually conversion between Cu_3Zn_7/γ-Al_2O_3 catalyst and DBD plasma. Even if it was simultaneous using, conversion was not increased by DBD plasma discharge when DBD plasma discharge area was not overlaid on Cu_3Zn_7/γ-Al_2O_3 catalyst.

In conversion increment result, the conversion increment was not detected when γ-Al_2O_3 used for catalyst. However, simultaneous use of γ-Al_2O_3 or Cu_3Zn_7/γ-Al_2O_3 catalyst with DBD plasma has a different discharge volume from individually use. Figure 18 is different DBD plasma volume for catalyst. None of catalyst condition can be used a full internal volume of reactor for DBD plasma discharge. Internal volume for DBD plasma discharge was decreased when reactor was filled with catalysts. Generally, void fraction of random packing sphere is 0.35 to 0.45 and nothing is 1.0[52, 53]. In other words, void fraction of reactor is 0.35 to 0.45 and 1.0 when it was not filled with any catalyst and filled with γ-Al_2O_3, respectively. Meaning of these two cases indicates different volume of internal gas

media for DBD plasma discharge.

The pure DBD plasma discharge and simultaneous use with γ-Al_2O_3 shows almost same power consumption and conversion increment for DBD plasma discharge. Consequentially, conversion increment per unit gas media volume was not same at both DBD plasma discharge condition. Furthermore, it was required overlay of DBD plasma discharge area and catalyst layer. Therefore, methanol conversion increment for DBD plasma discharge could be caused by interaction between catalyst and DBD plasma.

3.2 Selectivity in DBD plasma assisted condition

The efficiency or conversion for methanol conversion was only increased when DBD plasma discharge area was overlaid with catalyst. This conversion increment could be occurred from catalytic reaction or DBD plasma. Therefore, selectivity for DBD plasma discharge was compared to clarify the source of conversion increment. Table 3 describes selectivity comparison for DBD plasma discharge.

The increase of monoxide compound (CO) and hydrocarbon compounds (CH_4 and C_2H_6) were verified from pure DBD plasma discharge result. This can be assumed as result of DBD plasma effect for methanol reforming. On the contrary, H_2 and CO_2 were increased in typical methanol reforming process for catalyst. However, selectivity result of γ-Al_2O_3 and Cu_3Zn_7/γ-Al_2O_3 catalyst also showed similar tendency for DBD plasma discharge. This tendency of CO, CH_4 and C_2H_6 increment was also shown when DBD plasma discharge area was not overlaid with Cu_3Zn_7/γ-Al_2O_3 catalyst.

In general, high-voltage or high-powered plasma discharge causes dielectric heating[54, 55]. Even, DBD plasma what we called ‘non-thermal plasma’ also generate the dielectric heating. It also affected conversion increment because the catalytic activity can be increased by dielectric heating. This dielectric heating was shown maximum increment at room temperature (about +30°C) as Figure 19. On the contrary, it can negligible for experimental condition for 220°C.

Even dramatic increment of H_2 and CO_2 was not detected on Cu_3Zn_7/γ-Al_2O_3 catalyst when it used with DBD plasma discharge simultaneously or non-overlaid with Cu_3Zn_7/γ-Al_2O_3. Therefore, we expect that DBD plasma may affected by catalyst, and also affected on methanol conversion.

3.3 V-Q Lissajous method and discharge power

The tendency of interaction between catalyst and DBD plasma was also detected in V-Q Lissajous diagrams. Figure 20 shows consecutive 5 cycles of V-Q Lissajous diagram with comparison for catalyst. Tendency of V-Q Lissajous diagram can be classified as Figure 5 (a), (d) and (b), (c). Sharp-parallelogram shaped V-Q Lissajous diagram (a and d) was shown when DBD plasma discharge area was not overlaid with catalyst. On the contrary, diagonally sharp-elliptical shaped V-Q Lissajous diagram (b and c) was shown when DBD plasma discharge area was overlaid with Cu_3Zn_7/γ-Al_2O_3 catalyst or γ-Al_2O_3 support.

Basically, inter-electrode material can be affected on DBD plasma discharge because it has an electrical property like a resistance, dielectric constant, or etc[56-60]. This characteristic can be found in V-Q Lissajous results. In comparison with Figure 20 (a), (d) and (b), (c), state of electric charge was different for phase change of alternate current. It also indicates that DBD plasma discharge was not same for different catalyst condition.

V-Q Lissajous diagram also indicate power consumption for DBD plasma discharge. The power comparison of DBD plasma discharge is already presented in Table 2. The power consumption of DBD plasma discharge was changed by catalyst and discharge condition. Methanol conversion was not proportional to power consumption for DBD plasma discharge.

3.4 Carbon deposition on catalyst

SEM/EDS (Scanning Electron Microscopy/ Energy Dispersive X-ray Spectroscopy) result

about surface carbon deposition of Cu_3Zn_7/γ-Al_2O_3 catalyst is shown in Figure 21 and Table 4. After methanol reforming was performed, conifer needle shaped carbon nano-rod bundle was detected on SEM images.

The two types of carbon nano-rod bundle was detected on (b), (c), (d). The growth of carbon nanorod bundle was bigger and larger when DBD plasma discharge was not overlaid or occurred with catalyst. On the contrary, carbon nanorod bundle was smaller and dispersed when DBD plasma discharge area was overlaid on catalyst. The content of surface carbon was not significantly different from relative location between DBD plasma discharge and catalyst.

4. Conclusion of methanol conversion

The conversion of methanol was increased by DBD plasma discharge and DBD plasma-assisted catalyst process. Conversion increment or efficiency increment was only occurred when catalyst and DBD plasma was used simultaneously. The evidence of catalytic improvement like a dielectric heating or dramatic increment of H2 and CO2 selectivity was not detected on Cu_3-Zn_7/γ-Al_2O_3 catalyst when it used with DBD plasma discharge simultaneously or non-overlaid with Cu_3-Zn_7/γ-Al_2O_3. At the same time, selectivity of CO and hydrocarbon which compound was increased by DBD plasma discharge. Moreover, tendency of V-Q Lissajous diagram and surface carbon nanorod deposition pattern was changed by relative location between DBD plasma discharge and catalyst.

Table 1. Experimental parameters of methanol experiment

No	Catalyst	DBD plasma discharge	DBD plasma overlaid with catalyst
(1)	N/A (Blank)	N/A	N/A
		1 kHz, 7 kV, DBD	O
(2)	γ-Al_2O_3	N/A	N/A
		1 kHz, 7 kV, DBD	O
(3)	C_3Z_7A	N/A	N/A
		1 kHz, 7 kV, DBD (a)	O
		1 kHz, 7 kV, DBD (b)	X

Table 2. Conversion increment for DBD plasma assisted condition and discharge power (DBD : 1 kHz, 7 kV)

Catalyst	Methanol Conversion (%)			Discharge Power (W)
	Plasma Off (1)	Plasma On (2)	Increment (2)-(1)	
None	0.65	12.83	+12.18	1.93
γ-Al_2O_3	0.81	13.16	+12.35	1.94
C_3Z_7A(a)	81.32	95.95	+14.63	1.71
C_3Z_7A(b)	77.34	77.85	+0.51	1.70

Table 3. Selectivity comparison for catalytic conversion and DBD plasma assisted conversion of methanol (DBD : 1 kHz, 7 kV)

	None		γ-Al_2O_3		C_3Z_7A(a)		C_3Z_7A(b)	
	DBD off	DBD on	DBD off	DBD on	DBD off	DBD on	DBD off	DBD on
H_2	0.00	39.87	47.68	31.20	43.14	42.07	41.30	43.75
CH_4	0.00	14.59	0.56	24.67	0.29	1.84	0.34	2.76
CO	3.93	59.93	4.70	43.46	51.27	54.98	50.29	50.52
CO_2	38.82	1.30	35.45	2.73	13.43	11.04	14.34	12.28
C_2H_6	0.00	1.48	0.00	2.63	0.00	0.03	0.01	0.14

Table 4. EDS analysis result of Cu_3Zn_7/γ-Al_2O_3 catalyst for each different conditions. (a) fresh catalyst, (b) after using catalytic conversion, (c) after using DBD plasma-assisted conversion, (d) after individual using of DBD plasma and catalyst

Conditions	Al (Wt.%)	O (Wt.%)	Cu (Wt.%)	Zn (Wt.%)	C (Wt.%)
(a)	21.08	47.62	11.82	11.98	7.50
(b)	20.45	47.02	9.53	9.71	13.29
(c)	18.92	43.79	12.00	12.48	12.81
(d)	25.88	48.13	5.72	9.14	11.13

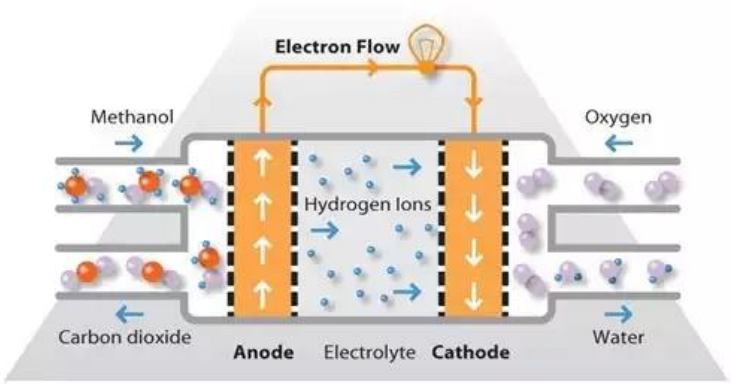

Figure 11. Operating principle of the direct methanol fuel cell

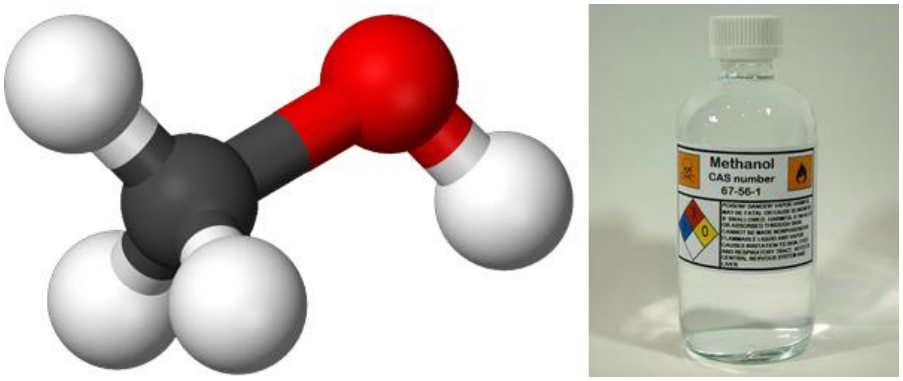

Figure 12. 3D structure of methanol molecule and state in atmospheric condition

Figure 13. Shape comparison of gamma-alumina sphere and pellet

Figure 14. $Cu_3Zn_7/\gamma\text{-}Al_2O_3$ catalyst after finished impregnation

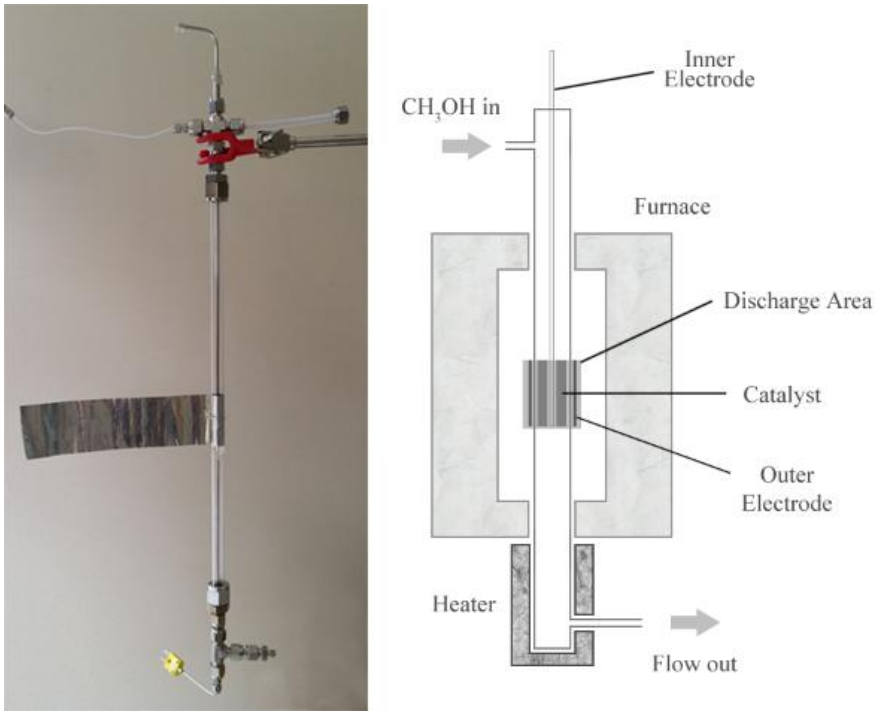

Figure 15. schematics of catalyst-DBD plasma hybrid reactor for methanol experiment

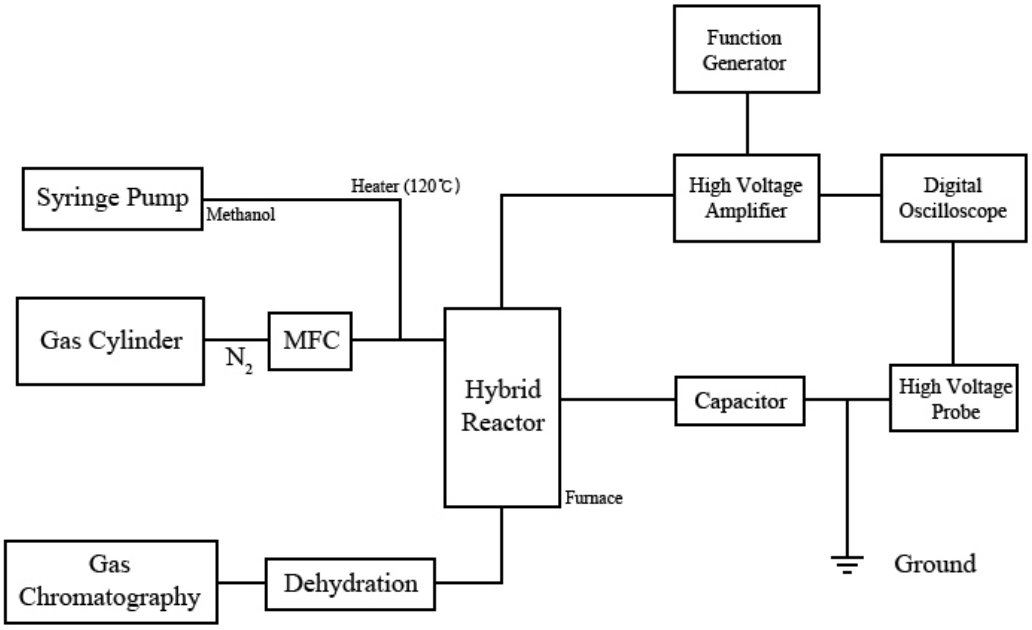

Figure 16. Schematics of experimental apparatus for methanol experiment

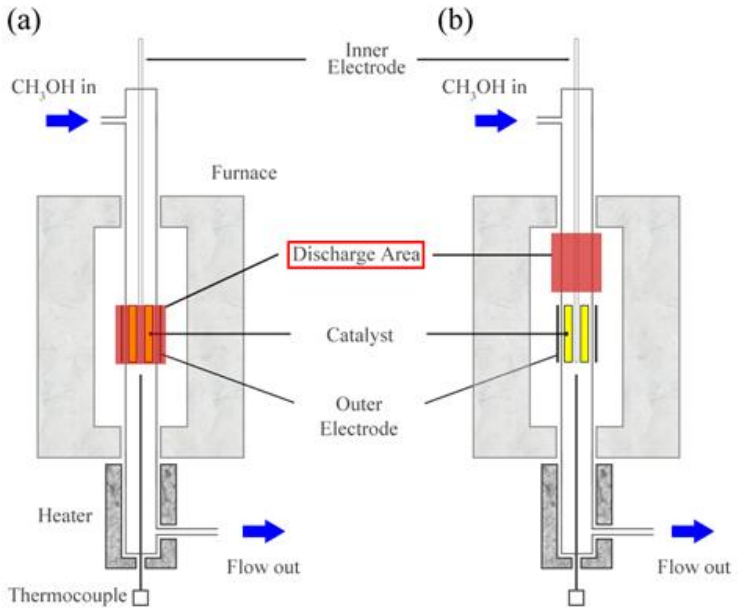

Figure 17. Relative position of DBD plasma and catalyst in methanol experiment : (a) DBD plasma discharged over catalyst, (b) DBD plasma discharged in front of catalyst

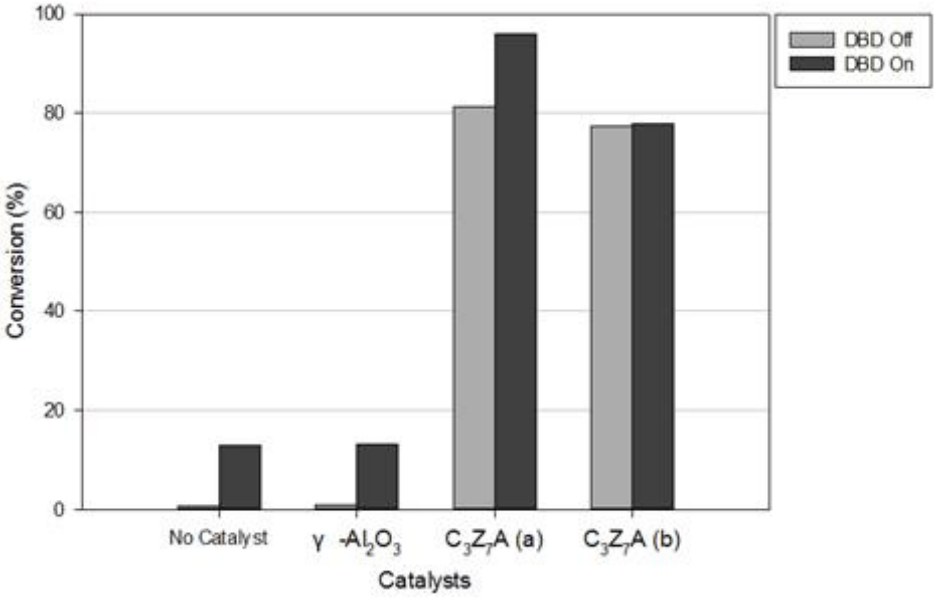

Figure 18. Catalytic and DBD plasma assisted methanol conversion at 220°C

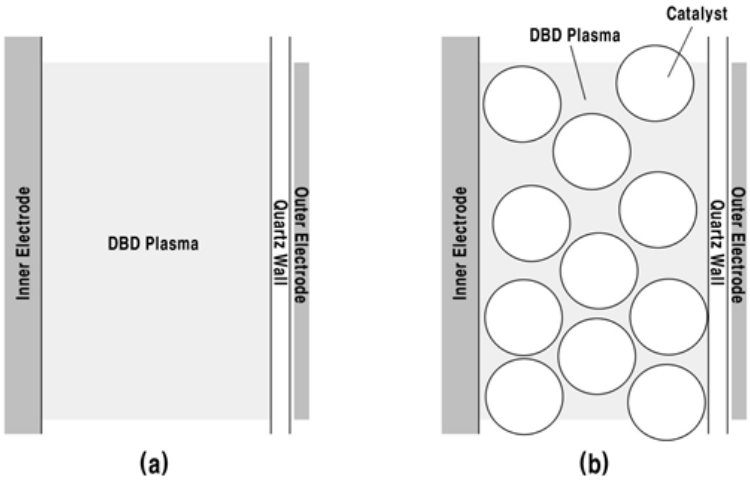

Figure 19. Different volume of generated DBD plasma for (a) empty space, (b) packed catalyst in the reactor

Figure 20. Dielectric heating over copper-zinc catalyst at room temperature

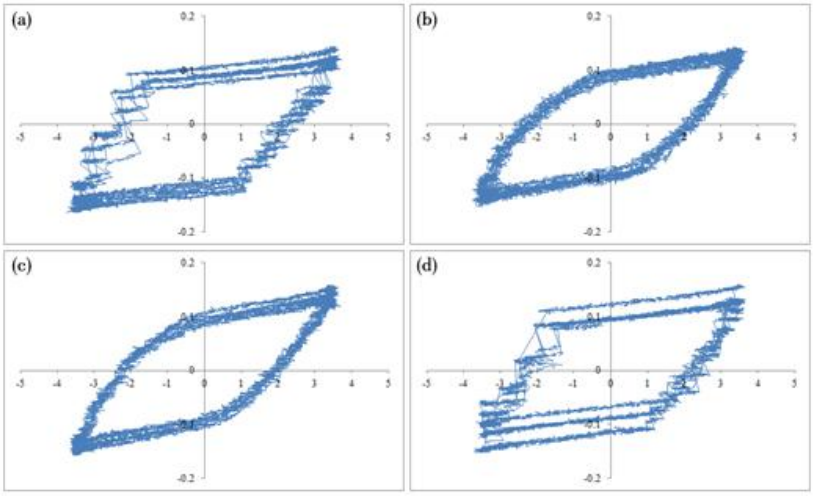

Figure 21. V-Q diagrams of DBD plasma generation for (a) empty reactor, (b) γ-Al_2O_3 support, (c) Cu_3Zn_7/γ-Al_2O_3 catalyst, (d) forward area of Cu_3Zn_7/γ-Al_2O_3 catalyst

III. Methane Conversion

1. Overview of Methane

The methane is main component of natural gas and maintain gas state at room temperature. It is consists of one carbon atom and four hydrogen atoms, and can express CH_4 in chemical formula.

Major use of methane is combustion fuel and feedstock for syngas production or upgrading[61]. The methane is also contained four hydrogen atoms for single molecule as methanol but this hydrogen atoms are hard to separate directly. Therefore, oxygen contained compounds such as carbon dioxide or steam is usually used to separate hydrogen from the methane. For example, steam reforming of methane is produced carbon monoxide and hydrogen, and dry reforming is produced carbon monoxide and hydrogen.

$$CH_4 + H_2O \rightarrow CO + 3H_2 \quad (7)$$

$$CO_2 + CH_4 \rightarrow 2H_2 + 2CO \quad (8)$$

This conventional catalytic conversion is generally conducted at high temperature such as over 800ºC with nickel-based catalyst[62-64]. In high temperature condition such as over 800ºC, catalyst is encountered critical issues on its endurance what related with sintering, oxidation, carbon deposition and deactivation[65]. Therefore, many studies for decrease reaction temperature has been studied and many new catalysts and processes are developed in today. Non-thermal plasma or its assisted catalytic process is also studied to decrease reaction temperature because the ionized or excited atoms and molecules, and radicals can generated by plasma[66-70].

The plasma which has studied for methane conversion process can classified two types such as thermal plasma and non-thermal plasma. The thermal plasma has usually used alone or pre/post-treatment and has shown good performance in various processes because it

can extremely high temperature (over 1,000ºC) in a short time. On the contrary, heat generation and power consumption of non-thermal plasma is much lower than thermal plasma. For these reasons, non-thermal plasma is easy to apply on previous process. Therefore, non-thermal plasma such as dielectric barrier discharge (DBD) plasma has been studied for low-temperature methane conversion process.

2. Experimental

2.1 Catalyst Preparation

The methane experiment was conducted with copper-zinc oxide based catalyst. It is one of the famous catalyst in chemical industry and often used for low temperature shift reaction. However, nickel based catalyst had used to methane conversion process with high temperature. This means copper-zinc catalyst is not suitable catalyst in this process. There are several reasons to use copper-zinc catalyst in this study. First of all, this study is focused on plasma-assisted process at low-temperature like a below 300ºC because we want to investigate and utilize non-thermal plasma interaction with catalyst. Moreover, the catalyst will be exposed on electrical discharge for DBD plasma generation, and we had expected that surface material of catalyst makes interaction to DBD plasma. For this reason, loading of catalyst was aimed higher loading as possible in this experiment. Also, we already confirmed negative effect of impregnated nickel catalyst on DBD plasma generation in preceding study and copper or copper-zinc material has a better electrical conductivity than nickel. Therefore, we used copper-zinc oxide based catalyst and mixed 10% promoter materials on copper-zinc oxide catalyst to investigate its effect and interaction on plasma assisted condition.

The 10% promoter mixed copper-zinc catalysts were prepared to verify the effect of catalyst materials for interaction. The 6 different materials like a cobalt (Co), iron (Fe), magnesium (Mg), manganese (Mn), nickel (Ni), titanium (Ti) was selected for promoter

materials because it has easy to obtain and cheaper than novel metal like a platinum (Pt). Especially, nickel was selected to investigate interaction between catalytic activity and DBD plasma. Mole ratio of copper-zinc-promoter material was controlled by 3 : 6 : 1.

Promoter mixed copper-zinc catalysts were prepared by incipient wetness impregnation method. The copper, zinc and promoter material was dissolved in minimum required water and diluted with acetone solution. These prepared precursor solutions were poured on sphere shaped γ-Al_2O_3 support which has 1.1 mm diameter. It was dried on room temperature for 48 hours and then calcined at 300℃ for 1 hour. More detailed information of these catalysts is summarized in Table 5.

2.2 Non-catalytic materials

The non-catalytic material and its interaction with DBD plasma was also investigated to identify source of synergy effect. Most of previous studies about DBD plasma assisted process are used catalyst, and they discussed on catalytic activity enhancement. The inverse case like a conversion increase from plasma activity enhancement by catalyst or material is not considered. However, we confirmed this inverse case related performance increase in methanol experiment. The DBD plasma assisted γ-Al_2O_3 was shown better methanol conversion than pure DBD plasma discharge. Therefore, non-catalytic material verification experiment was planned in methane experiment.

The spherical shaped glass bead and γ-Al_2O_3 was used for experiment. The glass bead has a 3 mm diameter and γ-Al_2O_3 has a 2.5 mm and 3.15 mm diameter. This glass bead and γ-Al_2O_3 was prepared to verify the interaction between DBD plasma and non-catalytic material. The glass bead and γ-Al_2O_3 has no catalytic activity for methane conversion. Therefore, it is suitable to verify aforementioned inverse case related performance increase and part of the mechanism on DBD plasma assisted catalyst process. Moreover, γ-Al_2O_3 was also used as support material for aforementioned promoter mixed copper-zinc catalyst and has occupied over a half of mass contents of catalyst. This means that DBD plasma

interaction can be affected by γ-Al_2O_3 support. This is the another reason to investigate effect of γ-Al_2O_3 on DBD plasma discharge even it is a non-catalytic material on methane conversion.

2.3 Catalyst-DBD plasma hybrid reactor

In methane experiment, we used catalyst-DBD plasma hybrid reactor again but there are minor changes of configuration to used on methane experiment. For example, outer electrode was changed from thin aluminum film to helical iron wire. Also, injection tube line for methanol was removed from the reactor. The inlet and outlet components of reactor was simplified because methane experiment is gas-phase reaction.

The dimension of quartz glass tube and internal electrode is same as previous methanol experiment. This quartz glass has a 402 mm × 13 mm × 10.9 mm (length × outer diameter × inner diameter) dimensions and diameter of internal electrode is 3.15 mm. Simplified stainless steel tube components were connected on both ends of quartz glass tube which was used for gas inlet and outlet. The reactor was also installed inside of programmable furnace and vertically for ground.

The plasma was generated between overlapped area of electrodes. These electrodes were consists of stainless steel rod and helical-shaped steel wire. The stainless steel rod was installed inside of reactor and was overlapped with center axis of reactor. The steel wire was installed outside wall of reactor. It had a 30 mm length overlapping area between anode and cathode for DBD plasma generation. Same as methanol experiment, catalyst was always filled in this 30 mm length overlapping area. Figure 25 shows picture and schematic of catalyst-DBD plasma hybrid reactor.

2.4 Experimental setup

Experimental apparatus were consists of reactor, plasma generation device, gas supply

and analysis device. Syringe pump and electric band heater what was used in methanol experiment was excluded in methane experiment, and gas supply device was changed. Figure 26 shows overall setup of experimental apparatus. The high-voltage was applied for DBD plasma generation and was supplied by function generator (Agilent 33220A) and high voltage amplifier (Trek Model 20/20C). The electrical discharge characteristics like a discharge voltage and gap capacitance between electrodes were measured and analyzed by 1024pF capacitor, high-voltage probe (Tektronix P6015A), digital oscilloscope (LeCroy WaveSurfer 424). Discharge power of DBD plasma generation was calculated by V-Q Lissajous method.

Mass flow controller (MKP TSC-210) and control unit (Sehwa KRO-4001) was used to control and maintain the gas supply rate of input gases. Basically, every experiment used nitrogen (N2, 99.999%) and methane (CH4, 99.999%). The nitrogen gas was used as carrier gas and DBD plasma discharge media. The methane gas was used for reforming gas. After input gases were passed through the reactor, output gases were passed through dehydration chamber before it moved into gas chromatography device (YL6100GC).

2.5 Experimental parameters

Table 6 shows two different experimental conditions and parameters. The experiments were planned for interaction verification and comparison of DBD plasma. Therefore, major experimental parameter was focused on material which was placed between inter-electrodes. These inter-electrodes material was consisted of non-catalytic material and catalytic material. In experiment (A), non-catalytic materials like a glass bead and γ-Al_2O_3 was selected to verify the correlation and requirement of catalytic synergistic effect from DBD plasma. On the contrary, promoter mixed copper-zinc catalysts were selected for experiment (B) which was compared synergistic efficiency between metal oxide catalysts and DBD plasma.

Except aforementioned inter-electrode material like a catalyst, experimental condition like a surrounding temperature of reactor, electrical input for DBD plasma discharge, flow rate

of nitrogen and methane was set up differently for an experiment (A) and (B). Supply rate of N_2 and CH_4 gases was controlled 50 mL/min (N_2) and 25 mL/min (CH_4) for an experiment (A). At the same time, 1 kHz and 7 kV sinusoidal alternating current electrical input was supplied for DBD plasma discharge. In experiment (B), supply rate of N_2 and CH_4 gases was changed for 45 mL/min (N_2) and 5 mL/min (CH_4). Electrical input was also changed for 1 kHz and 8 kV for DBD plasma discharge.

Every experiment was used same amount of catalyst which was matched with DBD plasma discharge volume. The DBD plasma was always discharged on catalyst location when DBD plasma was used. Before an experiment, hydrogen treatment was performed for removal of residual oxygen in reactor and reduction of catalyst. It was performed at 250℃ for 2 hours. The environment temperature of hybrid reactor was always maintained 250℃.

2.6 Conversion, selectivity and discharge power

Methane conversion, selectivity of hydrogen and C_2 and C_3 hydrocarbon product was analyzed from measured value. The methane conversion was calculated by mass ratio between introduced methane and converted product from methane which was detected on gas chromatography device. Selectivity of hydrogen and hydrocarbons like a C_2 and C_3 products were also measured and calculated. It is defined as below equation (9) - (13).

$$\text{Conversion of } CH_4\ (\%) = \frac{\text{Mass of converted product from } CH_4}{\text{Mass of introduced } CH_4} \times 100 \quad (9)$$

$$\text{Selectivity of } H_2\ (\%) = \frac{\text{Mole of produced } H_2}{2 \times \text{Moles of converted } CH_4} \times 100 \quad (10)$$

$$\text{Selectivity of CO}\ (\%) = \frac{\text{Mole of produced CO}}{\text{Moles of converted } CH_4} \times 100 \quad (11)$$

$$\text{Selectivity of } CO_2\ (\%) = \frac{\text{Mole of produced CO}}{\text{Moles of converted } CH_4} \times 100 \quad (12)$$

$$\text{Selectivity of } C_xH_y\ (\%) = \frac{\text{Mole of produced } C_xH_y}{x \times \text{Moles of converted } CH_4} \times 100 \quad (13)$$

The discharge power of DBD plasma was also measured to clearly identify DBD plasma phenomenon. It can be calculated by using V-Q Lissajous method like as equation (14).

$$W = 4 f C_d V_0 \left\{ V_m - \left(\frac{C_a - C_d}{C_d} \right) \right\} \quad (14)$$

In this equation, f is frequency of input electricity, C_a and C_d is air gap and dielectric capacitance, V_0 and V_m is the breakdown voltage, and maximum voltage. Discharge power is also calculated by measuring the enclosed area of V-Q Lissajous diagram[3].

3. Results and discussions

3.1 Catalytic conversion of CH_4

General catalytic methane reforming or decomposition process is performed over 700 ~ 1,000ºC with Ni catalyst. Below 500ºC temperature, it is hard to expect good methane conversion. The result of experiment (A) and (B) was also has a poor catalytic methane conversion. The experiment was performed at 250ºC and it was not used DBD plasma discharged. In other words, the result is indicates performance of catalytic methane conversion.

Figure 27 is an example of catalytic conversion of CH_4 which was performed with empty reactor, glass bead and γ-Al_2O_3. In 250ºC condition, catalytic conversion was shown nearly zero conversion. Promoter mixed copper-zinc catalyst result was also shown similar result and it is shown in Figure 28.

Every result has a nearly zero methane conversion when DBD plasma was not discharged at 250ºC. Especially, nickel mixed copper-zinc catalyst ($Cu_3Zn_6Ni_1$) was also has a nearly zero conversion. There are no significant differences of methane conversion

between non-catalytic material and promoter mixed copper-zinc catalyst. It also means that catalytic methane conversion was not occurred within experimental range and negligible.

3.2 Plasma-assisted conversion of non-catalytic material

The methane conversion was increased for DBD plasma discharge even it was worked with non-catalytic material like a glass bead and γ-Al_2O_3. Figure 29 shows methane conversion for empty reactor, glass bead and γ-Al_2O_3. Before DBD plasma discharge, the methane conversion was zero. On the contrary, it was increased to 1.35% when DBD plasma was discharged on empty reactor. The conversion increment was also confirmed on glass bead and γ-Al_2O_3 when DBD plasma was discharged. The methane conversion was increased to 1.79% and 1.44% for glass bead and γ-Al_2O_3, respectively.

Comparison with empty reactor and non-catalytic material, effect of DBD plasma was increased by non-catalytic material. Especially, it was hard to expect from enhancement of catalytic activity because glass bead and γ-Al_2O_3 does not have any catalytic activity for methane. The evidence of interaction was also detected in discharge power result. It was also has a different discharge power for material which was placed in discharge gap. Specific energy density (SED) and its CH_4 conversion efficiency comparison were shown in Figure 30. The glass bead has the best conversion and higher discharge power for DBD plasma discharge. However, discharge power was not always match with conversion result like a γ-Al_2O_3 result. The empty reactor has a higher conversion increment for DBD plasma, whereas γ-Al_2O_3 was used more discharge power than empty reactor. Furthermore, different diameter was not affected on conversion and discharge power for γ-Al_2O_3 result. Only material was played role like a variable parameter for DBD plasma discharge. Therefore, we expect that different result was occurred from interaction between DBD plasma and non-catalytic material.

3.3 Promoter and DBD plasma-assisted conversion

The interaction between DBD plasma and material which was placed between inter-electrodes was also verified from promoter mixed copper-zinc catalyst result. Aforementioned, promoter mixed copper-zinc catalyst has no catalytic methane conversion without DBD plasma discharge for experimental temperature. However, methane conversion of promoter mixed copper-zinc catalyst was increased when DBD plasma was discharged on catalyst layer. Figure 31 shows methane conversion increment for DBD plasma discharge.

The different interaction for DBD plasma was also confirmed on experimental result. The pure DBD plasma has a 6.987% conversion increment under same experimental condition. Simultaneously work of DBD plasma and γ-Al_2O_3 or other promoter mixed copper-zinc catalysts was shown higher conversion result. Even γ-Al_2O_3 has a 4.5% higher conversion increment than pure DBD plasma discharge result. Magnesium and manganese mixed copper-zinc catalyst ($Cu_3Zn_6Mg_1$, $Cu_3Zn_6Mn_1$) has the best conversion increment for DBD plasma discharge. The conversion was increased 33.607% for magnesium mixed copper-zinc catalyst ($Cu_3Zn_6Mg_1$) and manganese was 44.940%. On the contrary, the worst result within promoter mixed copper-zinc catalyst was confirmed on $Cu_3Zn_6Ni_1$ for DBD plasma discharge.

These results may be caused from enhancement of catalytic activity or pure DBD plasma effect. For example, catalytic activity can be enhanced by dielectric heating or radical generation of DBD plasma. However, nickel has the worst conversion increment within experimental cases. This means that conversion increment was not caused from catalytic enhancement and dielectric heating of DBD plasma was not increased gas temperature over 500ºC because nickel used as catalyst for general catalytic methane reforming process.

The conversion increment also can be affected by catalyst loading. For example, catalyst loading can be increased catalytic activity at same condition. Therefore, we considered

effect of catalyst loading for conversion increment. In terms of the catalyst loading, $Cu_3Zn_6Mg_1$, $Cu_3Zn_6Ni_1$ and Cu_3Zn_6, $Cu_3Zn_6Fe_1$, $Cu_3Zn_6Ti_1$ has a similar loading, respectively. The former catalyst has a 33.310%, 9.626% conversion increment, while the latter has a 12.131%, 17.580%, 14.952%. Relation between catalyst loading and conversion increment was not identified in most of the experiment result. Even $Cu_3Zn_6Mg_1$, $Cu_3Zn_6Ni_1$ and Cu_3Zn_6, $Cu_3Zn_6Fe_1$, $Cu_3Zn_6Ti_1$ have a similar loading, different conversion increment was confirmed on result.

3.4 Discharge power and efficiency

The methane conversion was increased by DBD plasma discharge. The conversion was differently increased over every result. Each experiment was differently consumed electrical power for DBD plasma discharge whereas electrical input was same as 1 kHz, 8 kV and sine waveforms. The conversion increment and discharge power is compared in Table 7. The $Cu_3Zn_6Co_1$ catalyst has used minimum discharge power and $Cu_3Zn_6Ti_1$ catalyst has used maximum discharge power within experimental range. It is inconsistent with those of previous conversion result. Compare to similar discharge power results, discharge power of γ-Al_2O_3, $Cu_3Zn_6Mg_1$, $Cu_3Zn_6Mn_1$ and $Cu_3Zn_6Ni_1$ was shown similar result, whereas conversion increment of methane is not. The correlation between conversion increment and discharge power of DBD plasma is summarized in Figure 32. The result shows relation with methane conversion increment for unit discharge power. Comparison with similar discharge power as pure DBD plasma and pure copper-zinc catalyst, $Cu_3Zn_6Mn_1$ has 4~6 times higher methane conversion for same discharge power. Most of the sample has a higher methane conversion than pure DBD plasma when it was worked with DBD plasma discharge.

Both experiments have a different inter-electrode gap condition like a Figure 33. The glass bead, γ-Al_2O_3 and promoter mixed copper-zinc catalyst has a lesser free-internal volume for gas media. It means that discharge volume of DBD plasma also has decreased.

If strength or effectiveness of DBD plasma was not changed for unit volume, discharge power and methane conversion will be varied in direct proportion to discharge volume. However, glass bead, γ-Al_2O_3 and promoter mixed copper-zinc catalyst have a higher conversion with DBD plasma discharge. At the same time, methane conversion and discharge power have not risen proportionately. Each promoter mixed copper-zinc catalyst has a different discharge power and methane conversion increment. It is indicates that strength or effectiveness of DBD plasma can be changed by inter-electrode material like a 10% promoter materials which were mixed on copper-zinc catalyst.

3.5 Hydrocarbon and H_2 selectivity

The methane can be converted C_2 and C_3 hydrocarbon. It is required high temperature in common catalytic process or pyrolysis. On the contrary, plasma discharge can achieve hydrocarbon conversion at atmosphere condition or low temperature. It also confirmed from our experiment result. We compared C_2H_2, C_2H_4, C_2H_6 and C_3H_8 selectivity for DBD plasma discharge. Before DBD plasma applied, C_2 and C_3 hydrocarbon was not detected at experimental condition. Hydrocarbon product was only detected in DBD plasma discharged condition. The comparison about hydrocarbon selectivity under different catalyst is summarized in Table 8. Difference of hydrocarbon selectivity among the catalyst was not confirmed for DBD plasma discharge. The same hydrocarbon product has a similar selectivity for catalyst and DBD plasma discharge. On the contrary, different hydrocarbon product has a different selectivity. The C_2H_6 has the highest selectivity then C_3H_8 is second highest result. C_2H_2 and C_2H_4 have shown similar and least selectivity.

The methane can be directly converted to C_2 or C_3 hydrocarbon. The overall reaction is described below Equation (15) to (18):

$$2CH_4 \rightarrow C_2H_2 + 3H_2 \qquad \Delta H = 377.18 \text{ kJ/mol} \qquad (15)$$

$$2CH_4 \rightarrow C_2H_4 + 2H_2 \qquad \Delta H = 202.21 \text{ kJ/mol} \qquad (16)$$

$$2CH_4 \rightarrow C_2H_6 + H_2 \qquad \Delta H = 65.85 \text{ kJ/mol} \qquad (17)$$

$$3CH_4 \rightarrow C_3H_8 + 2H_2 \qquad \Delta H = 82.225 \text{ kJ/mol} \qquad (18)$$

The reaction is endothermic reaction, and enthalpy change is related with hydrocarbon selectivity. It also indicates that lower ΔH required hydrocarbon like a C_2H_6 and C_3H_8 can be easily converted from methane at same temperature condition. The experimental result about hydrocarbon selectivity has some correlation for those theoretical ΔH requirements. Inverse proportion between ΔH and hydrocarbon selectivity was confirmed. The lower ΔH required hydrocarbon product has a shown selectivity.

On the contrary, hydrogen selectivity under DBD plasma discharge was significantly increased and varied for different catalyst condition. It has a similar tendency for methane conversion result. The hydrogen selectivity was maximized by using $Cu_3Zn_6Mg_1$, $Cu_3Zn_6Mn_1$ catalyst with DBD plasma. Correlation between hydrogen selectivity and methane conversion was corresponded within experimental range. Figure 34 shows the selectivity increment of hydrogen for DBD plasma discharge. The $Cu_3Zn_6Mg_1$, $Cu_3Zn_6Mn_1$ has also shown higher hydrogen selectivity with DBD plasma discharge. Especially, hydrogen selectivity of $Cu_3Zn_6Mn_1$ was increased from 5.921 to 73.971% with DBD plasma discharge. The selectivity increment of hydrogen was also confirmed on other experimental result. It indicates that methane cracking activity was increased by DBD plasma discharge.

The environmental temperature of reactor was always maintained by electrical furnace during experiment. At the same time, lower input electrical frequency and voltage was applied to decrease the dielectric heating effect. We also measured dielectric heating temperature by using infra-red thermometer. The measurement result was indicated about 300ºC. The temperature of catalyst layer was increased about 50ºC and was similar for every promoter mixed copper-zinc catalyst.

We expect that it was occurred from catalyst-assisted DBD plasma. Aforementioned our experimental results, methane conversion and discharge efficiency of DBD plasma was increased by interaction with promoter material mixed copper-zinc catalyst. It was also

influenced to methane cracking activity of DBD plasma. Methane was decomposed to carbon and hydrogen or hydrocarbon radicals. The conversion and hydrogen selectivity result is explained these methane cracking activity. The methane conversion and hydrogen selectivity was increased when DBD plasma was discharged. At the same time, it was also confirmed in carbon balance comparison. Figure 35 is comparison result of carbon balance. The carbon balance was decreased for DBD plasma discharged result. It is also indicates increment of methane cracking activity. On the contrary, C_2 and C_3 hydrocarbon formation from radical or carbon and hydrogen were influenced by temperature or dielectric heating. The temperature of catalyst layer was always shown similar result, and hydrocarbon formation was not shown different result for different catalyst. Only, relation between ΔH and hydrocarbon selectivity was confirmed for same catalyst condition.

3.6 CO/CO_2 formation

The experiments were performed with primary discharge media N_2 and reaction target CH_4. However, CO and CO_2 what contains oxygen were detected during the experiments. It was only detected in plasma assisted γ-Al_2O_3 and Cu-Zn based catalysts experiments and not detected in absence of catalyst or plasma discharge condition. Figure 36 and Figure 37 is CO and CO_2 selectivity comparison for different catalysts and plasma discharge conditions. The γ-Al_2O_3 and Mg, Mn and Ti mixed Cu-Zn catalyst shows better CO selectivity and CO_2 selectivity was shown similar tendency to CH_4 conversion. The manganese mixed copper-zinc catalyst shown better CO/CO_2 selectivity with plasma-assisted condition.

Basically, hydrogen treatment for surface oxygen removal was always performed before experiments and oxygen was not supplied to reactor during the experiments. Nevertheless, the oxygen contained species like a CO and CO_2 was only detected with plasma assisted γ -Al_2O_3 and Cu-Zn based catalysts. It indicates that oxygen may be originated from γ-Al_2O_3 and Cu-Zn based catalysts and influenced by plasma. In order to investigate source of

oxygen, EDS analysis was performed for γ-Al_2O_3. Table 9 is comparison of surface contents variation for plasma discharge. The plasma discharge makes increase of oxygen contents on the γ-Al_2O_3 surface. Based on this result, we assumed that absorbed oxygens are detached from the internal layer or deep inside area of the porous structure, and then flow out to the surface. After flow out, it can be bonded with decomposed carbon or absorbed on surface because that oxygen is exposure on electron collisions what can provide excitation or ionization. Thus, the CO and CO_2 are produced and oxygen contents of the surface are increased. However, exact source of oxygen and mechanism is need to further investigation.

3.7 Optical emission spectroscopy

Excited atoms and molecules are emits photons when they are restored to the low and ground states[71]. The optical emission spectroscopy is used this photon emission characteristic to investigate state of plasma. The OES experiments were performed with pure DBD plasma and plasma-assisted γ-Al_2O_3 support and Mn and Ni mixed Cu-Zn catalyst what shows best and worst performance in direct methane conversion experiments. DBD plasma was generated with 1 kHz and 9 kV and only 45 mL/min of CH_4 was supplied into reactor.

Figure 39 is comparisons of optical emission spectra from DBD plasma for different catalyst conditions. Noticeable differences are occurred for presence or absence of intermediate material like a γ-Al_2O_3 support or catalysts. This difference is significantly detected within 170 to 520 nm wavelength range. The emission pattern of the DBD plasma was completely changed when γ-Al_2O_3 support or catalysts were placed between electrodes. It indicates that intermediate material like a γ-Al_2O_3 support or catalyst can change plasma generation characteristics and it influences on generated species like an excited molecules and radicals.

The difference of emission spectra was also detected in $Cu_3Zn_6Mn_1$ and $Cu_3Zn_6Ni_1$

catalyst. It was shown similar emission spectra for γ-Al_2O_3 support but it is not a completely matched within experimental range. Emission intensity of $Cu_3Zn_6Mn_1$ and $Cu_3Zn_6Ni_1$ catalyst was weaker than γ-Al_2O_3 support. The γ-Al_2O_3 support has shown stronger emission intensity and additional emission bands. However, this higher intensity on γ-Al_2O_3 support is not related with CH_4 conversions. The γ-Al_2O_3 support was shown relatively good CO selectivity and C_2 or C_3 selectivity. On the contrary, emission intensity of DBD plasma was significantly reduced with $Cu_3Zn_6Ni_1$ catalyst. It indicates that activity of DBD plasma is suppressed or degraded on Ni mixture. We expect this result can explain why $Cu_3Zn_6Ni_1$ catalyst was shown poor performance on plasma assisted condition. Actually, CH_4 conversion and most of the selectivities are shown the worst result with $Cu_3Zn_6Ni_1$ catalyst.

The difference between $Cu_3Zn_6Mn_1$ and $Cu_3Zn_6Ni_1$ catalyst was also confirmed near 430 nm wavelengths what can observe C-H bands. Figure 40 is shown emission spectra near 430 nm with different intermediate conditions. The intensity of γ-Al_2O_3 support, $Cu_3Zn_6Mn_1$ and $Cu_3Zn_6Ni_1$ catalyst near 430 nm is shown inverse proportion for CH_4 conversion. The emission intensity was significantly reduced with $Cu_3Zn_6Mn_1$ catalyst but it was shown best CH_4 conversion. On the contrary, emission intensity of γ-Al_2O_3 support and $Cu_3Zn_6Ni_1$ catalyst was higher than $Cu_3Zn_6Mn_1$ catalyst but CH_4 conversion was shown the worst result. Based on photon emission mechanism as mentioned earlier, the higher C-H intensity indicates that excited hydrocarbon species like a CH_4 are restored to the low and ground states. It also indicates decomposition or conversion of hydrocarbon is not detected as C-H bands. Actually, H_2 and CO_2 selectivity with $Cu_3Zn_6Mn_1$ catalyst was significantly higher than γ-Al_2O_3 support and $Cu_3Zn_6Ni_1$ catalyst.

Based on above results, we expect interaction of DBD plasma and intermediate material as below. The intermediate material which has placed between electrodes is influenced on plasma generations. Especially, plasma generation was affected by impregnated catalysts on γ-Al_2O_3 support, and as a result CH_4 conversion and selectivity was shown completely

different result.

4. Conclusions of methane conversion

The interaction between DBD plasma and promoter mixed copper-zinc catalyst was investigated for plasma-assisted methane conversion process. The promoter such as cobalt, iron, magnesium, manganese, nickel and titanium mixed copper-zinc catalyst was shown zero catalytic methane conversion at 250ºC. On the contrary, methane conversion activity was confirmed in DBD plasma assisted condition. The plasma assisted methane conversion was also confirmed on non-catalytic material such as glass bead, γ-Al_2O_3 support and pure DBD plasma discharge condition. In case of catalyst, Mn promoter was shown the best methane conversion as 44.94% and Ni promoter was worst as 9.98% but non-catalytic material like a γ-Al_2O_3 support was shown 11.85% at 250ºC. The performance of plasma assisted methane conversion was shown different results for a promoter material.

The OES analysis was performed with pure DBD plasma, γ-Al_2O_3 support, Mn and Ni promoter. We confirmed that intermediate material which has placed between electrodes is influenced on plasma generations such as ionized species. The intensity about excited or ionized hydrogen species was much significantly detected in Mn promoter than Ni promoter. At the same time, intensity about C-H excitation was nearly zero in Mn promoter. Based on this result, we assumed that role of Mn promoter provides highly reactive hydrogen species and increases methane decomposition activity.

In plasma assisted condition, most of the methane was decomposed or converted into hydrogen and carbon monoxide/dioxide at low temperature. The source of oxygen for CO/CO_2 formation was also investigated with EDS analysis. We confirmed that plasma discharge makes increase of oxygen contents on the γ-Al_2O_3 surface. Therefore, we assumed that absorbed oxygens are detached from the internal layer or deep inside area of the porous structure, and then flow out to the surface. However, this controvertible oxygen source need to further study.

Table 5. Detailed information of prepared catalysts (Support : γ-Al_2O_3)

Catalyst	Shape / Diameter	Loading (wt.%)
Cu_3Zn_6	Spherical / 1.1 mm	24.74
$Cu_3Zn_6Co_1$	Spherical / 1.1 mm	34.39
$Cu_3Zn_6Fe_1$	Spherical / 1.1 mm	25.22
$Cu_3Zn_6Mg_1$	Spherical / 1.1 mm	27.23
$Cu_3Zn_6Mn_1$	Spherical / 1.1 mm	43.83
$Cu_3Zn_6Ni_1$	Spherical / 1.1 mm	28.34
Cu3Zn6Ti1	Spherical / 1.1 mm	24.33

Table 6. Experimental conditions and parameters about DBD plasma-assisted non-catalytic and catalytic materials

Experiment	Catalyst			Gas Feed		DBD Plasma Discharge	
	Name	Shape	Diameter (mm)	N_2 (mL/min)	CH_4 (mL/min)	Frequency (kHz)	Voltage (kV)
(A)	Empty	N/A	N/A	50	25	1	7
	Glass	Sphere	3	50	25	1	7
	γ-Al_2O_3	Sphere	2.5	50	25	1	7
	γ-Al_2O_3	Sphere	3.15	50	25	1	7
(B)	Empty	N/A	N/A	45	5	1	8
	γ-Al_2O_3	Sphere	1.1	45	5	1	8
	Cu_3Zn_6	Sphere	1.1	45	5	1	8
	$Cu_3Zn_6Co_1$	Sphere	1.1	45	5	1	8
	$Cu_3Zn_6Fe_1$	Sphere	1.1	45	5	1	8
	$Cu_3Zn_6Mg_1$	Sphere	1.1	45	5	1	8
	$Cu_3Zn_6Mn_1$	Sphere	1.1	45	5	1	8
	$Cu_3Zn_6Ni_1$	Sphere	1.1	45	5	1	8
	$Cu_3Zn_6Ti_1$	Sphere	1.1	45	5	1	8

Table 7. CH_4 conversion and discharge power for DBD plasma assisted condition

Catalyst	CH_4 Conversion (%)			Discharge Power (W)
	DBD Off (1)	DBD On (2)	Increment (2)-(1)	
DBD Only	0.312	7.299	6.987	2.20
γ-Al_2O_3	0.292	11.850	11.558	2.24
Cu_3Zn_6	0.327	12.458	12.131	2.51
$Cu_3Zn_6Co_1$	0.320	15.758	15.438	1.93
$Cu_3Zn_6Fe_1$	0.322	17.902	17.580	1.96
$Cu_3Zn_6Mg_1$	0.297	33.607	33.310	2.25
$Cu_3Zn_6Mn_1$	0.328	44.940	44.612	2.26
$Cu_3Zn_6Ni_1$	0.352	9.978	9.626	2.21
$Cu_3Zn_6Ti_1$	0.300	15.252	14.952	2.32

Table 8. Selectivity of C_2 and C_3 hydrocarbons for different promoter under DBD plasma assisted condition

	Selectivity (%)			
Catalyst	C_2H_4	C_2H_6	C_2H_2	C_3H_8
DBD Only	1.70	14.03	2.10	3.84
γ-Al_2O_3	1.88	15.25	2.22	3.56
Cu_3Zn_6	0.93	13.62	0.81	2.78
$Cu_3Zn_6Co_1$	0.74	14.97	0.88	2.92
$Cu_3Zn_6Fe_1$	0.89	11.09	0.77	3.52
$Cu_3Zn_6Mg_1$	0.34	11.89	0.35	2.42
$Cu_3Zn_6Mn_1$	0.43	14.41	0.47	3.15
$Cu_3Zn_6Ni_1$	0.99	13.96	0.42	2.18
$Cu_3Zn_6Ti_1$	1.95	15.68	1.59	5.15

Table 9. Surface contents variation of γ-Al_2O_3 after exposed DBD plasma discharge

Element	Weight percent (wt.%)		
	Fresh	Exposed after 1 kHz DBD Plasma	Exposed after 3 kHz DBD Plasma
Al	37.50	35.31	34.04
O	62.50	64.69	65.96

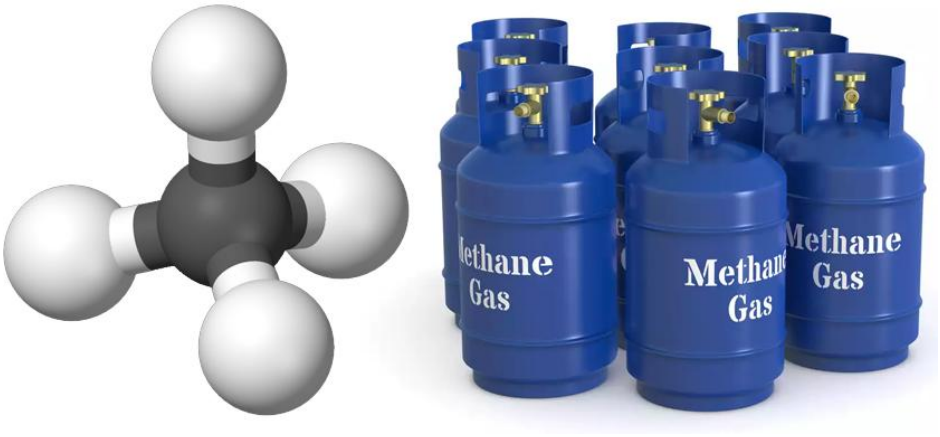

Figure 22. 3D structure of methane molecule and state in atmospheric condition

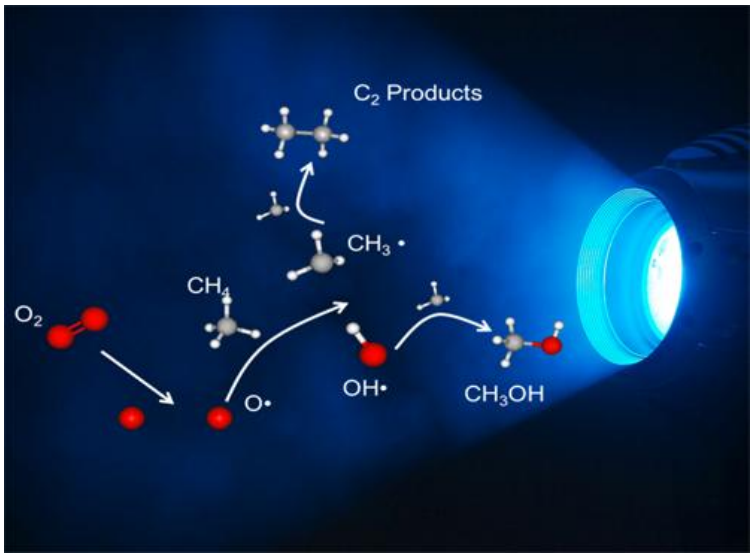

Figure 23. Example of methane conversion for various feedstocks and products

Figure 24. Preparation of 10% promoter mixed copper-zinc catalysts

Figure 25. After calcined 10% promoter mixed copper-zinc catalysts

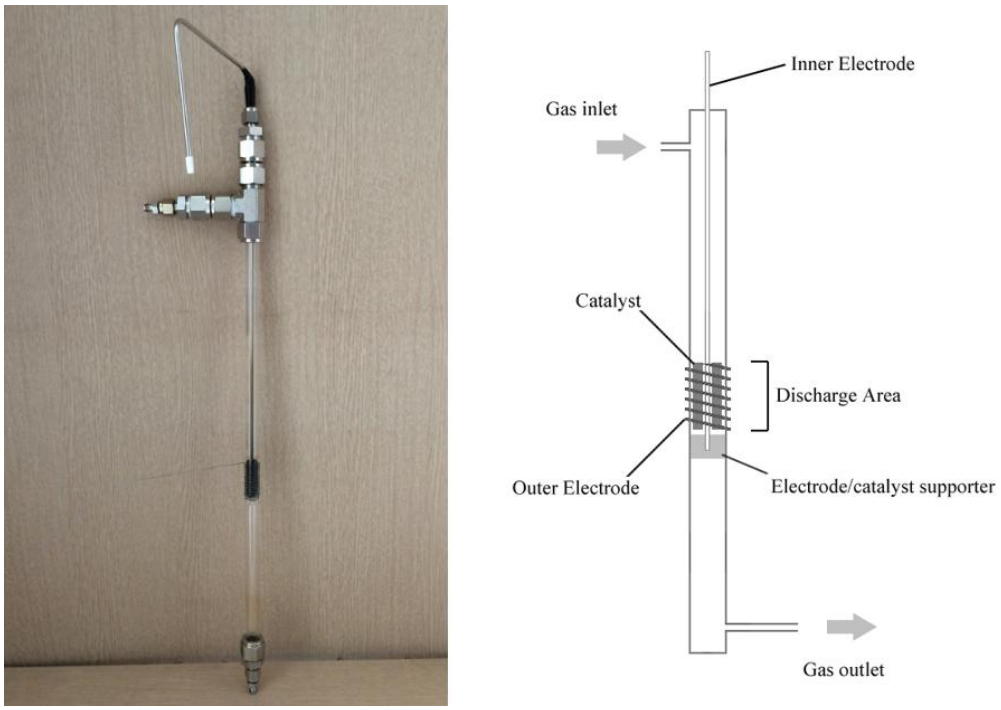

Figure 26. Picture and schematic of catalyst-DBD plasma hybrid reactor for methane experiment

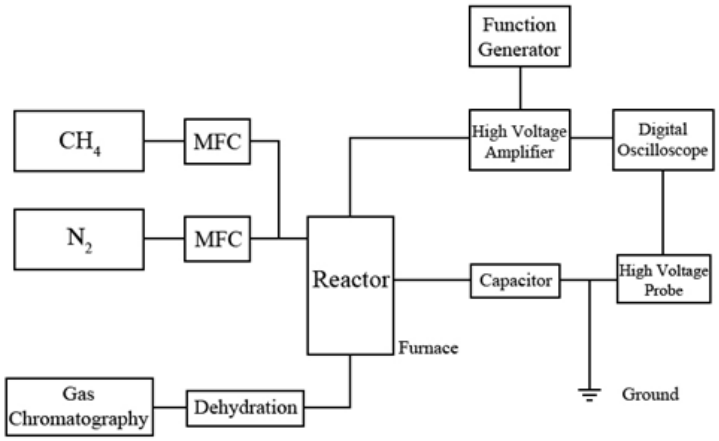

Figure 27. Schematic diagram of apparatus for methane experiment

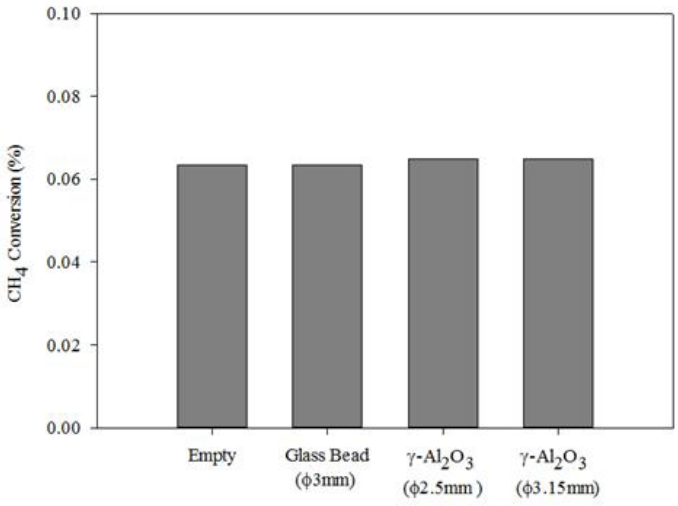

Figure 28. Thermal/catalytic CH_4 conversion with non-catalytic materials at 250°C

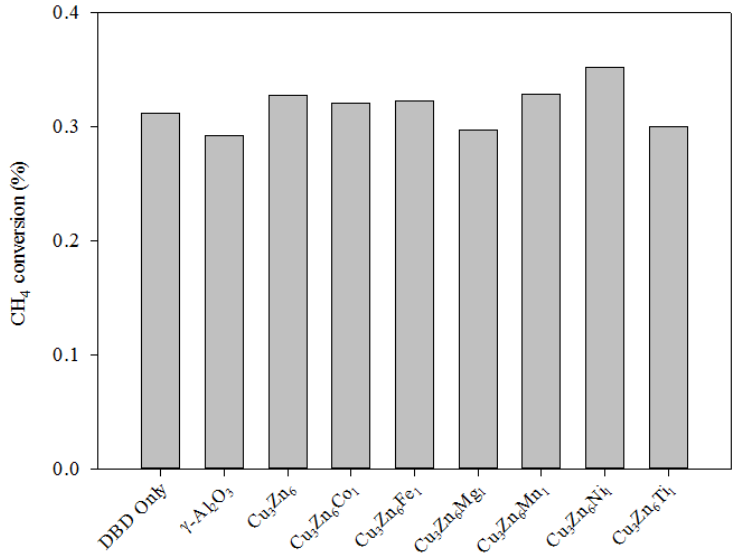

Figure 29. Thermal/catalytic CH_4 conversion with promoter mixed catalyst at 250°C

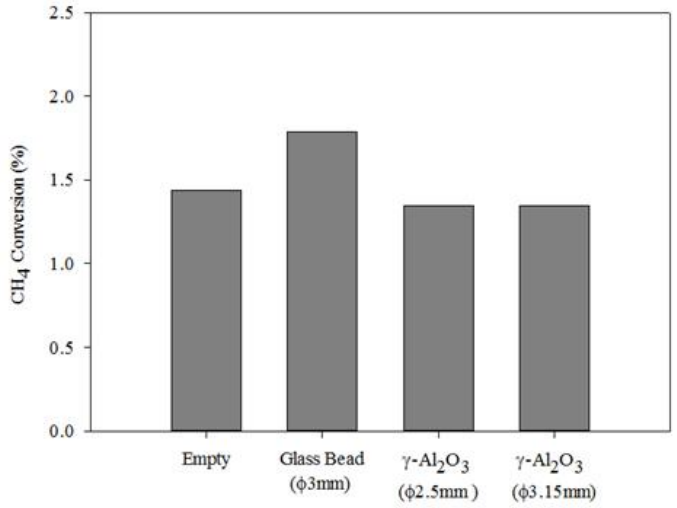

Figure 30. DBD plasma-assisted methane conversion of non-catalytic materials at 250°C

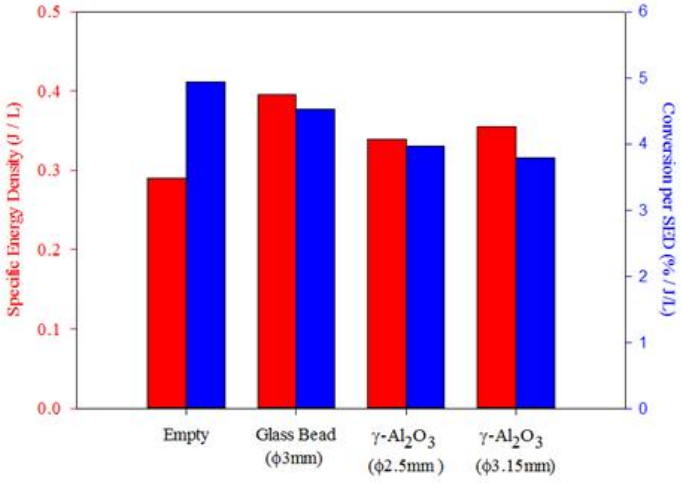

Figure 31. Specific energy density and conversion of DBD plasma assisted CH_4 conversion with non-catalytic materials at 250°C

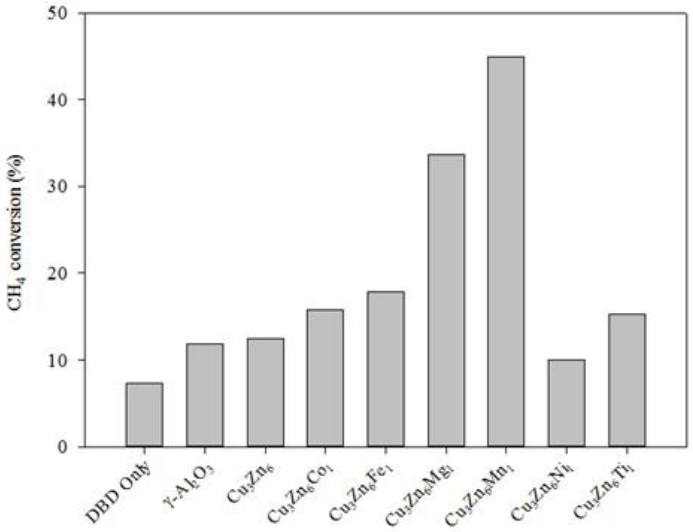

Figure 32. Methane conversion of promoter mixed copper-zinc catalyst and γ-Al_2O_3 for DBD plasma assisted condition at 250°C

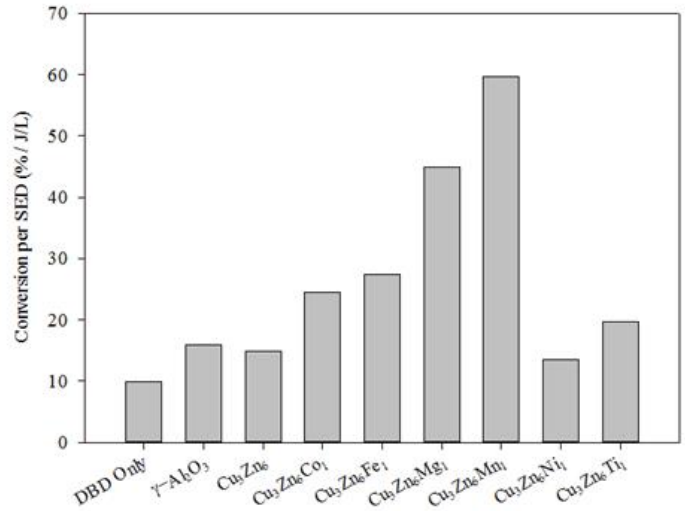

Figure 33. CH_4 conversion efficiency of promoter mixed copper-zinc catalyst and γ-Al_2O_3 on DBD plasma assisted condition at 250°C

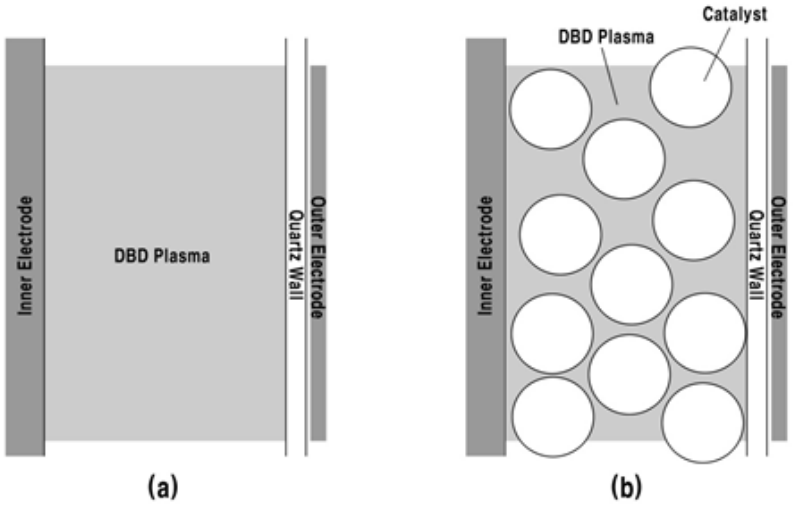

Figure 34. Different internal gap conditions for packed catalyst between electrodes

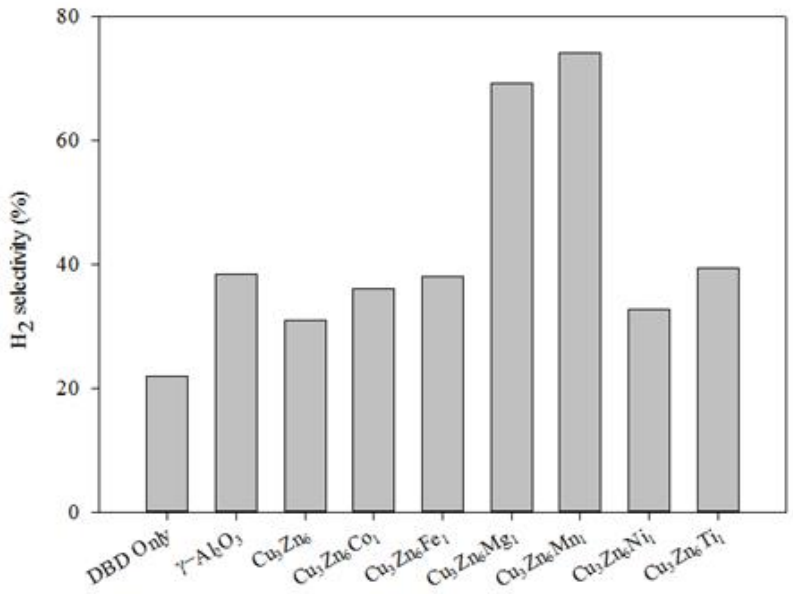

Figure 35. H_2 selectivity on promoter mixed copper-zinc catalyst and γ-Al_2O_3 for DBD plasma assisted condition at 250°C

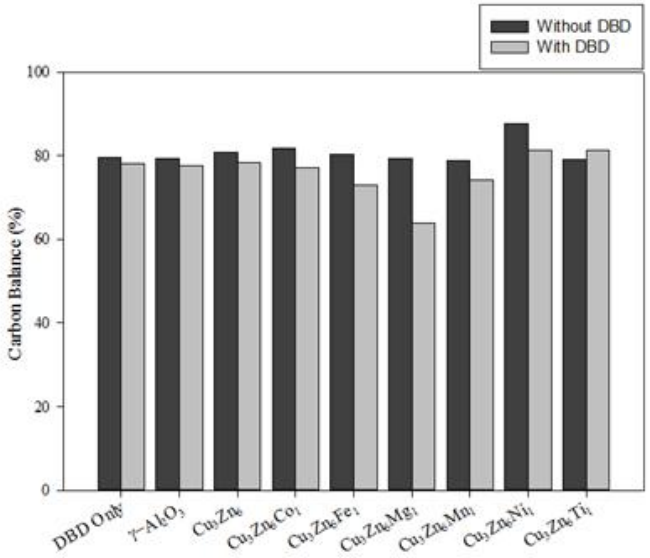

Figure 36. Comparison of carbon balance before and after DBD plasma discharge

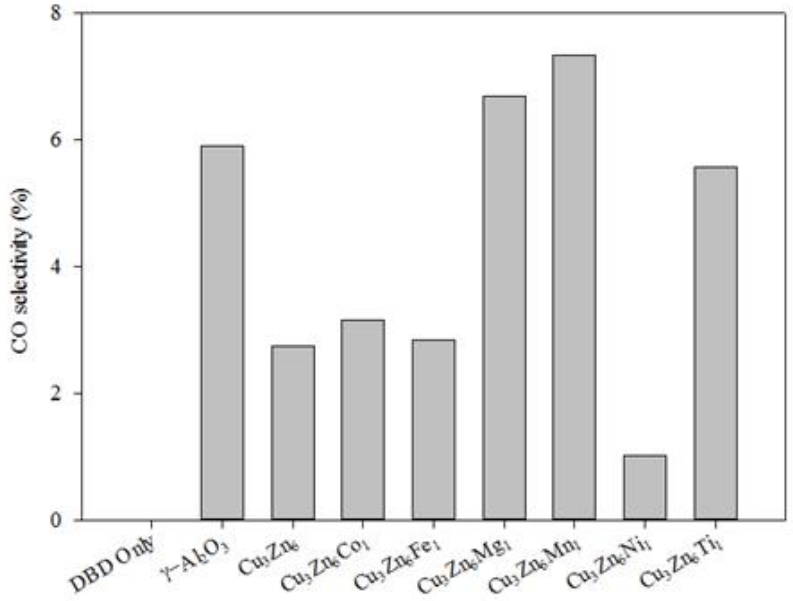

Figure 37. CO selectivity of promoter mixed copper-zinc catalyst and γ-Al_2O_3 for DBD plasma assisted condition at 250℃

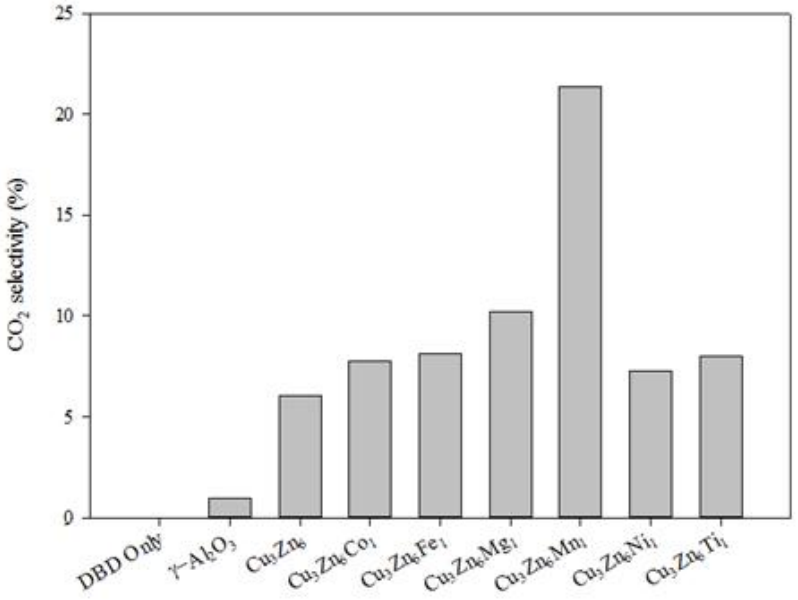

Figure 38. CO_2 selectivity of promoter mixed copper-zinc catalyst and γ-Al_2O_3 on DBD plasma assisted condition at 250℃

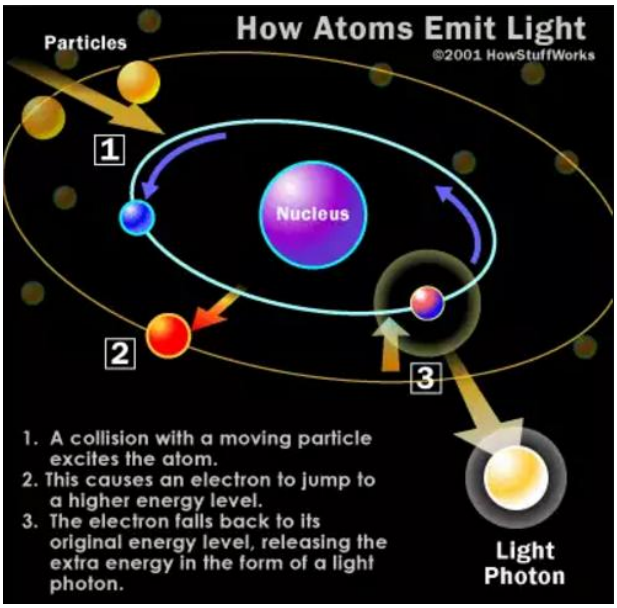

Figure 39. Photon emission mechanism from the atom

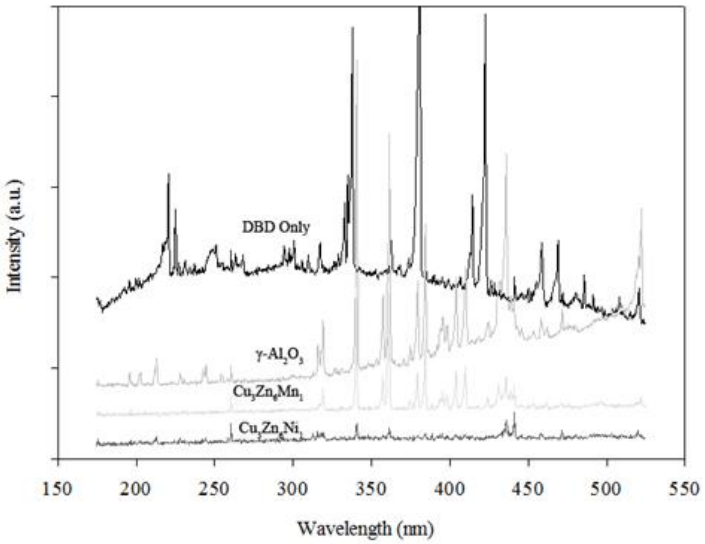

Figure 40. Optical emission spectra of pure DBD plasma and DBD plasma assisted γ-Al_2O_3 and Mn, Ni promoter mixed copper-zinc catalyst (150 groove)

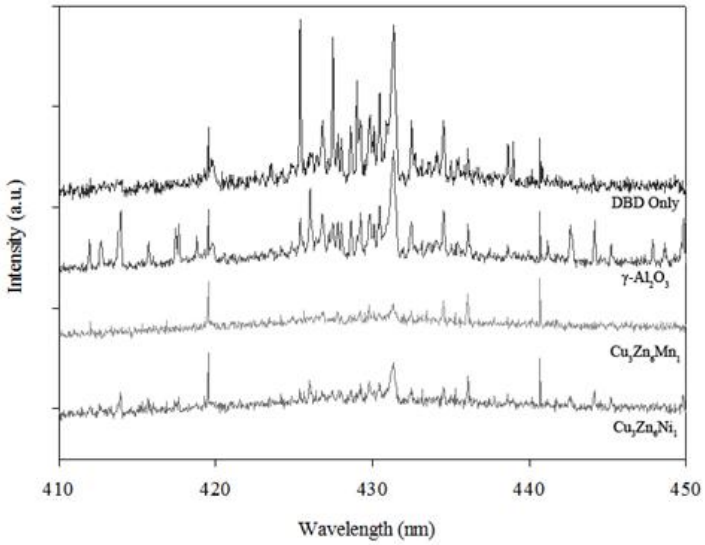

Figure 41. Optical emission spectra of pure DBD plasma and DBD plasma assisted γ-Al_2O_3 and Mn, Ni promoter mixed copper-zinc catalyst (1200 groove)

IV. Interaction Visualization

1. Overview of visualization

In previous chapter, different performance of DBD plasma assisted catalyst process was investigated and confirmed by using small-amount promoter material. The conversion, selectivity and discharge efficiency were shown different result for promoter material. Moreover, surface material such as impregnated catalyst was also affected on DBD plasma assisted catalyst process. Especially, effect on plasma activity by catalyst material was confirmed by optical emission spectroscopy.

Based on these results, we expect what DBD plasma assisted catalyst process has interdependent characteristic like a DBD plasma-assisted catalytic enhancement and catalyst-assisted DBD plasma activity enhancement. For example, catalyst and its catalytic performance can affected by active species (excited atoms and molecules, and radicals) and dielectric heating what is generated by DBD plasma. On the contrary, DBD plasma generation and its effect can changed by catalyst what is play a role like a additional dielectric barrier because it is located between electrodes.

The DBD plasma-assisted catalytic enhancement like a dielectric heating effect and active species generation is also confirmed in previous chapters. Therefore, we planned visualization experiment to verify and secure a solid proof of catalyst-assisted DBD plasma activity enhancement.

2. Experimental

The experiments were performed with asymmetric DBD plasma actuator. The body plate what is also used as dielectric barrier was prepared by using acrylic plate and copper film was placed both side to used as electrode. The upper side of actuator plate, hemispheric and semi-recessed hole was drilled to place catalyst between the electrode. Figure 41 and 42 shows asymmetric DBD plasma actuator what is used in this experiment.

Experimental apparatus was consists of actuator, dark room and plasma generation device. The high-voltage was applied for DBD plasma generation and was supplied by function generator (Agilent 33220A) and high voltage amplifier (Trek Model 20/20C). The electrical discharge characteristics like a discharge voltage and gap capacitance between electrodes were measured and analyzed by 1024pF capacitor, high-voltage probe (Tektronix P6015A), digital oscilloscope (LeCroy WaveSurfer 424). It is same as previous chapters.

The dark room has a cube shape and was built by using black plastic plates. Plasma generation device used same devices what is mentioned previous chapters. The picture of generated plasma on the actuator was taken by using commercial digital camera. Figure 43 is schematic of visualization experiment.

The shutter speed and exposure time was adjusted to photograph more clear image. After a picture was taken, post-processing was performed to remove noise and get more clear image.

The materials what was placed between electrodes like a 1) different angle of copper film, 2) γ-Al_2O_3, MgO/γ-Al_2O_3, TiO/γ-Al_2O_3, ZnO/γ-Al_2O_3, 3) oxidation states of Cu_3Zn_6/γ -Al_2O_3 was used in visualization experiment. Also, experiments were performed at room temperature and DBD plasma actuator was surrounded by room air.

3. Results and discussions

3.1 Electrical induction and transfer

First visualization experiment was performed with copper film what is same as electrodes. The copper film was placed parallel, orthogonal and diagonal between the electrodes. Copper has a good electrically conductive and is already well-known as well. Therefore, visualization experiment was performed by using copper first.

Normally, DBD plasma was generated between electrodes horizontal gap in this actuator configuration. However, between the placed copper film and upper electrode, concentrated

streamer filaments and micro-discharge filaments were coexisted and micro-discharge filaments was also existed near a placed copper film.

The placed copper film was played role like a extended electrode. It means that electrons which was emitted from the upper electrode was transferred to placed copper film and was re-emitted from placed copper film. In the other word, electrical induction and transfer was caused by placed copper film and electrical conductivity of catalyst may affected on discharge and generation of plasma.

3.2 Streamer extension and development

Second visualization experiment was performed with impregnated metal oxide catalysts. The γ-Al_2O_3, MgO/γ-Al_2O_3, TiO/γ-Al_2O_3, ZnO/γ-Al_2O_3 was placed between the electrodes and bottom of half was buried under semi-recessed hole because catalyst can be blown away by induced flow of generated plasma.

The streamer generation and development on rear-side of catalyst was shown big different for catalyst materials. Especially, γ-Al_2O_3 was shown the worst result and MgO/γ-Al_2O_3, TiO/γ-Al_2O_3, was shown good result for streamer extension and development. DBD plasma streamer generation on rear-side of γ-Al_2O_3 which was used catalyst support was partially vanished but away from vanished region was covered by diffused streamers from nearby. On the contrary, streamer generation was extended and well-developed at rear-side of MgO/γ-Al_2O_3, TiO/γ-Al_2O_3 catalyst. Especially, MgO/γ-Al_2O_3 was shown the longest streamer extension and development at its rear-side area.

Above rear-side streamer generation was also shown similar trend for methane direct conversion results which was conducted by research team of KRICT (Korea Research Institute of Chemical Technology)[72]. The MgO/γ-Al_2O_3 was shown the best methane direct conversion performance (16.2%) and TiO/γ-Al_2O_3 was second best (14.1%). Except this two catalyst, conversion of methane with γ-Al_2O_3 and pure DBD plasma was 10.5% and 7%, respectively. The result of γ-Al_2O_3 and pure DBD plasma for methane direct

conversion was shown γ-Al_2O_3 was better but rear-side streamer extension was shown similar result. However, discharge power consumption of each condition were 3.61W for MgO/γ-Al_2O_3, 3.68W for TiO/γ-Al_2O_3, 3.86W for pure DBD plasma discharge and 4.15W for γ-Al_2O_3. Only γ-Al_2O_3 used more discharge power in experiment of KRICT team and this parameter makes difference. Also, discharge power for DBD plasma is same as dissipation of energy between electrodes and if it is higher, that means more energies are required to make discharge for same condition. Therefore, vanished region of streamers was occurred at rear-side of γ-Al_2O_3 because same energy was supplied in this visualization experiment.

3.3 Oxidation and streamer development

The catalyst is easily exposed in oxygen or hydrogen for room or working temperature. Also, oxidation or reduction condition of catalyst is changed during the pre-treatment or experiment. For example, oxygen in oxidized catalyst and its surface oxygen is removed in hydrogen pre-treatment or reduction process. On the contrary, catalyst is easily oxidized when it used on oxygen contained process. The oxidation state or adsorption of oxygen is affected on catalytic performance of the catalyst. This oxidation or adsorption of oxygen is also changed electrical properties of catalyst. For example, copper can turned into copper(I) oxide (CuO), copper(II) oxide (Cu_2O) and copper peroxide (CuO_2) but each copper oxide has a different electrical property because crystal structure and band gap is changed. Therefore, visualization experiment about oxidation/reduction condition of catalyst was performed with copper-zinc catalyst (Cu_3Zn_7/γ-Al_2O_3) because it is easily oxidized and reduced.

Figure 49 shows result of oxidation and reduction state for streamer generation. The result was shown difference streamer development at rear-side of catalyst. The oxidized copper-zinc catalyst which was exposed oxygen rich flow at 300ºC for 2 hours was shown streamer development at the rear-side. At the same time, concentrated streamer filaments

was occurred between front-side of catalyst and upper-electrode of DBD plasma actuator. On the contrary, reduced copper-zinc catalyst which was treated in hydrogen rich flow for 2 hours was shown vanished streamer region at rear-side of the catalyst. Concentrated streamer filaments was not observed in reduced copper-zinc catalyst experiment.

4. Conclusions of visualization

The evidence of catalyst assisted DBD plasma generation was confirmed in visualization experiment. The streamer generation characteristics near the catalyst was investigated by using asymmetric DBD plasma actuator, and result shown different rear-side streamer development characteristics for material of catalysts. The streamer development on γ-Al_2O_3, MgO/γ-Al_2O_3, TiO/γ-Al_2O_3, ZnO/γ-Al_2O_3 was shown similar trend for its DBD plasma assisted catalytic chemical conversion process. Also, oxidation state of catalyst and its effect on streamer development was investigated.

Summarized with previous results, the material or element what consist of catalyst is also very important parameter for DBD plasma assisted catalyst process. In other word, the conventional catalyst what has a good catalytic performance is not always good solutions for DBD plasma assisted catalyst process. Therefore, we propose new requirement about catalyst for DBD plasma assisted catalyst process. New parameter is related performance of catalyst-assisted DBD plasma and its streamer development characteristic. It means that catalyst-assisted DBD plasma generation characteristic is also important and must be considered on DBD plasma assisted catalyst process.

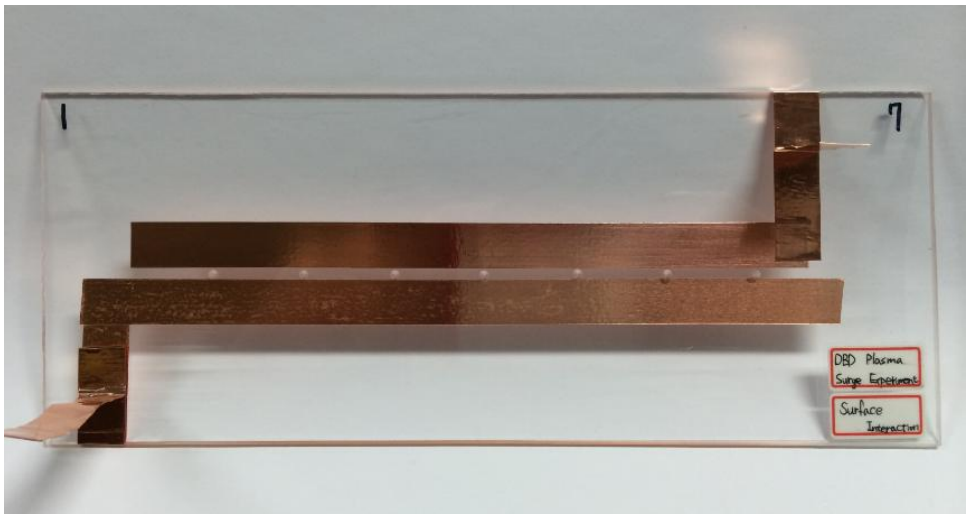

Figure 42. Picture of asymmetric DBD plasma actuator for visualization experiment

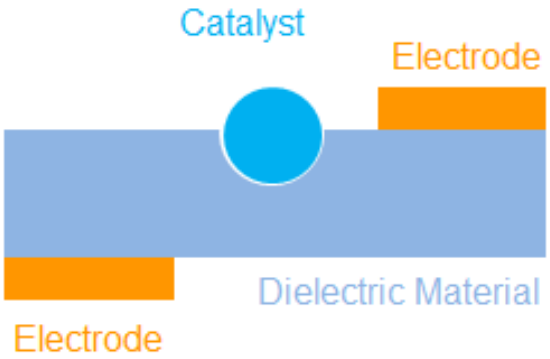

Figure 43. Cross-section of asymmetric DBD plasma actuator for visualization experiment

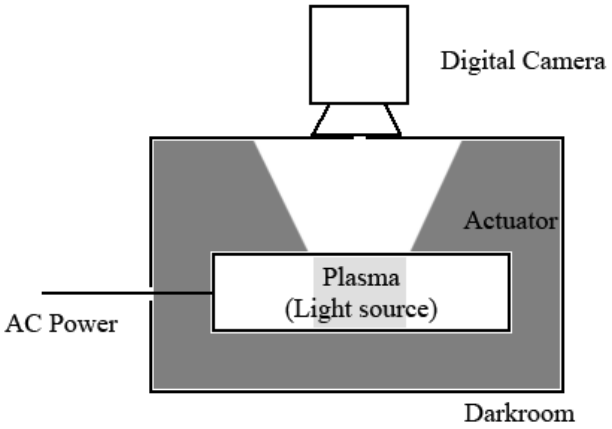

Figure 44. Schematic of experimental apparatus for visualization experiment

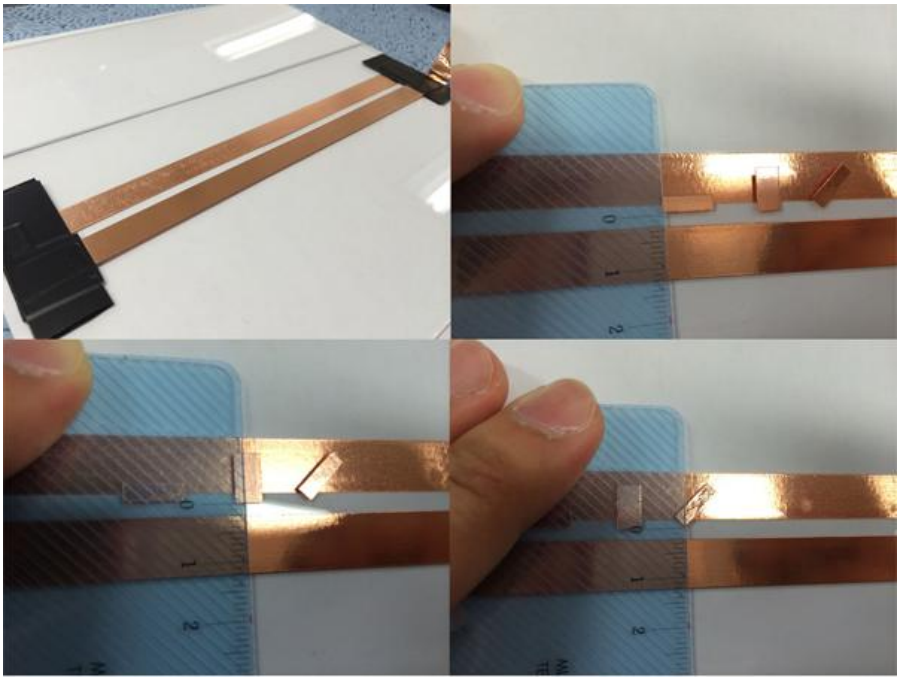

Figure 45. Copper film placed on inter-electrode area of the actuator

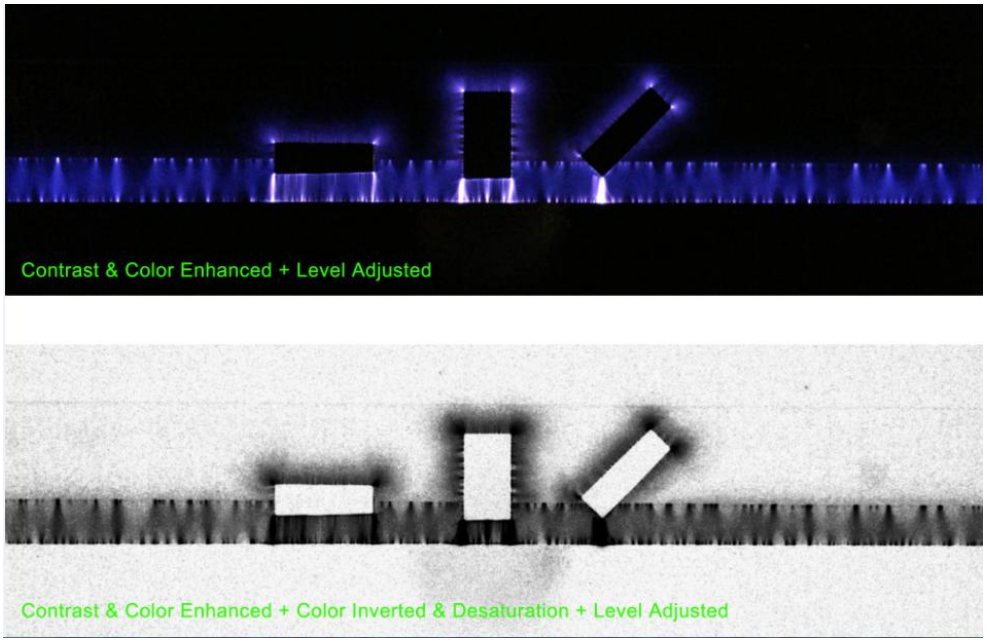

Figure 46. Visualization of streamer generation characteristics of copper film what placed on inter-electrode area

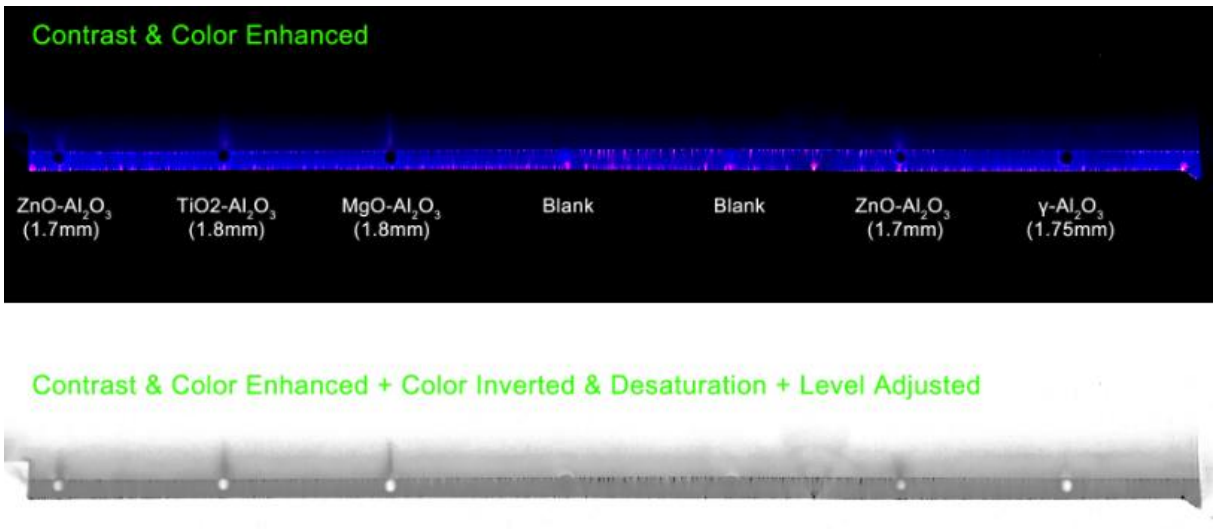

Figure 47. Extended streamer generation and development on rear-side of catalyst

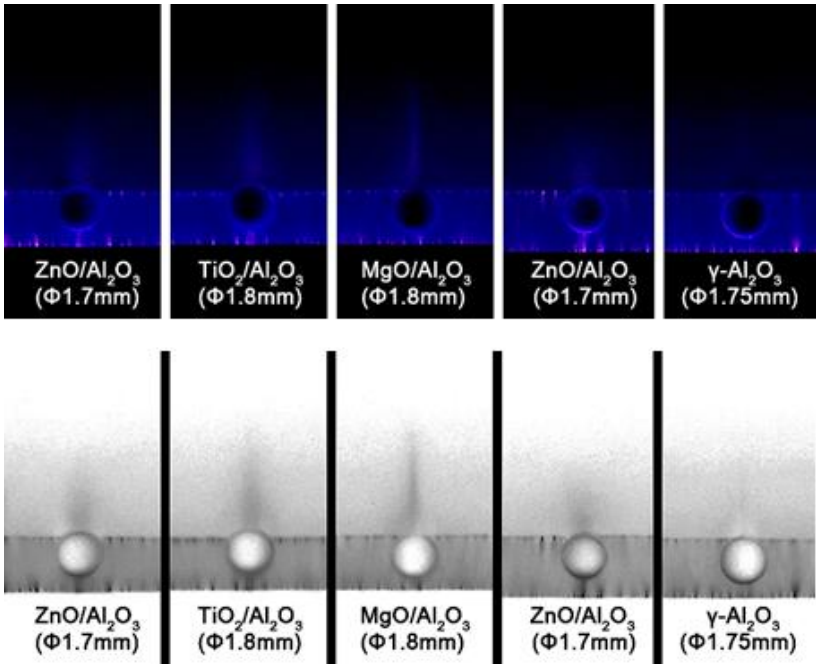

Figure 48. Comparison of rear streamer extension for different catalysts

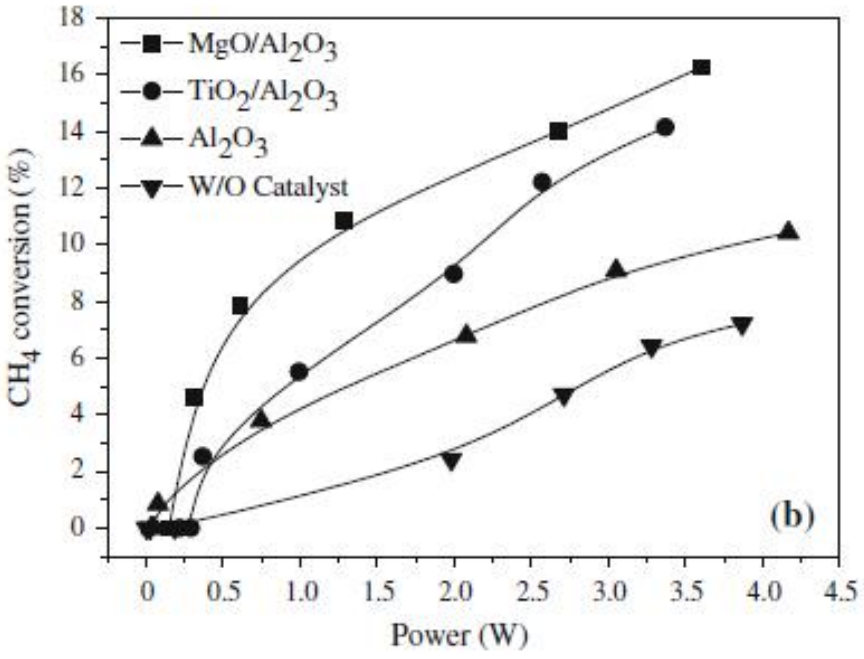

Figure 49. Methane direct conversion data of KRICT research team for same catalyst

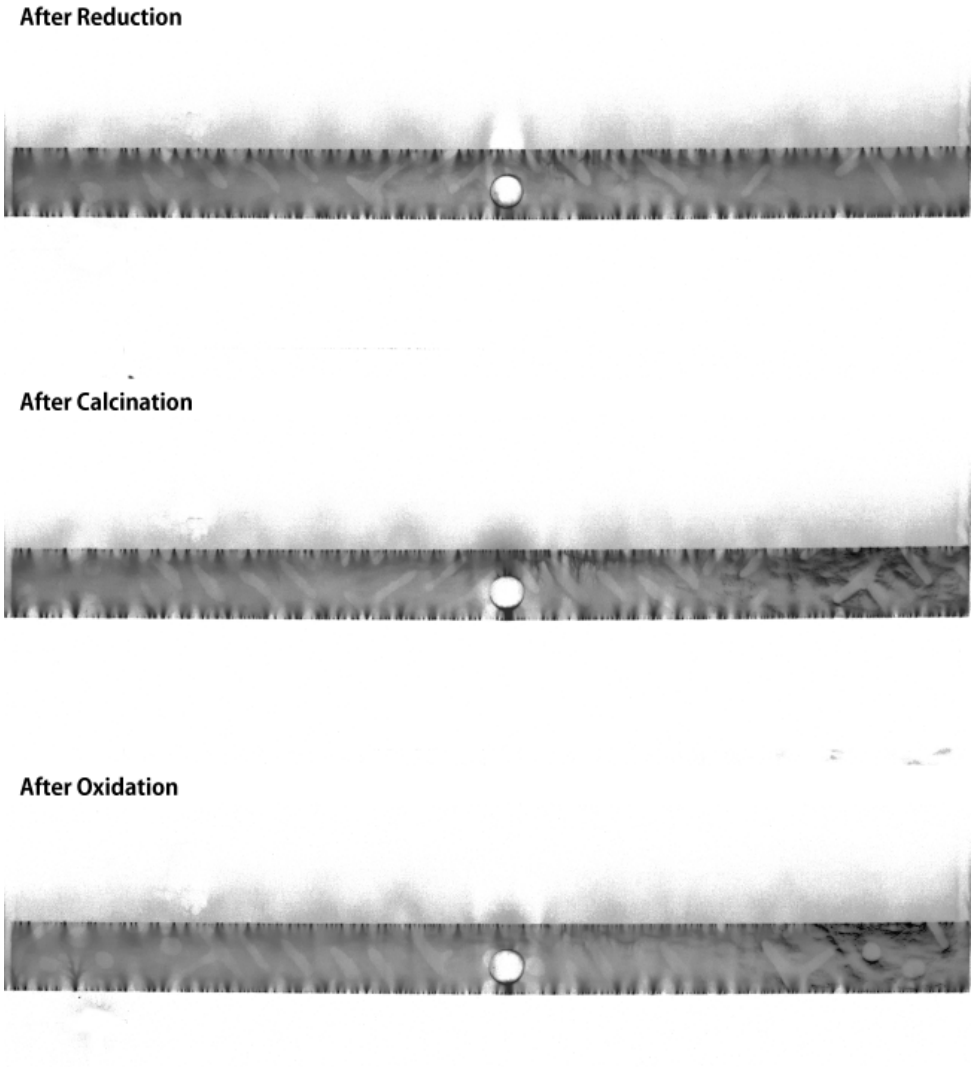

Figure 50. Oxidation and reduction state of catalyst and rear-side streamer generation characteristics

V. CO_2 Methanation

1. Overview of CO_2 methanation

The characteristics of DBD plasma assisted catalyst process is discussed in previous chapters. Now we know that DBD plasma and catalyst have an interaction like a DBD 'DBD plasma-assisted catalytic performance' and 'catalyst-assisted DBD plasma generation'. The plasma-assisted catalytic enhancement is related with dissociation of molecular or active species generation by electron collision and dielectric heating effect from DBD plasma. The other one, catalyst-assisted DBD plasma generation enhancement is related with increased energy of emitted electron and electrical induction and transfer. This means that catalyst and DBD plasma is an interdependent relation in DBD plasma assisted catalyst process. Based on above-mentioned characteristics, we determined to use DBD plasma assisted process for improvement of CO_2 methanation process. The final goal of my research is achieved atmospheric CO_2 methanation process by using interaction of DBD plasma and catalyst.

The methanation of carbon dioxide (CO_2) is one of the important challenges, recently. There are two reasons why the CO_2 methanation is important; the first one is CO_2-related environmental issues and the second one is a potential of "Power to Gas (P2G)" process [44-46]. Since the industrial revolution, atmospheric concentration of CO_2 has kept increasing; as a result, the increased CO_2 concentration causes climate change and global warming issues [37, 38].

The major source of CO_2 emissions is from the combustion of fossil fuels like an internal combustion engine. However, human beings cannot stop using the fossil fuels to prevent CO_2 emissions because the modern human life highly depends on the fossil fuel-based economy system. For this reason, reasonable and alternative solutions about prevent CO_2 emission is a recycling or utilizing the emitted CO_2.

Either recycling or utilizing the CO_2 can be achieved by Sabatier reaction. The Sabatier reaction is a well-known process to convert the CO_2 into a useful product like methane (CH_4) and water as Equation (19):

$$CO_2 + 4H_2 \rightarrow CH_4 + 2H_2O \qquad \triangle H = -165.0 \text{ kJ/mol} \qquad (19)$$

The CO_2 methanation process has a great potential in environmental, industrial and economical aspects, because fuels or fuel sources can be regenerated from the CO_2 that is a waste gas. Based on the renewable energy growth, the CO_2 methanation can be used for "Power to Gas" process that converts the electrical power to a gas fuel. It means that the excess power can be utilized and stored in a form of storable gas state such as the CH_4.

For this reason, the CO_2 methanation process has been widely studied in the literature. Typically, the CO_2 methanation has been achieved on the group VIII base-metal catalysts such as Ni and Ru[73-77]. However, the catalytic methanation process using the Sabatier reaction is usually activated over 300°C and 20 bar[78-80]. This temperature and pressure requirement makes the process complex because the heater, pressurization device, and pressurized reactor are required. It means that the system has the limitation for miniaturization and simplification, which makes it hard to be applied to various industrial applications. Therefore, the alternative approach to lower the temperature and pressure to activate the CO_2 methanation process is required.

The non-thermal plasma has many advantages in various chemical processes. A few groups have reported the study on CO and CO_2 hydrogenation using the non-thermal plasma [31-34]. Therefore, the non-thermal plasma-assisted CO_2 methanation process was investigated in this study. Among non-thermal plasma techniques, dielectric barrier discharge (DBD) was used to generate the plasma on the catalyst. The activation and enhancement of the CO_2 methanation under the plasma in atmospheric condition and its mechanism between the plasma and catalyst will be discussed in this chapter.

2. Experimental

2.1 Catalyst preparation

The cobalt, iron, iron-manganese, nickel, rhodium and ruthenium catalyst was tested for DBD plasma-assisted CO_2 methanation process. These elements are often used as catalyst for many chemical conversion process including Fischer-Tropsch synthesis and the catalytic CO_2 methanation process[81-83]. The incipient wetness impregnation method was used to prepare catalyst and 1/16 inch diameter spheric γ-Al_2O_3 was used as catalyst support.

Each precursor powders were dissolved in distilled water and then the solution was added to the γ-Al_2O_3 support. The impregnated catalyst was dried at room temperature for 24 hours. After dried, the catalyst was calcined at 350°C for 2 hours; as a result, the Ru/γ -Al_2O_3 catalyst was obtained.

In the plasma catalysis, the catalyst is exposed to the plasma streamer. It means that the catalyst can influence the generation and propagation of the plasma streamer. When the streamer is generated, it first would be contacted with the surface layer of the catalyst. Not enough the catalyst loading, the probability of the interaction between the streamer and the catalyst are reduced. The loading fraction of Ru in the Ru/γ-Al_2O_3 catalyst was 5.369 wt.%, which is enough for the catalyst to be loaded in the interior of the catalyst when impregnated.

2.2 Catalyst-DBD plasma hybrid reactor

Overall configuration and layout of reactor is also similar to previous reactors but inside bumps what was used to fix the inner electrode were removed and fix method of inner electrode was changed. In this reactor configuration, we used quartz wool to support catalyst and bottom component of tube fitting was used to fix center location of inner electrode. Figure 51 shows reactor for CO_2 methanation experiment. The reactor consists of the quartz glass tube, and two electrodes. The quartz glass had an axis-symmetrical shape

with 402 mm × 13 mm × 10.9 mm (length × outer diameter × inner diameter) in dimension. Stainless steel fittings were connected on both ends of direction, which was used for the gas supply.

The reactor has two electrodes; one is the stainless steel rod and the other is the helix-shaped steel wire. The stainless steel rod was installed inside the reactor as being aligned with the center axis of the reactor. On the other hand, the steel wire was installed around the outside of the reactor. These electrodes were 45 mm which was the length overlapped in the axial direction of quartz tube. Thus, the plasma was generated in the overlapped area between two electrodes. The prepared catalysts were filled in this overlapped area which was matched with the plasma discharge area. It means that the plasma was generated in the identical volume in which the catalysts were packed and its average weight is 3g. The glass wool was used to fix the catalysts in the predetermined location. The reactor was installed vertically to the ground to remove water gravitationally from the plasma discharge area and catalyst bed, and the gas down flow configuration was used.

2.3 Experimental apparatus

The schematic diagrams of the experimental apparatus are shown in Figure 53 including the plasma reactor setup to perform the CO_2 methanation under the plasma generation (Figure 53 (a)), and the optical emission spectroscopy (OES) to analyze the plasma characteristics during the plasma-catalytic reaction (Figure 53 (b)). The identical reactor was used for the CO_2 methanation and OES analysis under the plasma generation.

The high-voltage was applied to generate the DBD plasma on the catalyst. Waveform of electrical input was generated from function generator (Agilent 33220A), and applied voltage was amplified through the high-voltage amplifier (Trek Model 20/20C). The electrical discharge characteristics such as the onset voltage and frequency of the discharge were measured by the high-voltage probe (Tektronix P6015A), digital oscilloscope (LeCroy

WaveSurfer 424). The capacitor of 1,024 pF was connected with the gap capacitance between electrodes in series to analyze the discharge power. Discharge power of DBD plasma was calculated by V-Q Lissajous method. Figure 54 is typical V-Q Lissajous diagram of DBD plasma assisted condition with $Ru/\gamma\text{-}Al_2O_3$ catalyst. From the preliminary tests, it was confirmed that the onset voltage of the discharge was 9 kV and at the discharge voltage higher than 9 kV, the arc transition had taken place as the discharge frequency increased higher than 2 kHz. In addition, the change of the discharge frequency was more dominant factor to determine the performance than the discharge voltage. Therefore, the discharge voltage was fixed to 9 kV for all experiments.

The mass flow controller (MKP TSC-210) and control unit (Sehwa KRO-4001) were used to adjust and maintain the gas supply rates. The ultrahigh purity (99.999%) gases including N_2, H_2, CO_2, and Ar were used for all experiments. N_2 gas was used as a carrier gas and played a role of a major discharge media, and space velocity based on the unit weight of the catalyst was 18,625 $ml \cdot h^{-1} \cdot g_{cat.}^{-1}$ in case of the total flow rate of 50 mL/min without Ar addition, whereas it was 29,800 $ml \cdot h^{-1} \cdot g_{cat.}^{-1}$ in case of 80 mL/min with Ar addition.

The moisture in product gases was filtered through a dehydration chamber before supplied into a gas chromatography (YL6100GC). The composition of the product gas was analyzed by the gas chromatography that can detect the hydrogen, nitrogen, oxygen, carbon monoxide, carbon dioxide, methane, acetylene, ethylene, ethane, and propane. Average values of experiments three times conducted are presented and the deviation of all values was less than ±1.5%. Also, definition of conversion and selectivity are expressed in Equation (20) to (22).

The OES system consists of monochromator (Dongwoo Optron Monora 500i) and optical CCD detectors (Andor iDus DV420A-OE). It is connected with PC and its software (Andor Solis) to acquire a diagnosed data of DBD plasma.

$$\text{Conversion of } CO_2\ (\%) = \frac{\text{Mass of converted product from } CO_2}{\text{Mass of introduced } CO_2} \times 100 \quad (20)$$

$$\text{Selectivity of } CH_4\ (\%) = \frac{\text{Mass of produced } CH_4}{\text{Mass of converted } CO_2} \times 100 \quad (21)$$

$$\text{Selectivity of CO}\ (\%) = \frac{\text{Mass of produced CO}}{\text{Mass of converted } CO_2} \times 100 \quad (22)$$

3. Results and discussions

3.1 Catalyst screening

The prepared catalysts for DBD plasma-assisted CO_2 methanation were selected by investigation of existing researches and publications. It means that prepared catalysts was not verified suitability for DBD plasma-assisted condition. We already mentioned relation about catalyst-assisted DBD plasma generation and DBD plasma-assisted catalytic performance in previous chapters. Therefore, catalyst screening was performed to investigate suitability for DBD plasma-assisted condition.

First screening test was performed with 1 kHz and 9 kV discharge condition and gas supply was controlled at 30 mL/min for N_2, 15 mL/min for H_2 and 5 mL/min for CO_2. Figure 55 shows test result and it was performed at atmospheric condition. The CO_2 conversion and selectivity for CH_4 what is related with CO_2 methanation activity was shown interesting result. In DBD plasma-assisted condition, cobalt and nickel catalyst was shown better CO_2 conversion and ruthenium was shown similar performance as pure DBD plasma but ruthenium and pure DBD plasma was shown better CH_4 selectivity. Therefore, iron and iron-manganese catalyst was excluded and second screening test was performed with cobalt, nickel and ruthenium catalyst.

Figure 56 shows second screening test result. The discharge condition was 3 kHz and 9 kV, and gas supply and another experimental condition was same as first screening test. In second test, performance of ruthenium catalyst was significantly better than cobalt and

nickel catalyst. Basically, catalytic CO_2 conversion and methanation was zero at atmospheric condition. However, CO_2 conversion and CH_4 selectivity which was related with CO_2 methanation activity was significantly increased on DBD plasma assisted ruthenium catalyst with 3 kHz. For these reasons, we decide to use ruthenium catalyst for further investigations.

3.2 CO_2 methanation of DBD plasma assisted Ru Catalyst

The DBD plasma-assisted CO_2 methanation was performed under atmospheric temperature and pressure conditions. The discharge voltage and frequency were 9 kV and 3 kHz. The CO_2 conversion and CH_4 selectivity when the plasma was applied only in the empty reactor, the catalyst was used only without the plasma, and both the plasma and catalyst were used simultaneously are shown in Figure 57 and Table 10. Basically, the CO_2 conversion, and CH_4 and CO selectivity were zero in the absence of the plasma. The Ru/γ-Al_2O_3 catalyst also had no reactivity in the absence of the plasma. On the contrary, the CO_2 conversion of 8.21% and CO selectivity of 43.84% were obtained by using the plasma only but the CH_4 selectivity was much low by 1.42%. However, the CO_2 conversion and CH_4 selectivity were 12.80% and 73.30%, respectively, while the CO selectivity decreased, when the DBD plasma was applied on the Ru/γ-Al_2O_3 catalyst.

The CO_2 conversion and CO selectivity was high when the plasma was applied only but the CH_4 selectivity was low. On the contrary, the CO_2 conversion was nearly zero when the Ru/γ-Al_2O_3 catalyst was used only because the catalyst was not activated at the atmospheric temperature. The CO_2 conversion and CH_4 selectivity were both high when the plasma and the catalyst were used simultaneously but the CO selectivity significantly decreased. The results indicated that plasma leads to the increase of the deoxygenation of CO_2 and thereby it enhances the activity of methanation through the interaction with the Ru/γ-Al_2O_3 catalyst.

3.3 Discharge frequency and methanation

The effect of the discharge frequency on the CO_2 conversion and CH_4 selectivity is shown in Figure 58. The discharge frequency increased in the increment of 0.5 kHz, while the discharge voltage was maintained into 9 kV because it was higher than the onset voltage of discharge. At 1 kHz, the small amount of CO_2 was converted into CH_4 even though the DBD plasma was generated on the Ru/γ-Al_2O_3 catalyst. However, the CO_2 conversion and CH_4 selectivity gradually increased with the increase of the discharge frequency.

The CO_2 conversion and CH_4 selectivity were directly proportional to the discharge frequency. Especially, CH_4 selectivity suddenly increased at the increase of the discharge frequency from 2.5 to 3.0 kHz. The discharge frequency is a determining factor of the energy deposition to activate the methanation. The specific energy density (SED) as a function of the discharge frequency is shown in Figure 59. SED shows the similar tendency for CH_4 selectivity, the SED increased rapidly after the discharge frequency of 2.0 kHz was applied. It was indicated that the CO_2 methanation was enhanced when the sufficient discharge energy was applied to the catalyst. If either the discharge energy was lack or the catalyst was absent, the CO_2 deoxygenation was dominant, which leads to the increase of the CO selectivity.

It also means that the minimum discharge frequency is required to activate the Ru/γ-Al_2O_3 catalyst and to make it interact with the DBD plasma. The discharge frequency is one of the important parameters because ionization, excitation and radical generation can be influenced by the discharge frequency[84-86]. It might be also related with the aforementioned activation condition between the plasma and catalyst because the higher discharge frequency can provide more abundant ionized radicals and excited species. It was also confirmed that the CO_2 deoxygenation was improved by using the plasma only as summarized in Table 10. It means that the methanation was not just activated by using the plasma only. Moreover, this result shows the possibility of plasma assisted catalytic

methanation process when the plasma was applied on the catalyst and the discharge condition was satisfied as well.

3.4 Mixture ratio of H_2 and CO_2

The effect of the H_2/CO_2 mixture ratio on the CO_2 conversion and CH_4 selectivity is shown in Figure 60. The N_2, which is a primary discharge media, was supplied 30 mL/min and the H_2/CO_2 mixture ratio was varied by adjusting the H_2 and CO_2 flow rates under the constant total flow rate that was 50 mL/min. The CO_2 conversion and CH_4 selectivity increased the increase of the H_2/CO_2 mixture ratio. In particular, the CO_2 conversion increased from 12.80% to 23.20% when the H_2/CO_2 mixture ratio increased from 3 to 7. In the same condition, the CH_4 selectivity and carbon balance increased from 73.30% to 95.02%, and from 78.93% to 97.38%, respectively. On the other hand, the CO selectivity was decreased as the increase of the H_2/CO_2 mixture ratio.

This result can be explained from the relation of deoxygenation and methanation in the H_2 rich condition that is the high H_2/CO_2 mixture ratio. The carbon balance and CH_4 selectivity decreased but the CO selectivity increased at the low H_2/CO_2 mixture ratio. On the contrary, the carbon balance and CH_4 selectivity increased at the high H_2/CO_2 mixture ratio. The increase of carbon balance and CH_4 selectivity was because more carbon atoms were bonded with either 4 hydrogen atoms or 2 hydrogen molecules. Basically, the H_2 and CO_2 can turn into the dissociation, ionization or excitation by electron collision from the plasma. Therefore, at the high H_2/CO_2 mixture ratio, the hydrogen can be ionized and excited by the plasma so that the ionized hydrogen atoms and excited hydrogen molecules can be actively reacted with the CO_2 and CO, which leads to the increase of the carbon balance and CH_4 selectivity. The CO_2 can be dissociated into the carbon, CO, O, and O_2 by the electron collision[87, 88]. At the H_2/CO_2 mixture ratio, the carbon and O_2 were generated from the CO_2 dissociation but some carbon was deposited on the catalyst surface because there was no enough chance to be bonded with ionized hydrogen atoms and

excited hydrogen molecules. On the other hand, the plasma can generate abundantly ionized hydrogen atoms and excited hydrogen molecules, which can provide more chance to be bonded with the decomposed carbons.

3.5 Ar-N_2 discharge

The Ar has been widely used in various plasma applications because it is relatively easy to be ionized. It has been widely used as a primary or secondary gas with N_2 because the electric discharge of the N_2/Ar mixture can increase the concentration of plasma active species through Penning effect[89, 90]. In addition, the Ar can be recycled after the methanation process because it is inert, not participated in the reaction, and is simply separated from product gases using either the membrane or pressure swing adsorption process. Therefore, the N_2/Ar mixture was supplied in the reactor and the plasma discharge was performed to verify the effect of the Ar addition on the CO_2 methanation. The Ar was added in the flow rate of 30 mL/min without the change of the other flow rates (the flow rates of N_2, H_2 and CO_2 were fixed at 30, 15 and 5 mL/min) because the N_2 is a primary discharge media and CO_2 methanation can be affected by different gas mixture ratios. It means that the total flow rates were different between with and without the Ar addition; the total flow rate was 1.6 times higher when the Ar was added. The discharge condition was identical with the other experimental cases as 9 kV and 3 kHz.

The CO_2 conversion and CH_4 selectivity when the N_2 was used only was compared with those when the Ar was added with the N_2 are shown in Figure 61. Basically, the CO_2 conversion is inversely proportional to the total flow rate. However, CO_2 conversion in case of the N_2-Ar discharge was higher even though the total flow rate was 60% higher in comparison to the case of N_2 discharge. The CO_2 conversion increased 1.68% higher, while the CH_4 selectivity increased 11.60% in the N_2-Ar discharge condition. On the other hand, the CO selectivity increased 1.72% higher, which means that the methanation and deoxygenation were enhanced simultaneously when the Ar was added.

As aforementioned, the discharge can increase the concentration of plasma active species, which leads to the increase of the electron collision frequency. As a result, it induced the active CO_2 dissociation and also generated more active carbons with ionized and excited hydrogens. The increased active carbon and hydrogen ions can influence both the CO_2 methanation and deoxygenation because the increased electron collisions with the CO_2 species can lead to the increase of the deoxygenation. In addition, the increased electron collisions also induce ionization, excitation and radical generation which can provide more chance for carbon to be bonded with hydrogen.

3.6 Optical emission spectroscopy

The OES is one of the powerful non-contact diagnostic methods to monitor the excited and ionized species for plasma application. When the excited atoms and molecules are restored to the low and ground states, photons are released from the excited atoms and molecules; thereby, the optical emission can be detected by the OES. The type of elements as well as excitation and ionization state are determined based on the optical emission spectra of plasma[89, 91, 92]. For these reasons, the in-situ OES analysis was performed during the CO_2 methanation process on the Ru/γ-Al_2O_3 catalyst under the plasma.

The optical emission spectra of γ-Al_2O_3 and Ru/γ-Al_2O_3 catalysts were measured to investigate the effect of the presence of Ru under the plasma in the condition that the H2 and CO_2 flow rates are 15 mL/min and 5 mL/min as shown in Figure 62. The different emission peak and intensity were observed in both spectra, and discharge condition was 9 kV and 3 kHz. Intensity increase of emission bands and additional peaks were observed in the γ-Al_2O_3. On the contrary, several emission bands were suppressed and disappeared in the Ru/γ-Al_2O_3 catalyst. It means that discharge characteristics of the DBD plasma was changed by γ-Al_2O_3, thereby generating excited species with the different excitation state. In addition, it was kwon that the presence of the Ru influenced the discharge characteristics. However, the effect of the change in the discharge characteristics on the enhancement of

CO_2 methanation is not clearly identified. Therefore, additional OES analysis was performed at the different gas conditions.

The optical emission spectra at the different gas conditions are shown in Figure 63; one is the case that the H_2 and CO_2 mixture are supplied, which is the condition of methanation and the other is the case that H_2 was supplied only. The Ru/γ-Al_2O_3 catalyst was used for both cases. The similar spectra were observed in both cases, which indicated that the hydrogen was mainly ionized and returned to the lower or ground state when the plasma was applied on the catalyst in the condition of methanation. At the same time, the emission bands for Balmer series including H_α (656.5 nm), H_β (486.1 nm), H_δ (410.2 nm), H_ζ (388.9 nm), and H_η (383.5 nm) as well as Paschen series of H^+ (820 nm) were also identically detected in condition of methanation. It is indicated that hydrogen radicals with the different excitation states existed in the reaction because these emission series and bands are emitted from excited hydrogen atoms[93-96].

Based on the above result, it was suggested that the DBD plasma provides two enhancements to the CO_2 methanation; one is the dielectric heating and the other one is the excitation and ionization by electron collisions. When the plasma was applied to the catalyst, the local heating was induced by the dielectric heating so that the reaction temperature could be sustained without the additional heating such as an electric heater.

Actually, it was confirmed by an infrared thermography that the reaction temperature was maintained into 250°C when the electric discharge was applied to the Ru/γ-Al_2O_3 catalyst at 9 kV and 3 kHz. Figure 65 shows infrared thermography result for dielectric heating effect. However, the dielectric heating was not a major contribution to the improvement of the CO_2 methanation. Figure 66 is verification result of different between DBD plasma-catalyst interaction and dielectric heating effect. In order to prove the above, the CO_2 methanation was performed at the same temperature (250°C) using the Ru/γ-Al_2O_3 catalyst only without the plasma but the CO_2 conversion (3.06%) and CH_4 selectivity (34.95%) were 4 times and 2 times lower than those with the plasma, respectively.

Therefore, in addition to the dielectric heating, the electron collision is a major contribution to the improvement of the CO_2 methanation because the plasma provides electron collision to generate highly reactive plasma species such as an excited and ionized hydrogen species or dissociation of oxygen from the CO_2.

4. Conclusions of CO_2 methanation

The DBD plasma was used to activate the Ru/γ-Al_2O_3 catalyst for the CO_2 methanation at the atmospheric condition and the effect of the interaction between plasma and catalyst on the conversion and selectivity was investigated in the present study. It was confirmed that the CO_2 conversion increased with the DBD plasma regardless of the presence of the catalyst under the atmospheric condition. However, when the DBD plasma was used alone, most of the CO_2 conversion was induced by the CO_2 deoxygenation because CO_2 molecules were exposed to electron collisions and decomposed into CO. On the other hand, the Ru/γ-Al_2O_3 catalyst was not activated without the DBD plasma. The CO_2 methanation was activated when the DBD plasma was applied on the Ru/γ-Al_2O_3 catalyst. The CO_2 conversion and CH_4 selectivity increased with the increase of the discharge frequency and H_2/CO_2 ratio, and with the addition of Ar. CO_2 conversion and CH_4 selectivity was 23.20% and 97.38% in maximum when the discharge condition was 9 kV and 3 kHz, and the H_2/CO_2 ratio was 7.

The CO_2 methanation was activated by the interaction between the DBD plasma and Ru/γ-Al_2O_3 catalyst. Also, another famous elements were also investigated and confirmed its tendency as Figure 67. The interaction between the DBD plasma and Ru/γ-Al_2O_3 catalyst was confirmed by OES results that the presence of the catalyst in the plasma can influence the characteristics of the plasma discharge, thereby generating highly reactive plasma species such as the excited and ionized hydrogen species. In addition, the DBD plasma can induce the dielectric heating of the catalyst, resulting in the increase of catalytic activity when enough heating is provided. Therefore, it is expected that the enhancement of CO_2

methanation is occurred by the electron collision and the dielectric heating from the DBD plasma. However, it was confirmed that the electron collision was major contributions because the DBD plasma can provide electron collisions to generate highly reactive plasma species such as ionized and excited hydrogens, and the dissociation of carbon and oxygen from CO_2.

Table 10. Effect of presence of Ru/γ-Al_2O_3 catalyst and 3 kHz and 9 kV DBD plasma for CO_2 methanation

	CO_2 Conversion (%)		CH_4 Selectivity (%)		CO Selectivity (%)	
	No Catalyst	Ru/γ-Al_2O_3	No Catalyst	Ru/γ-Al_2O_3	No Catalyst	Ru/γ-Al_2O_3
DBD Off	0.03	0.01	0.15	0.10	0.13	0.01
DBD On	8.21	12.80	1.42	73.30	43.84	5.12

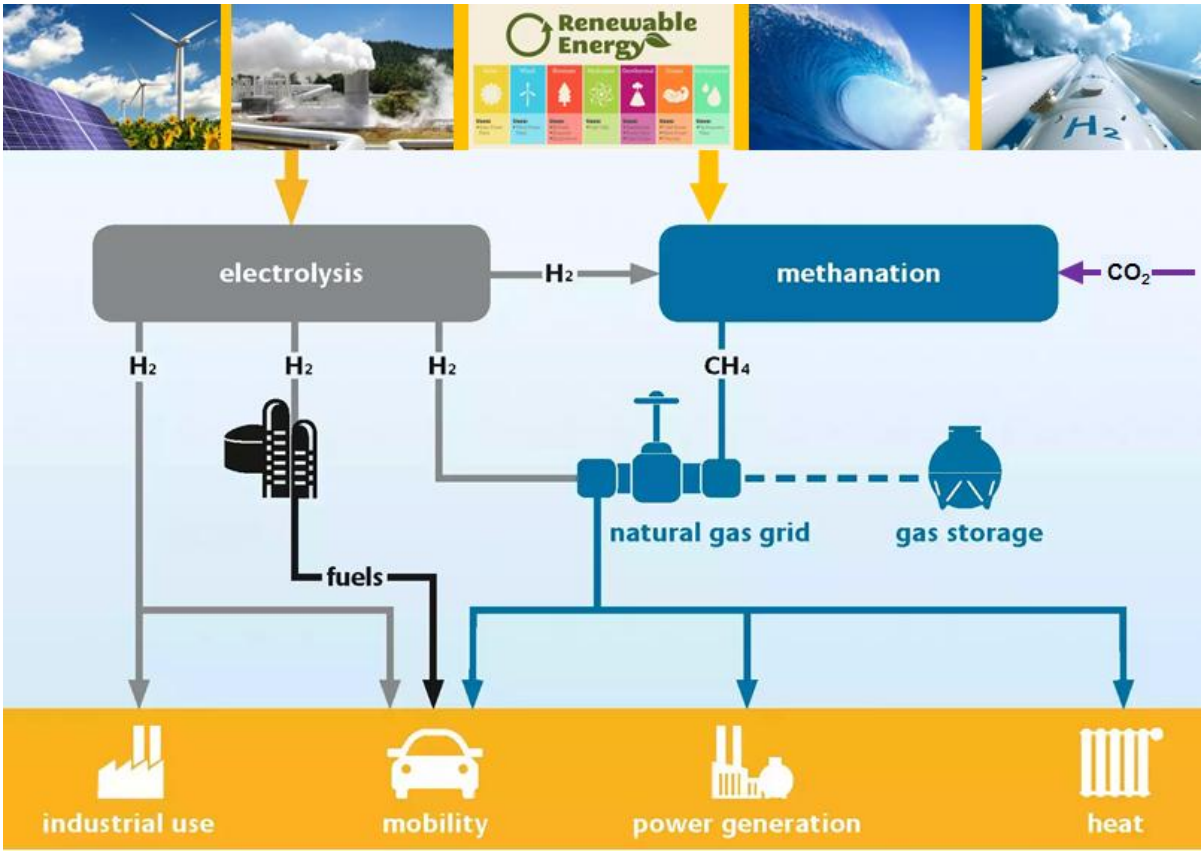

Figure 51. Relation of renewable energy and 'Power-to-Gas' and possible application

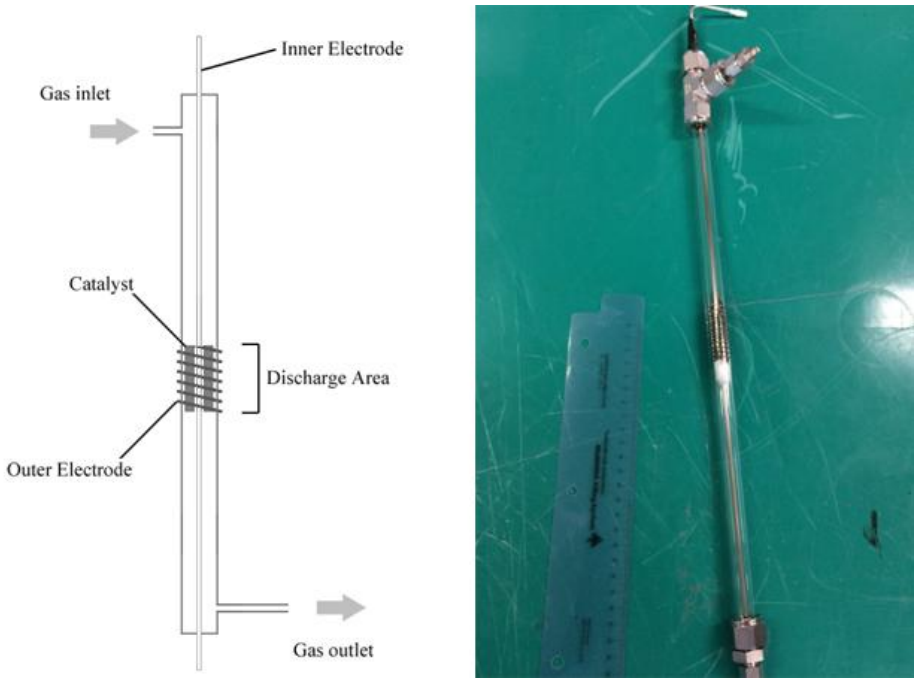

Figure 52. Picture and schematic of catalyst-DBD plasma hybrid reactor for CO_2 methanation experiment

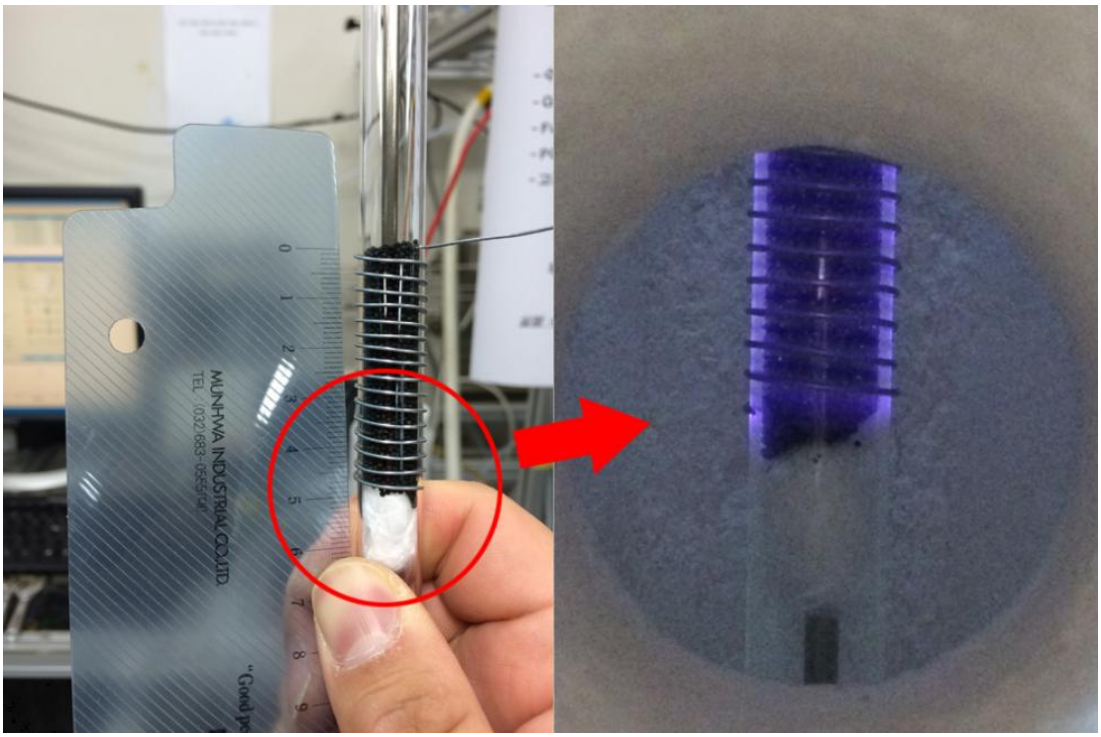

Figure 53. Catalyst packing and discharge area of the reactor for CO_2 methanation experiment

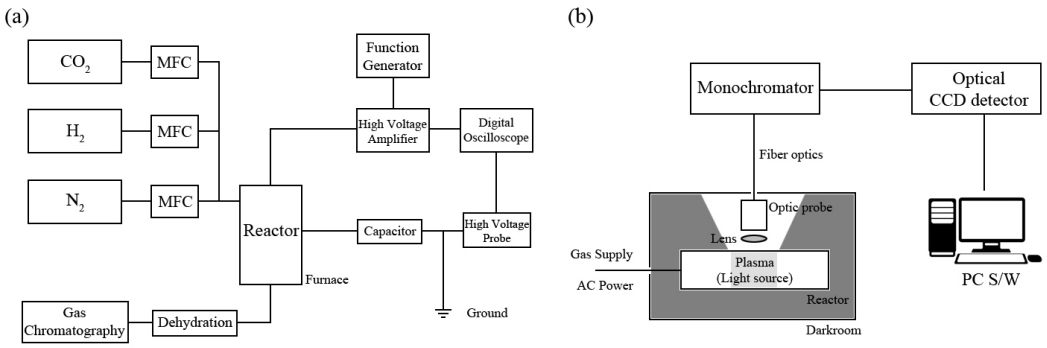

Figure 54. Schematic diagram of experimental apparatus for (a) methanation experiment, (b) optical emission spectroscopy experiment

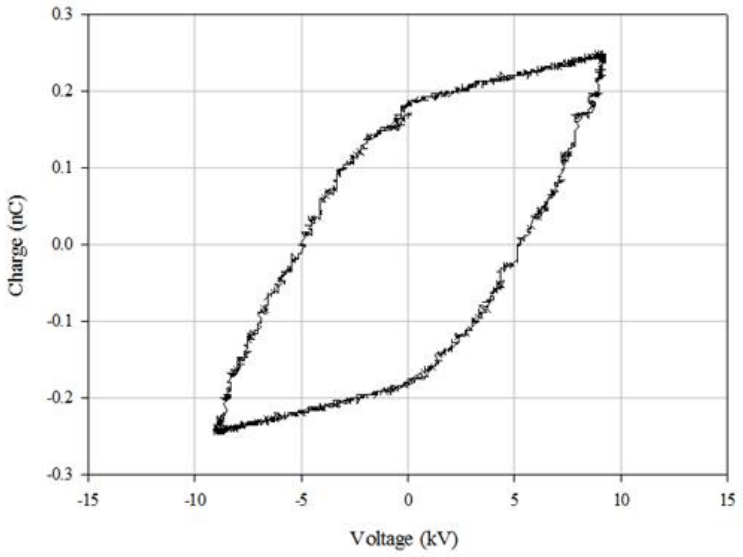

Figure 55. V-Q Lissajous diagram of DBD plasma (3 kHz, 9 kV) discharged on Ru/γ-Al_2O_3

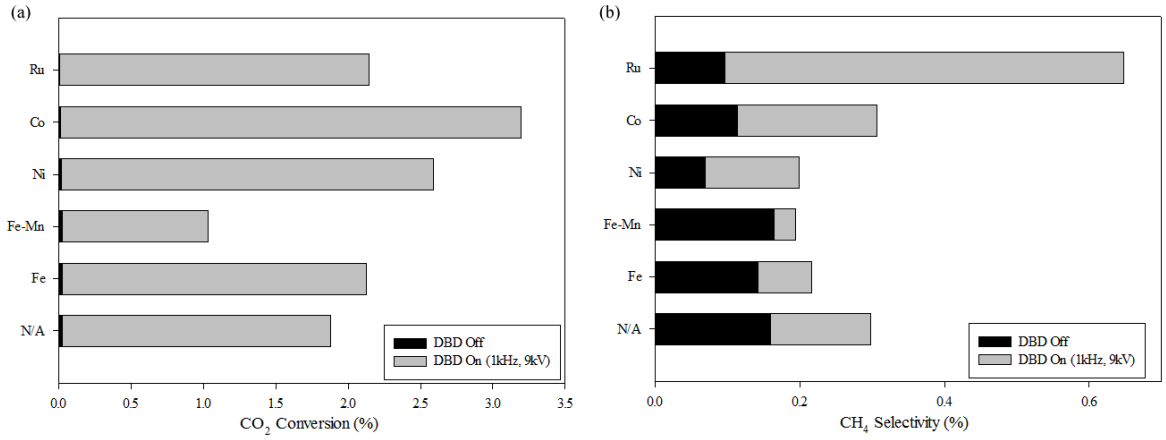

Figure 56. Result of first catalyst screening for DBD plasma assisted CO_2 methanation

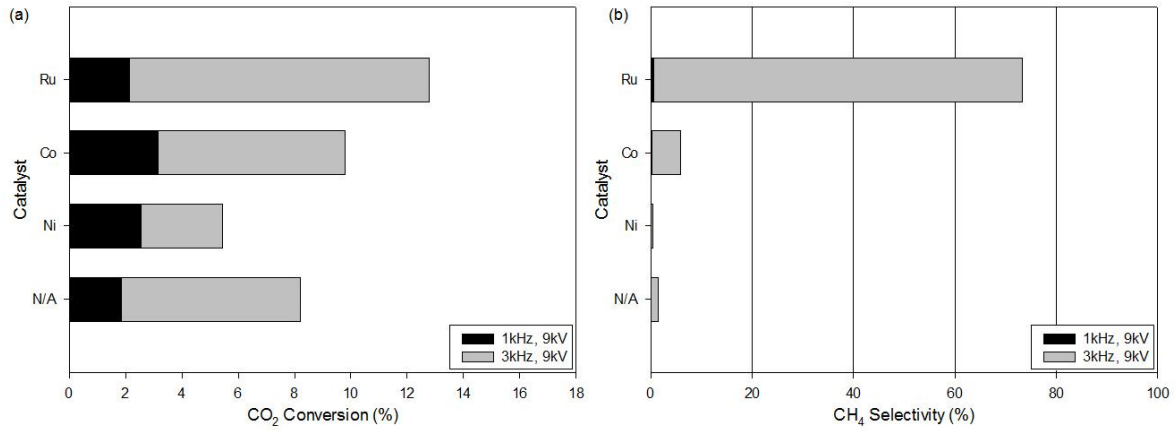

Figure 57. Result of second catalyst screening for DBD plasma assisted CO_2 methanation

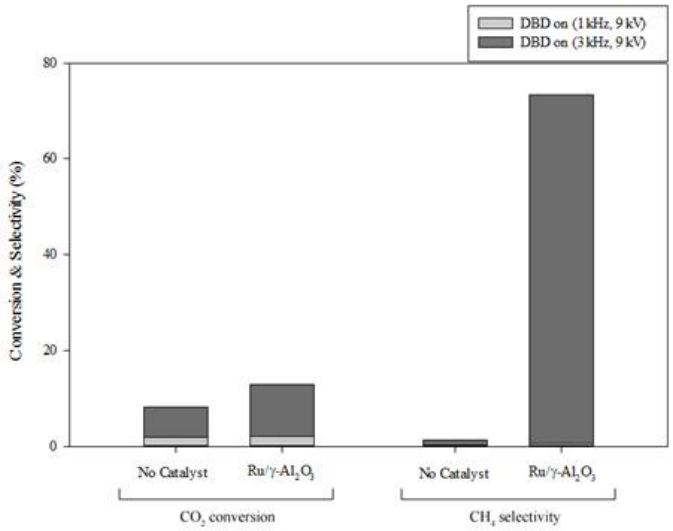

Figure 58. Comparison of CO_2 conversion and CH_4 selectivity under DBD plasma conditions (1 atm, 25°C)

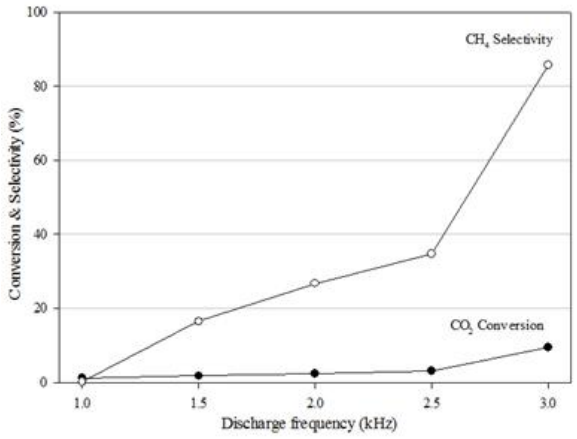

Figure 59. Effect of dielectric barrier discharge frequency for CO_2 conversion and CH_4 selectivity within 1.0 to 3.0 kHz (1 atm, 25°C)

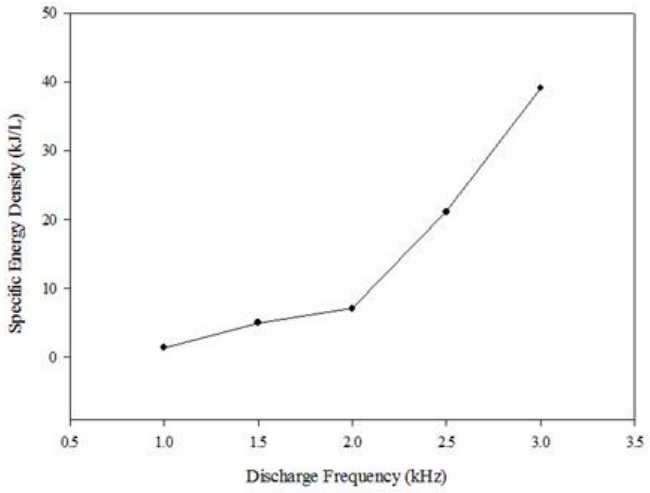

Figure 60. Specific energy density for CO_2 conversion and CH_4 selectivity within 1.0 to 3.0 kHz (1 atm, 25°C)

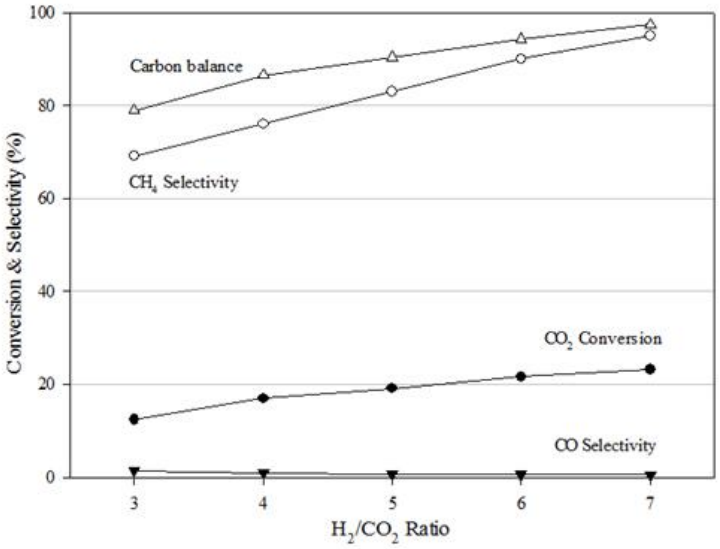

Figure 61. Effect of H_2/CO_2 mixture ratio on the CO_2 conversion and CH_4 selectivity for $Ru/\gamma\text{-}Al_2O_3$ with 3 kHz and 9 kV DBD (1 atm, 25°C)

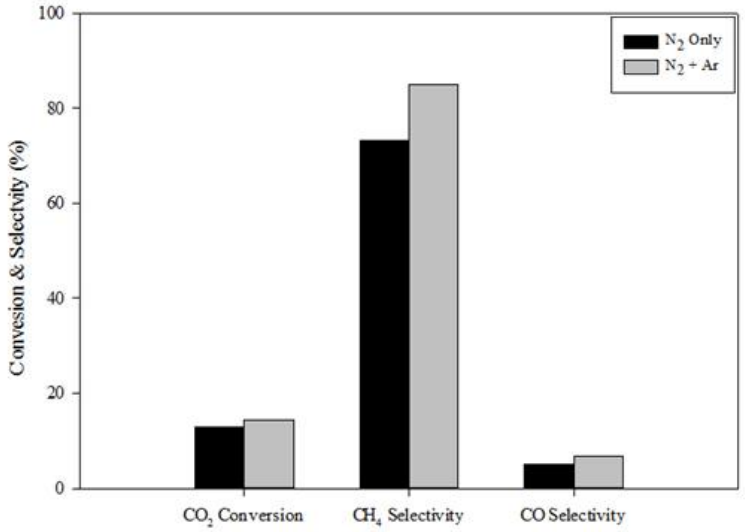

Figure 62. Effect of N_2 and Ar added N_2 dielectric barrier discharge over Ru/γ-Al_2O_3 with 3 kHz and 9 kV DBD (1 atm, 25°C)

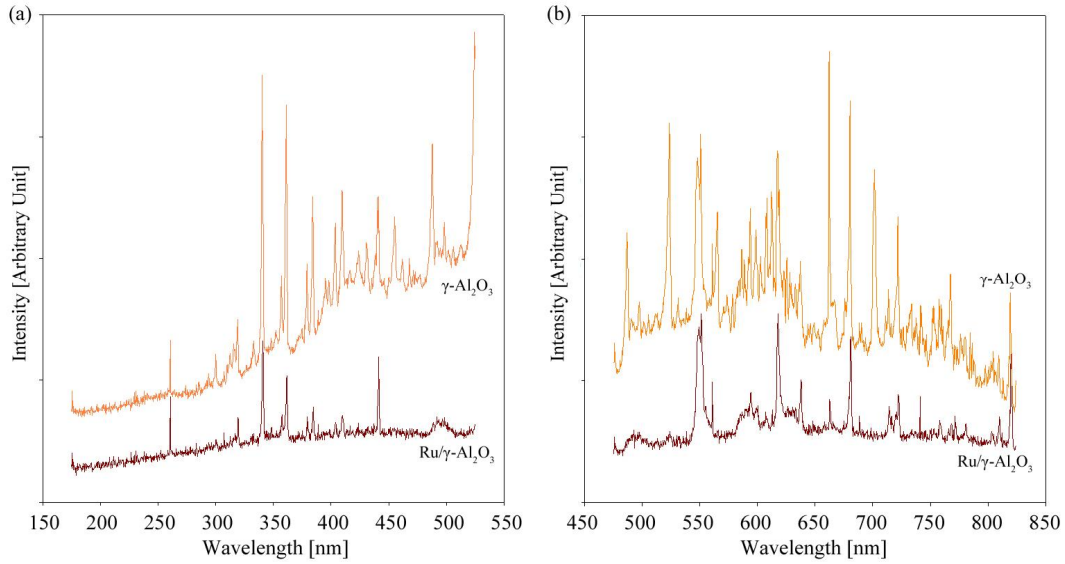

Figure 63. Optical emission spectra of γ-Al_2O_3 and Ru/γ-Al_2O_3 catalyst for 3 kHz and 9 kV DBD condition at (a) 150 to 550 nm and (b) 450 to 850 nm (1 atm, 25°C)

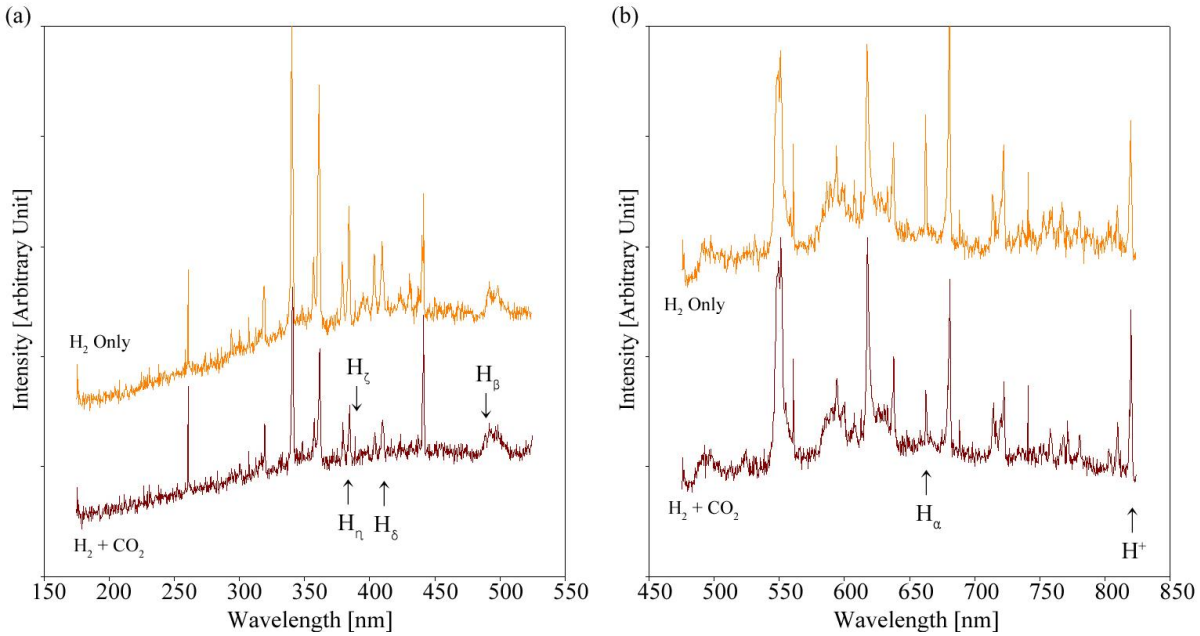

Figure 64. Optical emission spectra of H_2 and CO_2 + H_2 mixture gas discharge over Ru/γ-Al_2O_3 catalyst for 3 kHz and 9 kV DBD condition at (a) 150 to 550 nm and (b) 450 to 850 nm (1 atm, 25°C)

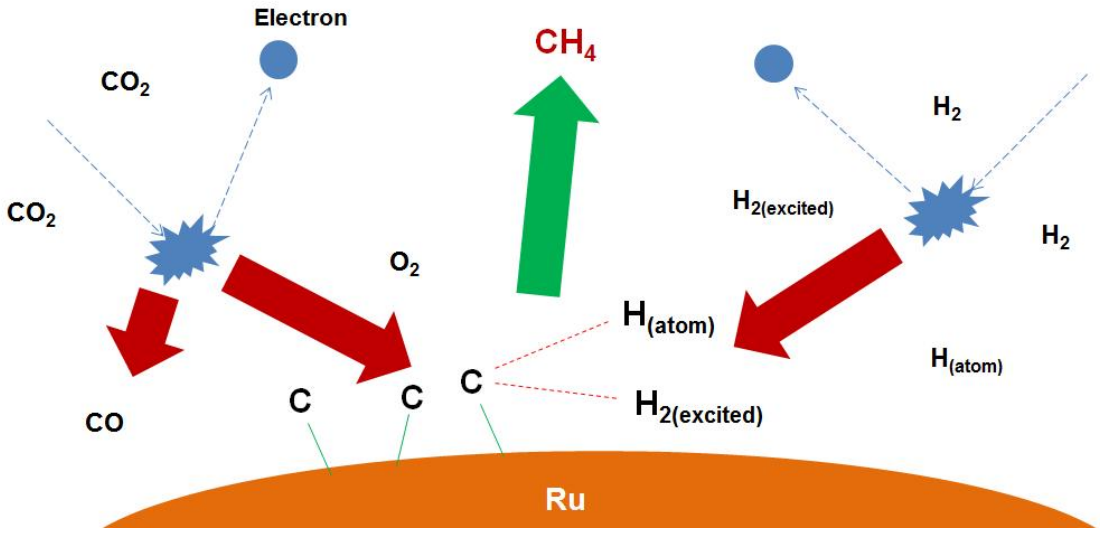

Figure 65. Effect of electron collision activity for CO_2 methanation process

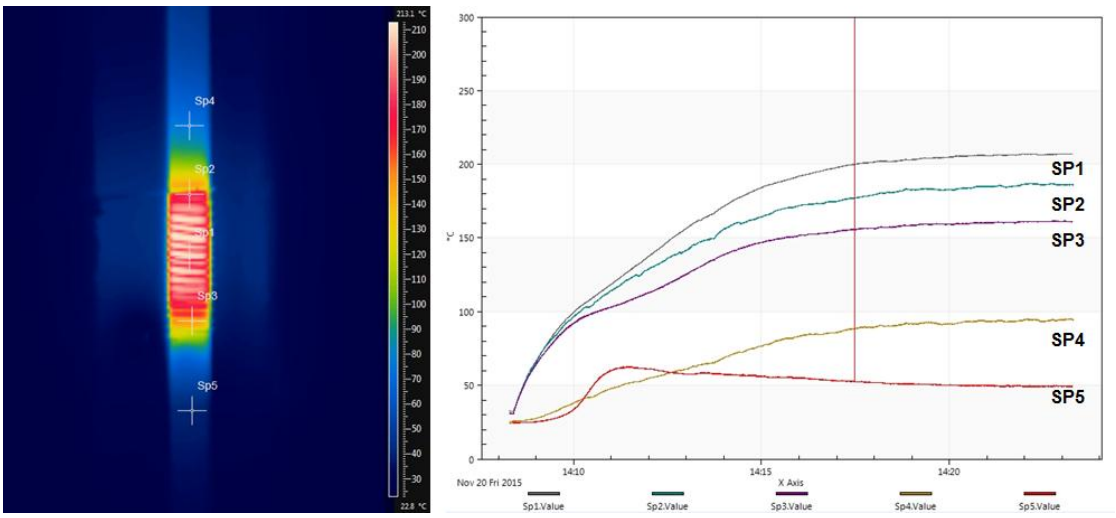

Figure 66. Infrared thermography of dielectric heating for 3 kHz, 9 kV DBD on Ru/γ-Al_2O_3 catalyst for atmospheric condition

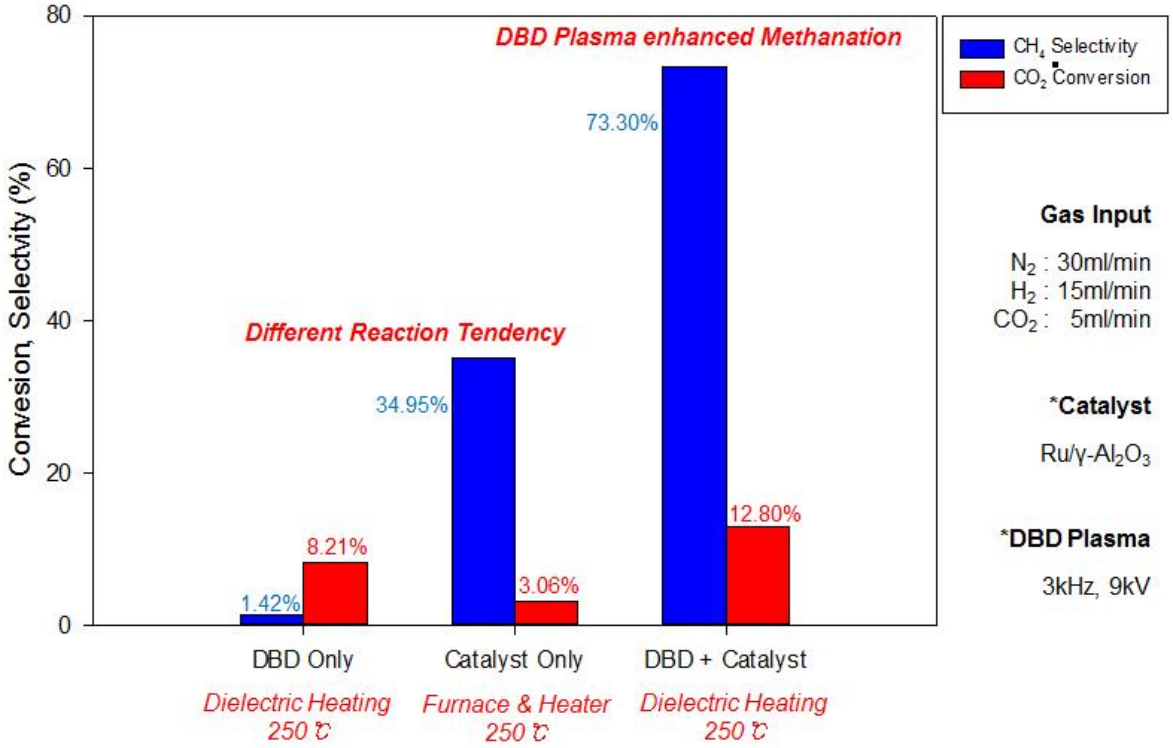

Figure 67. Verification result of different between DBD plasma-catalyst interaction and dielectric heating effect

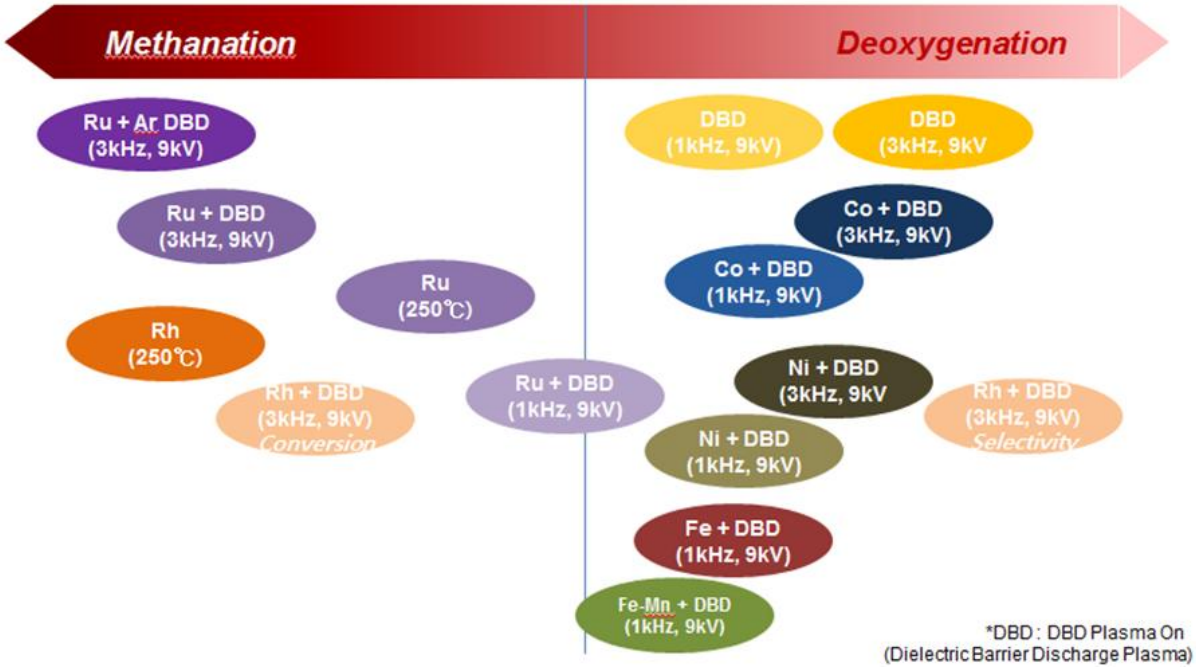

Figure 68. Interaction trend and performance for different condition

V. Interaction and Issues

1. Overview

In previous chapters, we discussed advantages of DBD plasma-catalyst interactions and its mechanisms. In my research, this interaction was only occurred when DBD plasma was discharged over catalyst area. It means catalyst should be exposed to electron collisions under the electric field. In plasma, radicals and excited species are also participated like a Figure 68. Therefore, the catalyst is influenced by the plasma species, thereby negative effects such as the performance degradation due to the surface damage is not negligible.

Except above direct effect from DBD plasma, indirect effect from DBD plasma is also affected on catalyst. Typical example is a carbon deposition on the surface of the catalyst when DBD plasma-assisted catalyst process is used for carbon-related process. The carbon is well-known electrical conductor and it may affect on discharge between electrodes and catalyst.

The performance enhancement or synergy effect of DBD plasma-assisted catalyst process is highlighted in many researches. We also focused on performance enhancement and its mechanism in previous chapters. However, practicality is also important to actual process because endurance is closely connected with economical side such as operating cost. Therefore, further investigation for endurance related characteristics of DBD plasma-assisted catalyst process was conducted and it will be discussed in this chapter.

2. Experimental

2.1 Catalysts

The promoter mixed catalysts and ruthenium catalyst what is used in previous methane conversion and CO_2 methanation chapters were used for experiment. The Mn and Ni promoter mixed impregnated catalyst ($Cu_3Zn_6Mn_1$ and $Cu_3Zn_6Ni_1$) was selected because the

performance degradation was detected at both catalysts but the CH_4 conversion was completely different under the DBD plasma. It was used to investigate a direct effect from DBD plasma and its related performance degradation issues.

On the contrary, ruthenium catalyst was selected to investigate carbon deposition what is related by dissociation and recombination of carbon. The methane direct conversion reaction and CO_2 methanation by using ruthenium catalyst was investigated because both reactions are related with carbon and methane. The methane can converted into C_2 and C_3 hydrocarbons or decomposed into carbon and hydrogens in methane direct conversion process. It means methane will be decreased by passing the ionized methane through the catalyst and carbon what decomposed from methane will be increased. On the contrary, carbon dioxide can decomposed into carbon and oxygens by passing the catalyst but decomposed carbon can exposed hydrogen rich condition in CO_2 methanation process. As a result, both cases have a different chance about recombination or bond with other species. We expect this different reaction characteristics are influenced on carbon deposition and endurance. Therefore, different carbon-related reaction process and carbon deposition was investigated with ruthenium catalyst.

2.2 Experiments

The Mn and Ni promoter mixed impregnated catalysts were exposed to the DBD plasma condition at 1 kHz and 9 kV for 4 hours. The applied discharge voltage was higher than the onset voltage of discharge because the breakdown voltage changed by the surface modification due to the damage. The reaction temperature was fixed to 250°C and supplied gas was controled 45 mL/min for N_2 and 5 mL/min for CH_4.

On the contrary, Ru catalyst was exposed on methane direct conversion and CO_2 methanation process. The discharge voltage and frequency was fixed at 3 kHz and 9 kV for DBD plasma-assisted condition, and supplied gas was controlled like a Table 11. The ruthenium catalyst was also exposed experimental condition for 4 hours.

3. Results and discussions

3.1 Performance degradation

The performance degradation of $Cu_3Zn_6Mn_1$ and $Cu_3Zn_6Ni_1$ are shown in Figure 69. The CH_4 conversion was increased after the DBD plasma discharged on both catalysts. In the $Cu_3Zn_6Mn_1$ catalyst, the CH_4 conversion was increased to 56.8% for 90 minutes but after then, it was decreased to 41.26% within 120 minutes. On the contrary, in the $Cu_3Zn_6Ni_1$ catalyst, the CH_4 conversion was increased to 10.88% for 30 minutes and then decreased to 6.52% for 90 minutes. The average decrements in CH_4 conversion of $Cu_3Zn_6Mn_1$ and $Cu_3Zn_6Ni_1$ were -0.23% and -0.45% per minute, and the total decrements in CH_4 conversion from the maximum conversion was -27.3% and -40.4%, respectively.

Generally, Ni has been widely used as a catalyst for the CH_4 conversion process. However, Ni had the worst performance and endurance under the DBD plasma condition. The poor performance of $Cu_3Zn_6Ni_1$ might be because the temperature at which experiments were performed was too low to activate the catalyst, but the $Cu_3Zn_6Mn_1$ showed the better performance than $Cu_3Zn_6Ni_1$ at the same temperature. In addition, the poor endurance is still not explained by the hypothesis that the temperature is too low to activate the catalyst.

Aforementioned, the catalyst is always exposed to electron collisions under the electric field and covered by numerous radicals and excited species during the DBD plasma reaction. Therefore, this difference of degradation and endurance may be related with the surface condition of catalyst.

3.2 Surface layer damage under DBD plasma

SEM images of $Cu_3Zn_6Mn_1$ and $Cu_3Zn_6Ni_1$ catalysts before and after exposed to the DBD plasma are shown in Figure 70. Noticeable difference appeared between Figure 70 (b) and Figure 70 (d). The loss of impregnated particles on the surface was observed in both catalysts after the exposure to the DBD plasma but this surface loss was significantly

higher in $Cu_3Zn_6Ni_1$ catalyst than $Cu_3Zn_6Mn_1$.

After exposed the DBD plasma, most of impregnated catalyst particles were disappeared from the surface of $Cu_3Zn_6Ni_1$ catalyst. This can explain why the $Cu_3Zn_6Ni_1$ catalyst showed the similar performance with the γ-Al_2O_3 support. On the contrary, the surface particles of $Cu_3Zn_6Mn_1$ catalyst were resistible well to the DBD plasma condition. Thus, impregnated nanoparticles of $Cu_3Zn_6Mn_1$ catalyst were sufficiently remained on the surface. This result might be explained as a relation between the performance and endurance because the $Cu_3Zn_6Mn_1$ catalyst had enough nanoparticles to be involved in CH_4 conversion reaction with the DBD plasma.

Under the DBD plasma condition, the surface of impregnated catalyst is consistently suffered from electron collisions, radicals and excited species which can cause the breakaway of impregnated catalyst particles from the surface of catalyst. As a result, the overall performance and endurance can be significantly decreased under the DBD plasma condition. However, the small amount of material such as Mn can prevent the catalyst surface from breakaway of impregnated catalyst particles. This result indicates that the breakaway of impregnated nanoparticles under the DBD plasma condition must be considered before using impregnated catalysts for the DBD plasma assisted process.

3.3 Carbon deposition on surface

Figure 71 shows SEM images of Ru/γ-Al_2O_3 catalyst surface at 800 times magnification after exposed at different reactions. Surface damage was clearly appeared in order of (d) > (c) > (a) = (b) = (e).

This surface damage pattern was occurred by a surface cracking and peeling. This was detected after exposed at the methane direct conversion reaction and at the DBD plasma assisted methane direct conversion reaction in Figure 71 (d). Especially, surface damage such as surface peeling and cracking was dominant at the DBD plasma discharge in the methane direct conversion reaction. On the contrary, damage on the Ru/γ-Al_2O_3 surface was

not clearly appeared after exposed to the CO_2 methanation.

SEM of Ru/γ-Al_2O_3 catalyst surface after exposed to the DBD plasma assisted methane direct conversion reaction is shown in Figure 72. Micro-cracking was detected on the catalyst surface but not detected on the support structure. Especially, this micro-cracking was formed with wrinkle shape at the entire surface.

EDS analysis on the catalyst surface was performed to reveal the reason of the surface damage. The weight ratio of elements on the catalyst surface is presented in Table 12. Carbon was only detected on the catalyst surface at the case of DBD plasma assisted methane direct conversion reaction.

3.4 Plausible mechanism of carbon related surface damage

Several things that cause the surface damage such as a peeling and cracking were confirmed. The damage was detected on the DBD plasma assisted methane direct conversion but not detected on the CO2 methanation reaction. At the same time, surface carbon deposition was also detected at the case of DBD plasma assisted methane direct conversion reaction. Moreover, average carbon balance of CO_2 methanation was greater than 90, nearly 100%. On the contrary, methane direct conversion was from 70 to 80% in the average carbon balance.

Based this result, we propose plausible mechanism of surface modification which can caused negative effect under DBD plasma assisted condition as shown in Figure 73.

After the DBD plasma is discharged on the catalyst, the local streamer is generated between Ru/γ-Al_2O_3 catalysts. The streamer causes methane decomposition to be enhanced because it has an increased electron energy and local temperature. This enhancement makes it increased the deposition of surface carbon which has a high electric conductivity. The surface carbon enhances local streamer, through which electrical current also increased. The enhanced streamer increases dielectric heating locally, which leads to the thermal expansion of catalyst surface layers. As a result, catalyst surface layers are destroyed or damaged by

the thermal stress as the catalyst surface layer is expanded because the thermal expansion rate of Ru-impregnated catalyst surface layer is different with that of internal alumina support.

This thermal expansion of catalyst surface layer is highly related with endurance and stability of catalysts. Performance degradation of the catalyst under the DBD plasma discharge is also related in Figure 69 what is mentioned previous discussion. Methane conversion under plasma assisted $Cu_3Zn_6Mn_1$ catalyst was increased rapidly but 90 minutes after the DBD plasma discharged, performance and carbon balance was gradually decreased because the discharging of DBD plasma caused methane decomposition increased, which lead to the increase of surface carbon and surface local temperature. Eventually, the thermal expansion damage was applied on the catalyst surface by the DBD plasma as the plasma discharge time elapsed after 90 minutes. Therefore, the conversion was decreased gradually due to the loss of surface catalysts.

4. Conclusions of interaction and issues

The performance and degradation what related with surface modification from interaction of catalyst and DBD plasma was investigated to achieve more stable DBD plasma-assisted catalyst process. The relation of performance degradation with the surface damage on the impregnated catalysts was confirmed by SEM analysis. The $Cu_3Zn_6Ni_1$ catalyst had a higher loss from the surface of the impregnated catalyst under the DBD plasma assisted condition. On the other hand, the surface particles of $Cu_3Zn_6Mn_1$ catalyst were more robust under the DBD plasma assisted condition and thereby the performance and endurance of the $Cu_3Zn_6Mn_1$ catalyst were higher than the $Cu_3Zn_6Ni_1$ catalyst.

Moreover, reaction process what can be related with carbon deposition is also important parameter for endurance of DBD plasma-assisted catalyst process. The carbon deposition on catalyst surface can generate concentrated streamer generation and it can causes thermal stress on impregnated layer of the catalyst.

For this reason, parameters what related with surface damage on the impregnated catalysts under the DBD plasma must be considered for the DBD plasma assisted impregnated catalyst process.

VI. Conclusions

The characteristics and mechanism of DBD plasma assisted catalyst process on C1 chemistry was investigated in my research. The experiments about DBD plasma-assisted methanol, methane direct conversion, visualization was performed to investigate characteristics and mechanism of DBD plasma assisted catalyst process. Unlike the expression, DBD plasma and catalyst in DBD plasma assisted catalyst process is not a unilateral dependence relation. In other word, catalyst what have a good catalytic performance is not always make a good result with DBD plasma assisted condition. Of course, DBD plasma can provide useful things for catalysis such as dielectric heating, dissociation and active species generation (excited atoms and molecules, and radicals) but problem is that DBD plasma generation is also affected by element or material characteristic of catalyst when it placed between the electrodes. Therefore, material characteristics of catalyst on DBD plasma generation is also considered achieving the better DBD plasma-assisted catalyst process.

A close look at the DBD plasma and catalyst, the catalyst can provide more effective generation of DBD plasma and DBD plasma can provide electron emission and its collision related activity to catalyst. We investigated suitable application to utilize interaction characteristics of DBD plasma-assisted catalyst process. The DBD plasma-assisted CO_2 methnation process was selected and investigated because we expect that dissociation of CO_2 and active species generation by electron collision, catalysis activation by dielectric heating is suitable for CO_2 methanation process. We achieved atmospheric CO_2 methanation process by using DBD plasma assisted catalyst process and it has a 23.20% for CO_2 conversion and 97.38% CH_4 selectivity with impregnated ruthenium catalyst within experimental range. Dielectric heating effect is also investigated but interaction of DBD plasma and catalyst was shown 8 times better performance than catalytic methanation for same temperature as dielectric heating. Based on this result, we proposed DBD plasma-assisted CO_2 methanation for one of the ‘Power-to-Gas’ technology.

However, DBD plasma assisted catalyst process have a drawback and it must be understood to better utilization. The electron emission and collision from DBD plasma can give a many advantages. The advantages are already mentioned above but problem is that electron emission and collision can give physical damage to the catalyst. Dissociation activity of DBD plasma what is related with carbon deposition is also confirmed during the research. Therefore, physical stability of catalyst under DBD plasma and carbon deposition related issues from the application is must be considered to achieve better endurance.

In conclusion, the DBD plasma-assisted catalyst process is very attractive technology for many applications. It is not always perfect solution but it can give a new possibilities and improvements for many applications including chemical process. Therefore, understanding the interaction characteristics and mechanism of DBD plasma-assisted catalyst process is very important. Therefore, we have been studied this research since 2012, and we hope this work will be helpful to DBD plasma-assisted catalyst process and Power-to-Gas technology.

Table 11. Different carbon related conditions of ruthenium catalyst

	Reaction	Gas Supply (mL/min)	Reactor Heating	DBD plasma
(a)	CO_2 Methanation	N_2:30 H_2:15 CO_2:5	300°C (Heater)	No
(b)			300°C (Dielectric Heating)	Discharged
(c)	CH_4 Direct Conversion	N_2:45 CH_4:5	300°C (Heater)	No
(d)			300°C (Dielectric Heating)	Discharged
(e)	No	No	No	No

Table 12. The result of EDS analysis for weight ratio of catalyst surface layer

Element	Experimental case				
	(a)	(b)	(c)	(d)	(e)
C	-	-	-	19.06	-
O	43.02	52.12	50.93	32.37	51.52
Al	47.20	44.85	43.12	35.86	42.04
Ru	9.78	3.03	5.96	12.70	6.44

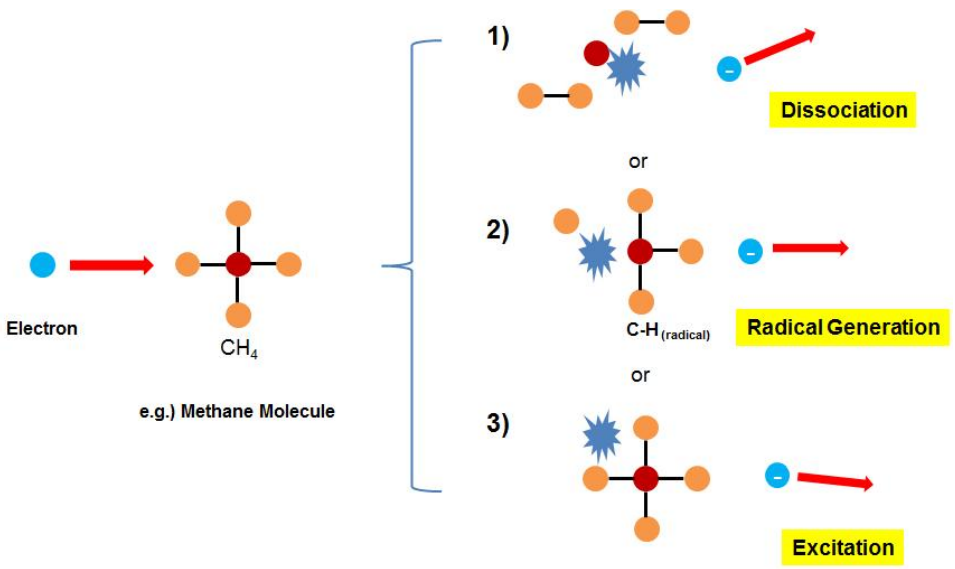

Figure 69. Effect of electron collision activity for molecule

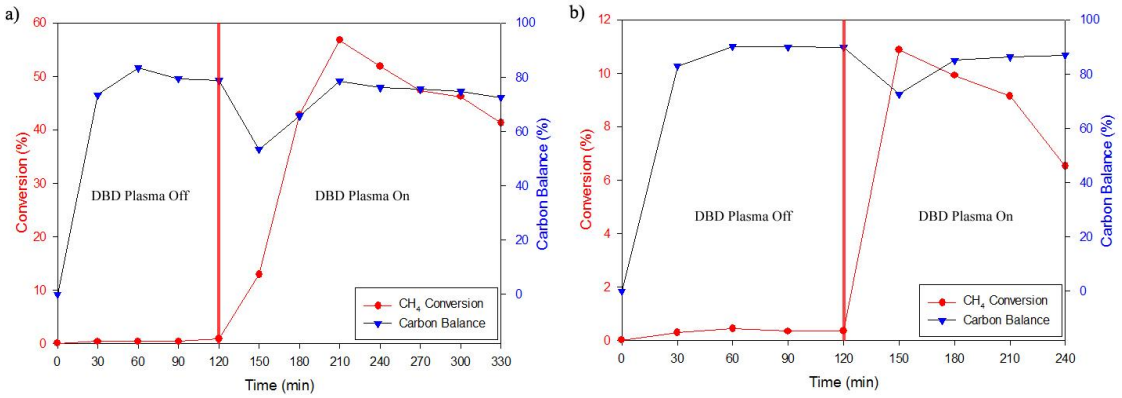

Figure 70. Performance degradation of $Cu_3Zn_6Mn_1$ and $Cu_3Zn_6Ni_1$ catalyst under DBD plasma assisted condition (1 kHz, 8 kV, 250°C)

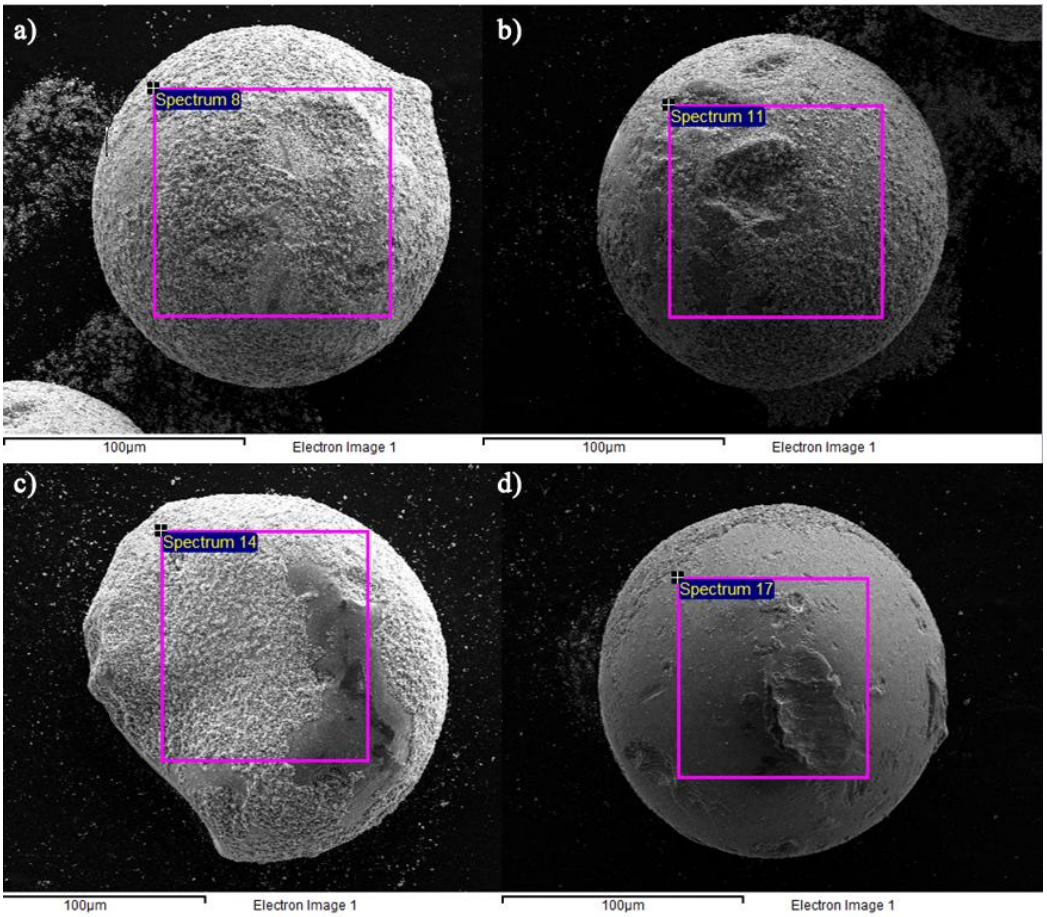

Figure 71. SEM images of (a) fresh $Cu_3Zn_6Mn_1$ catalyst, (b) 4 hours DBD plasma exposed $Cu_3Zn_6Mn_1$ catalyst, (c) fresh $Cu_3Zn_6Ni_1$ catalyst, (d) 4 hours DBD plasma exposed $Cu_3Zn_6Ni_1$ catalyst

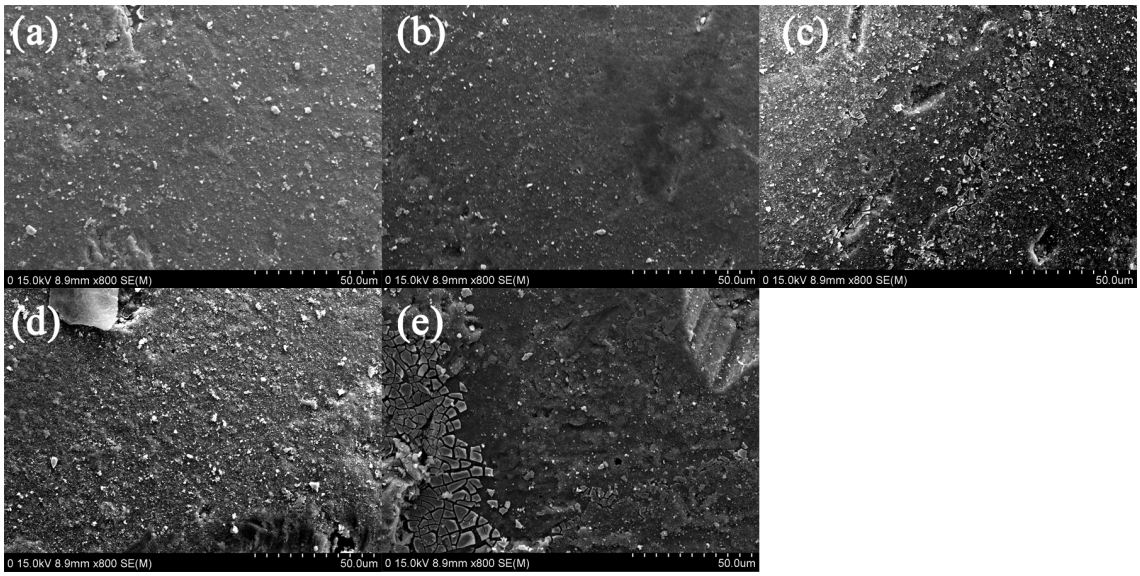

Figure 72. SEM images of Ru/γ-Al_2O_3 catalyst surface after exposed (a) catalytic methanation, (b) DBD plasma assisted methanation, (c) catalytic methane direct conversion, (d) DBD plasma assisted methane direct conversion and (e) fresh catalyst.

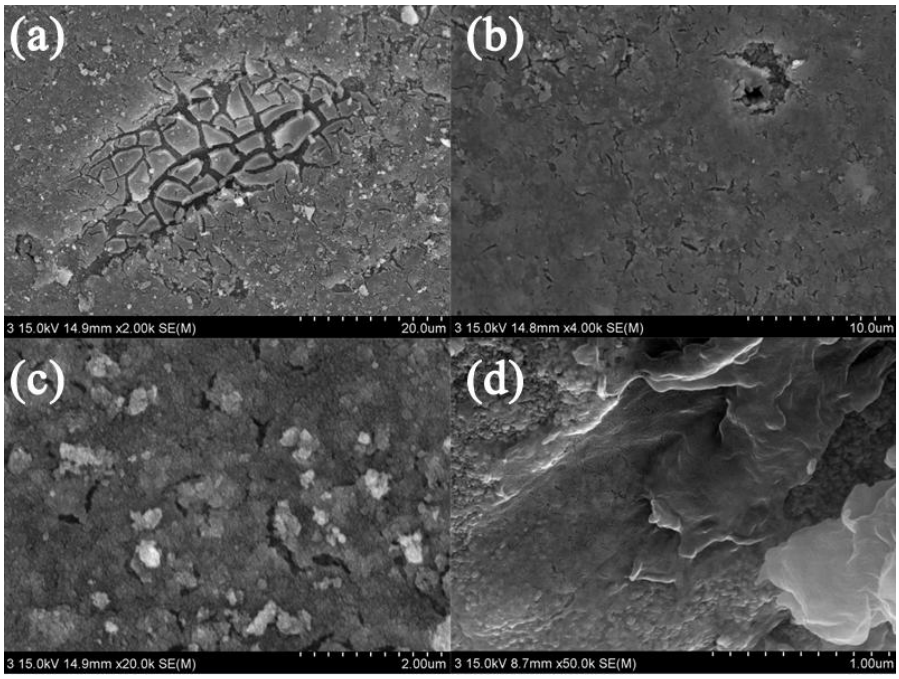

Figure 73. SEM images of surface damage on Ru/γ-Al_2O_3 catalyst after exposed at DBD plasma assisted methane direct conversion reaction: (a) 2,000, (b) 4,000, (c) 20,000 and (d) 50,000 times magnification.

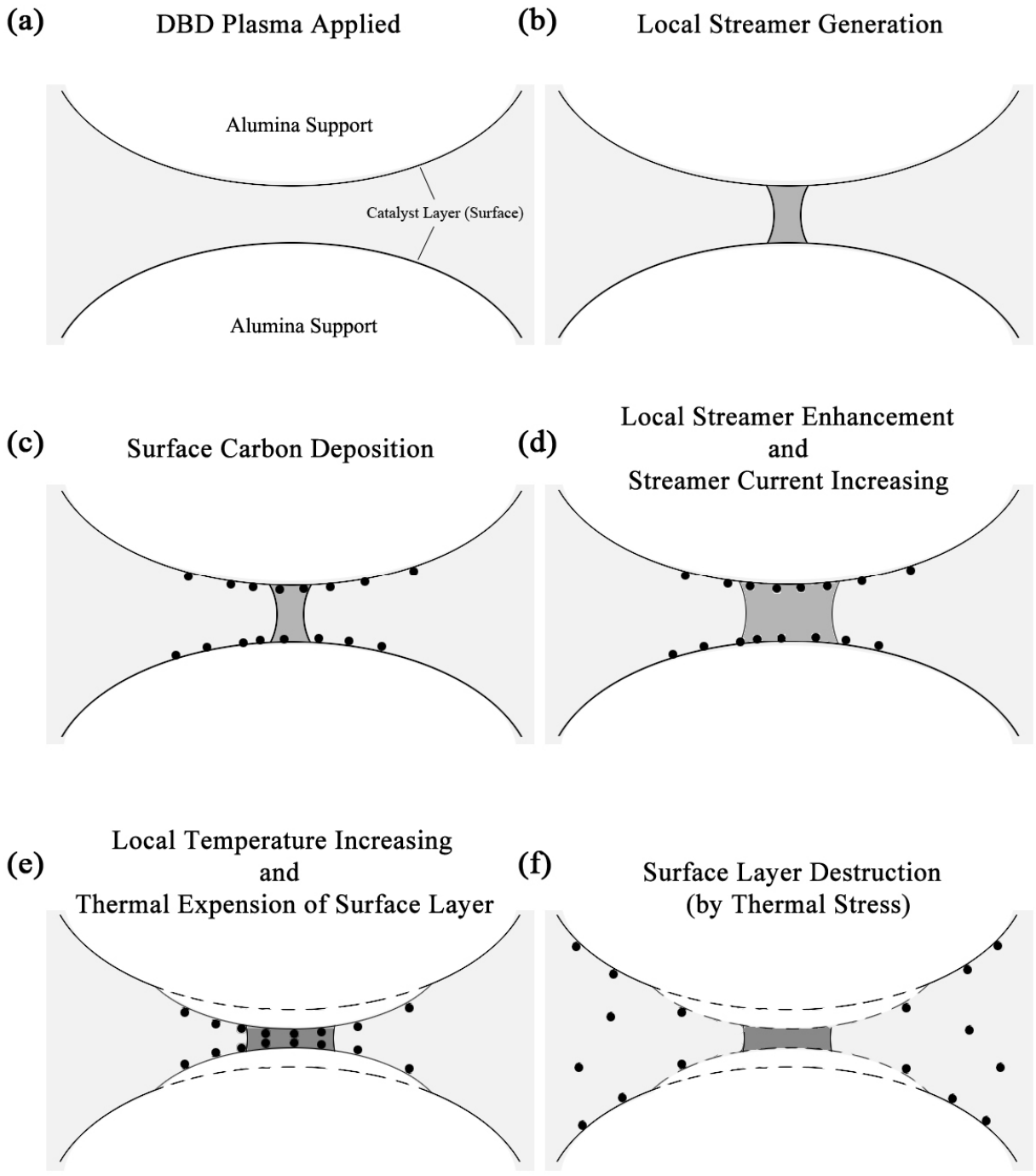

Figure 74. Plausible mechanism of surface modification and destruction of the catalyst layer under DBD plasma assisted condition

REFERENCES

[1] U. Kogelschatz, "Dielectric-barrier discharges: their history, discharge physics, and industrial applications." Plasma chemistry and plasma processing, 2013, 23(1), 1-46.

[2] B. H. Liu, Z. P. Li, "A review: hydrogen generation from borohydride hydrolysis reaction." Journal of Power Sources, 2009, 187(2), 527-534.

[3] T. C. Manley, "The electric characteristics of the ozonator discharge." Transactions of the electrochemical society, 84(1), 1943, 83-96.

[4] S. Samukawa, M. Hori, S. Rauf, K. Tachibana, P. Bruggeman, G. Kroesen, J. C. Whitehead, A. B. Murphy, A. F. Gutsol, S. Starikovskaia, U. Kortshagen, J. P. Boeuf, T. J. Sommerer, M. J. Kushner, U. Czarnetzki, N. Mason, "The 2012 plasma roadmap." Journal of Physics D: Applied Physics, 45(25), 2012, 253001.

[5] T. C. Corke, M. L. Post, D. M. Orlov, "Single dielectric barrier discharge plasma enhanced aerodynamics: physics, modeling and applications." Experiments in Fluids, 46(1), 2009, 1-26.

[6] D. Ishihara, Y. Noma, S. Stauss, M. Sai, T. Tomai, K. Terashima, "Development of a dielectric barrier discharge (DBD) cryo-microplasma: generation and diagnostics." Plasma Sources Science and Technology, 17(3), 2008, 035008.

[7] N. Mastanaiah, J. A. Johnson, S. Roy, "Effect of dielectric and liquid on plasma sterilization using dielectric barrier discharge plasma." PloS one, 8(8), 2013, e70840.

[8] M. Xi, Y. L. Li, S. Shang, D. H. Li, Y. X. Yin, X. Y. Dai, "Surface modification of aramid fiber by air DBD plasma at atmospheric pressure with continuous on-line processing." Surface and Coatings Technology, 202(24), 2008, 6029-6033.

[9] T. Shao, C. Zhang, K. Long, D. Zhang, J. Wang, P Yan, Y. Zhou, "Surface modification of polyimide films using unipolar nanosecond-pulse DBD in atmospheric air." Applied Surface Science, 256(12), 2010, 3888-3894.

[10] B. M. Obradović, G. B. Sretenović, M. M. Kuraica, "A dual-use of DBD plasma for simultaneous NO_x and SO_2 removal from coal-combustion flue gas." Journal of hazardous

materials, 185(2), 2011, 1280-1286.

[11] X. Tu, J. C. Whitehead, "Plasma-catalytic dry reforming of methane in an atmospheric dielectric barrier discharge: Understanding the synergistic effect at low temperature." Applied Catalysis B: Environmental, 125, 2012, 439-448.

[12] Q. Wang, H. Shi, B. Yan, Y. Jin, Y. Cheng, "Steam enhanced carbon dioxide reforming of methane in DBD plasma reactor." international journal of hydrogen energy, 36(14), 2011, 8301-8306.

[13] Y. P. Hu, G. Li, Y. Yang, X. Gao, Z. Lu, "Hydrogen generation from hydro-ethanol reforming by DBD-plasma." international journal of hydrogen energy, 37(1), 2012, 1044-1047.

[14] B. Sarmiento, J. J. Brey, I. G. Viera, A. R. Gonzalez-Elipe, J. Cotrino, V. J. Rico, "Hydrogen production by reforming of hydrocarbons and alcohols in a dielectric barrier discharge." Journal of Power sources, 169(1), 2007, 140-143.

[15] V. Nehra, A. Kumar, H. K. Dwivedi, "Atmospheric non-thermal plasma sources." International Journal of Engineering, 2(1), 2008, 53-68.

[16] L. Bian, L. Zhang, R. Xia, Z. Li, "Enhanced low-temperature CO_2 methanation activity on plasma-prepared Ni-based catalyst." Journal of Natural Gas Science and Engineering, 27, 2015, 1189-1194.

[17] Y. Li, B. W. Jang, "Non-thermal RF plasma effects on surface properties of Pd/TiO_2 catalysts for selective hydrogenation of acetylene." Applied Catalysis A: General, 392(1), 2011, 173-179.

[18] J. Wang, C. Liu, Y. Zhang, K. Yu, X. Zhu, F. He, "Partial oxidation of methane to syngas over glow discharge plasma treated $Ni-Fe/Al_2O_3$ catalyst." Catalysis Today, 89(1), 2004, 183-191.

[19] K. Li, X. Tang, H. Yi, P. Ning, Y. Xiang, J. Wang, C. Wang, X. Peng, "Research on manganese oxide catalysts surface pretreated with non-thermal plasma for NO catalytic oxidation capacity enhancement." Applied Surface Science, 264, 2013, 557-562.

[20] B. Roy, K. Loganathan, H. N. Pham, A. K. Datye, C. A. Leclerc, "Surface modification of solution combustion synthesized Ni/Al_2O_3 catalyst for aqueous-phase reforming of ethanol."

international journal of hydrogen energy, 35(21), 2010, 11700-11708.

[21] A. Ogata, H. H. Kim, S. Futamura, S. Kushiyama, K. Mizuno, "Effects of catalysts and additives on fluorocarbon removal with surface discharge plasma." Applied Catalysis B: Environmental, 53(3), 2004, 175-180.

[22] Y. F. Guo, D. Q. Ye, K. F. Chen, J. C. He, W. L. Chen, " Toluene decomposition using a wire-plate dielectric barrier discharge reactor with manganese oxide catalyst in situ." Journal of Molecular Catalysis A: Chemical, 245(1), 2006, 93-100.

[23] Y. Guo, D. Ye, K. Chen, "Toluene removal by a DBD-type plasma combined with metal oxides catalysts supported by nickel foam." Catalysis today, 126(3), 2007, 328-337.

[24] Z. Fan, K. Sun, N. Rui, B. Zhao, C. Liu, "Improved activity of $Ni/MgAl_2O_4$ for CO_2 methanation by the plasma decomposition." Journal of Energy Chemistry, 24(5), 2015, 655-659.

[25] Q. Wang, B. H. Yan, Y. Jin, Y. Cheng, "Dry reforming of methane in a dielectric barrier discharge reactor with Ni/Al_2O_3 catalyst: interaction of catalyst and plasma." Energy & Fuels, 23(8), 2009, 4196-4201.

[26] C. C. Chang, C. C. Hsu, C. T. Chang, Y. P. Chen, "Effect of noble metal on oxidative steam reforming of methanol over $CuO/ZnO/Al_2O_3$ catalysts." international journal of hydrogen energy, 37(15), 2012, 11176-11184.

[27] Y. P. Hu, G. Li, Y. Yang, X. Gao, Z. Lu, "Hydrogen generation from hydro-ethanol reforming by DBD-plasma." international journal of hydrogen energy, 37(1), 2012, 1044-1047.

[28] P. J. Lindner, R. S. Besser, "Hydrogen production by methanol reforming in a non-thermal atmospheric pressure microplasma reactor." International Journal of Hydrogen Energy, 37(18), 2012, 13338-13349.

[29] Q. Wang, B. H. Yan, Y. Jin, Y. Cheng, "Investigation of dry reforming of methane in a dielectric barrier discharge reactor." Plasma Chemistry and Plasma Processing, 29(3), 2009, 217-228.

[30] Q. Wang, H. Shi, B. Yan, Y. Jin, Y. Cheng, "Steam enhanced carbon dioxide reforming of

methane in DBD plasma reactor." international journal of hydrogen energy, 36(14), 2011, 8301-8306.

[31] E. Jwa, S.B. Lee, H.W. Lee, Y.S. Mok, "Plasma-assisted catalytic methanation of CO and CO_2 over Ni-zeolite catalysts." Fuel processing technology, 108, 2013, 89-93.

[32] M. Nizio, A. Albarazi, S. Cavadias, J. Amouroux, M. E. Galvez, P. Da Costa, "Hybrid plasma-catalytic methanation of CO_2 at low temperature over ceria zirconia supported Ni catalysts." International Journal of Hydrogen Energy, 41(27), 2016, 11584-11592.

[33] M. Nizio, R. Benrabbah, M. Krzak, R. Debek, M. Motak, S. Cavadias, E. Galvez, P. Da Costa, "Low temperature hybrid plasma-catalytic methanation over Ni-Ce-Zr hydrotalcite-derived catalysts." Catalysis Communications, 83, 2016, 14-17.

[34] Y. Zeng, X. Tu, "Plasma-Catalytic CO_2 Hydrogenation at Low Temperatures." IEEE Transactions on Plasma Science, 44(4), 2016, 405-411.

[35] J. C. Whitehead, "Plasma-catalysis: the known knowns, the known unknowns and the unknown unknowns." Journal of Physics D: Applied Physics, 49(24), 2016, 243001.

[36] International Energy Agency. "Key world energy statistics." International Energy Agency, 2007.

[37] S. Solomon, D. Qin, M. Manning, Z. Chen, M. Marquis, K.B. Averyt, M. Tignor, H.L. Miller, Contribution of Working Group I to the Fourth Assessment Report of the Intergovernmental Panel on Climate Change, Cambridge University Press, Cambridge, 2007.

[38] P. Tans, R. Keeling, ESRL Global Monitoring Division e Global Greenhouse Gas Reference Network, 2016. [WWW Document]. URL. http://www.esrl.noaa.gov/gmd/ccgg/trends/ (accessed 17.04.13.).

[39] International Energy Agency."Medium-Term Renewable Energy Market Report 2014." OECD/IEA, 2014.

[40] M. H. Lietzke, C. Mullins, "The thermal decomposition of carbon dioxide." Journal of Inorganic and Nuclear Chemistry, 43(8), 1981, 1769-1771.

[41] M. A. Oehlschlaeger, D. F. Davidson, J. B. Jeffries, R. K. Hanson, "Carbon dioxide thermal

decomposition: Observation of incubation." Zeitschrift fur Physikalische Chemie, 219, 2005, 555-567.

[42] STS-13 Mission Summary, NASA, WA, April 2010.
(Available: https://www.nasa.gov/pdf/436872main_STS131 mission summary.pdf)

[43] C. Junaedi, K. Hawley, D. Walsh, S. Roychoudhury, M. B. Abney and J. L. Perry, “Compact and Lightweight Sabatier Reactor for Carbon Dioxide Reduction,” AIAA Report, AIAA 2011-5033, 41st International Conference on Environmental Systems, Portland, Oregon, 2011.

[44] M. Bailera, P. Lisbona, L. M. Romeo, S. Espatolero, "Power to Gas projects review: Lab, pilot and demo plants for storing renewable energy and CO_2." Renewable and Sustainable Energy Reviews., 69, 2017, 292-312.

[45] M. Gotz, J. Lefebvre, F. Mors, A. M. Koch, F. Graf, S. Bajohr, R. Reimert, T. Kolb, "Renewable Power-to-Gas: A technological and economic review." Renewable Energy, 85, 2016, 1371-1390.

[46] G. Benjaminsson, J. Benjaminsson, R. Boogh Rudberg, "Powerto-gas - A technical review. Technical Report", Svenskt Gastekniskt Center AB, Malmo, 2013.

[47] M. Kulawska, M. Madej-Lachowska, "Copper/zinc catalysts in hydrogenation of carbon oxides." Chemical and Process Engineering, 34(4), 2013, 479-496.

[48] M. S. Spencer, "Precursors of copper/zinc oxide catalysts." Catalysis letters, 66(4), 2000, 255-257.

[49] Y. Li, Q. Fu, M. Flytzani-Stephanopoulos, "Low-temperature water-gas shift reaction over Cu-and Ni-loaded cerium oxide catalysts." Applied Catalysis B: Environmental, 27(3), 2000, 179-191.

[50] S Sa, JM Sousa, A Mendes, "Steam reforming of methanol over a $CuO/ZnO/Al_2O_3$ catalyst, part I: kinetic modelling." Chemical engineering science, 66(20), 2011, 4913-4921.

[51] X Du, Y Shen, L Yang, Y Shi, Y Yang, "Experiments on hydrogen production from methanol steam reforming in the microchannel reactor." International Journal of Hydrogen Energy, 37(17), 2012, 12271-12280.

[52] G. J. Auwerda, J. L. Kloosterman, A. J. M. Winkelman, J. Groen, V. van Dijk, "Comparison of experiments and calculations of void fraction distributions in randomly stacked pebble beds." PHYSOR 2010-Advances in Reactor Physics to Power the Nuclear Renaissance, Pittsburgh, Pennsylvania, USA, 9-14.

[53] G. D. Scott, D. M. Kilgour, "The density of random close packing of spheres. Journal of Physics D: Applied Physics, 2(6), 1969, 863."

[54] H. Sadat, N. Dubus, L. Pinard, J. M. Tatibouet, J. Barrault, "Conduction heat transfer in a cylindrical dielectric barrier discharge reactor." Applied Thermal Engineering, 29(5), 2009, 1259-1263.

[55] H. Sadat, N. Dubus, V. Le Dez, J. M. Tatibouet, "A simple model for transient temperature rise and fall in a dielectric barrier discharge reactor after ignition and shut down." Journal of Electrostatics, 68(1), 2010, 27-30.

[56] C. Wang, G. Zhang, X. Wang, "Comparisons of discharge characteristics of a dielectric barrier discharge with different electrode structures." Vacuum, 86(7), 2012, 960-964.

[57] C. Q. Wang, G. X. Zhang, "Effect of measurement elements on discharge characteristics of dielectric barrier discharge." Physics Procedia, 32, 2012, 664-668.

[58] T. L. Sung, S. Teii, C. M. Liu, R. C. Hsiao, P. C. Chen, Y. H. Wu, C. K. Yang, K. Teii, S. Ono, K. Ebihara, "Effect of pulse power characteristics and gas flow rate on ozone production in a cylindrical dielectric barrier discharge ozonizer." Vacuum, 90, 2013, 65-69.

[59] H. Zhang, K. Li, C. Shu, Z. Lou, T. Sun, J. Jia, "Enhancement of styrene removal using a novel double-tube dielectric barrier discharge (DDBD) reactor." Chemical Engineering Journal, 256, 2014, 107-118.

[60] P. Jitsomboonmit, M. Nisoa, S. Dangtip, "Experimental Study of Current-Voltage Characteristics and Optical Emission of Various Gases in Dielectric Barrier Discharge at Atmospheric Pressure." Physics Procedia, 32, 2012, 723-731.

[61] C. Karakaya, R. J. Kee, "Progress in the direct catalytic conversion of methane to fuels and chemicals." Progress in Energy and Combustion Science, 55, 2016, 60-97.

[62] R. Jin, Y. Chen, W. Li, W. Cui, Y. Ji, C. Yu, Y. Jiang, "Mechanism for catalytic partial oxidation of methane to syngas over a Ni/Al_2O_3 catalyst." Applied Catalysis A: General, 201(1), 2000, 71-80.

[63] J. H. Lunsford, "Catalytic conversion of methane to more useful chemicals and fuels: a challenge for the 21st century." Catalysis Today, 63(2), 2000, 165-174.

[64] G Gómez, JÁ Botas, DP Serrano, P Pizarro, "Hydrogen production by methane decomposition over pure silica SBA-15 materials." Catalysis Today, 277, 2016, 152-160.

[65] C. H. Bartholomew, "Mechanisms of catalyst deactivation." Applied Catalysis A: General, 212(1), 2001, 17-60.

[66] M. H. Pham, V. Goujard, J. M. Tatibouet, C. Batiot-Dupeyrat, "Activation of methane and carbon dioxide in a dielectric-barrier discharge-plasma reactor to produce hydrocarbons－Influence of La_2O_3/γ-Al_2O_3 catalyst." Catalysis today, 171(1), 2011, 67-71.

[67] Q. Wang, H. Shi, B. Yan, Y. Jin, Y. Cheng, "Steam enhanced carbon dioxide reforming of methane in DBD plasma reactor." international journal of hydrogen energy, 36(14), 2011, 8301-8306.

[68] P. Qin, H. Xu, H. Long, Y. Ran, S. Shang, Y. Yin, X. Dai, "Ni/MgO catalyst prepared using atmospheric high-frequency discharge plasma for CO_2 reforming of methane." Journal of Natural Gas Chemistry, 20(5), 2011, 487-492.

[69] Q. Wang, B. H. Yan, Y. Jin, Y. Cheng, "Dry reforming of methane in a dielectric barrier discharge reactor with Ni/Al_2O_3 catalyst: interaction of catalyst and plasma." Energy & Fuels, 23(8), 2009, 4196-4201.

[70] A. Indarto, D. R. Yang, J. Palgunadi, J. W. Choi, H. Lee, H. K. Song, "Partial oxidation of methane with Cu-Zn-Al catalyst in a dielectric barrier discharge." Chemical Engineering and Processing: Process Intensification, 47(5), 2008, 780-786.

[71] G. D. Stancu, F. Kaddouri, D. A. Lacoste, C. O. Laux, "Atmospheric pressure plasma diagnostics by OES, CRDS and TALIF." Journal of Physics D: Applied Physics, 43(12), 2010, 124002.

[72] P. Kasinathan, S. Park, W. C. Choi, Y. K. Hwang, "Plasma-enhanced methane direct conversion over particle-size adjusted MO_x/Al_2O_3 (M=Ti and Mg) catalysts." Plasma Chemistry and Plasma Processing, 34(6), 2014, 1317-1330.

[73] V. Jiménez, P. Sánchez, P. Panagiotopoulou, J. L. Valverde, A. Romero, "Methanation of CO, CO_2 and selective methanation of CO, in mixtures of CO and CO_2, over ruthenium carbon nanofibers catalysts." Applied Catalysis A: General, 390(1), 2010, 35-44.

[74] J. Xu, X. Su, H. Duan, B. Hou, Q. Lin, X. Liu, X. Pan, G. Pei, H. Geng, Y. Huang, T. Zhang, "Influence of pretreatment temperature on catalytic performance of rutile TiO_2-supported ruthenium catalyst in CO_2 methanation." Journal of Catalysis, 333, 2016, 227-237.

[75] G. Garbarino, D. Bellotti, P. Riani, L. Magistri, G. Busca, "Methanation of carbon dioxide on Ru/Al_2O_3 and Ni/Al_2O_3 catalysts at atmospheric pressure: Catalysts activation, behaviour and stability." International Journal of Hydrogen Energy, 40(30), 2015, 9171-9182.

[76] S. Danaci, L. Protasova, J. Lefevere, L. Bedel, R. Guilet, P. Marty, "Efficient CO_2 methanation over Ni/Al_2O_3 coated structured catalysts." Catalysis Today, 273, 2016, 234-243.

[77] M. S. Duyar, A. Ramachandran, C. Wang, R. J. Farrauto, "Kinetics of CO_2 methanation over Ru/γ-Al_2O_3 and implications for renewable energy storage applications." Journal of CO_2 Utilization, 12, 2015, 27-33.

[78] J. Kopyscinski, T. J. Schildhauer, S. M. Biollaz, "Production of synthetic natural gas (SNG) from coal and dry biomass – A technology review from 1950 to 2009." Fuel, 89(8), 2010, 1763-1783.

[79] J. M. Panek, J. Grasser, Practical experience gained during the first twenty years of operation of the great plains gasification plant and implications for future projects. U.S. DOE, Washington, 2006.

[80] T. Schaaf, J. Grünig, M.R. Schuster, T. Rothenfluh, A. Orth, "Methanation of CO_2-storage of renewable energy in a gas distribution system." Energy, Sustainability and Society, 4(1), 2014, 2.

[81] S. Sharma, Z. Hu, P. Zhang, E. W. McFarland, H. Metiu, "CO_2 methanation on Ru-doped

ceria." Journal of Catalysis, 278(2), 1011, 297-309.

[82] P. Panagiotopoulou, D. I. Kondarides, X. E. Verykios, "Selective methanation of CO over supported noble metal catalysts: Effects of the nature of the metallic phase on catalytic performance." Applied Catalysis A: General, 344(1), 2008, 45-54.

[83] I. Fechete, J. C. Vedrine, "Nanoporous materials as new engineered catalysts for the synthesis of green fuels." Molecules, 20(4), 2015, 5638-5666.

[84] N. Benard, E. Moreau, " Electrical and mechanical characteristics of surface AC dielectric barrier discharge plasma actuators applied to airflow control." Experiments in Fluids, 55(11), 2014, 1846.

[85] A. A. Abdelaziz, T. Ishijima, T. Seto, N. Osawa, H. Wedaa, Y. Otani, "Characterization of surface dielectric barrier discharge influenced by intermediate frequency for ozone production." Plasma Sources Science and Technology, 25(3), 2016,035012.

[86] S. Y. Liu, D. H. Mei, Z. Shen, X. Tu, "Nonoxidative conversion of methane in a dielectric barrier discharge reactor: prediction of reaction performance based on neural network model." The Journal of Physical Chemistry C, 118(20), 2014,10686-10693.

[87] M. J. Barton, A. Von Engel, "Electric dissociation of CO_2." Physics Letters A, 32(3), 1970, 173-174.

[88] L. F. Spencer, A. D. Gallimore, "Efficiency of CO_2 dissociation in a radio-frequency discharge." Plasma Chemistry and Plasma Processing, 31(1), 2011, 79-89.

[89] G. L. Scheffler, D. Pozebon, "Advantages, drawbacks and applications of mixed Ar-N_2 sources in inductively coupled plasma-based techniques: an overview." Analytical Methods, 6(16), 2014, 6170-6182.

[90] N. U. Rehman, Z. Anjum, A Masood, M Farooq, I. Ahmad, M. Zakaullah, "Metrology of non-thermal capacitively coupled N_2-Ar mixture plasma." Optics Communications, 296, 2013, 72-78.

[91] J. W. Coburn, M. Chen, "Optical emission spectroscopy of reactive plasmas: A method for correlating emission intensities to reactive particle density." Journal of applied physics, 51(6),

1980, 3134-3136.

[92] S. Ghosh, V. L. Prasanna, B. Sowjanya, P. Srivani, M. Alagaraja, D. Banji, "Inductively coupled plasma-optical emission spectroscopy: a review." Asian Journal of Pharmaceutical Analysis, 3(1), 2013, 24-33.

[93] F. Fendrych, A. Taylor, L. Peksa, I. Kratochvilova, J. Vlcek, V. Rezacova, V. Petrak, Z. Kluiber, L. Fekete, M. Liehr, M. Nesladek, "Growth and characterization of nanodiamond layers prepared using the plasma-enhanced linear antennas microwave CVD system." Journal of Physics D: Applied Physics, 43(37), 2010, 374018.

[94] R. Bogdanowicz, "Investigation of H_2: CH_4 plasma composition by means of spatially resolved optical spectroscopy." Acta Phys. Pol. A, 114, 2008, 6.

[95] C. G. Parigger, E. Oks, "Hydrogen Balmer series spectroscopy in laser-induced breakdown plasmas." Int. Rev. Atom. Mol. Phys, 1, 2010, 13-23.

[96] N. Konjević, M. Ivković, N. Sakan, "Hydrogen Balmer lines for low electron number density plasma diagnostics." Spectrochimica Acta Part B: Atomic Spectroscopy, 76, 2012, 16-26.